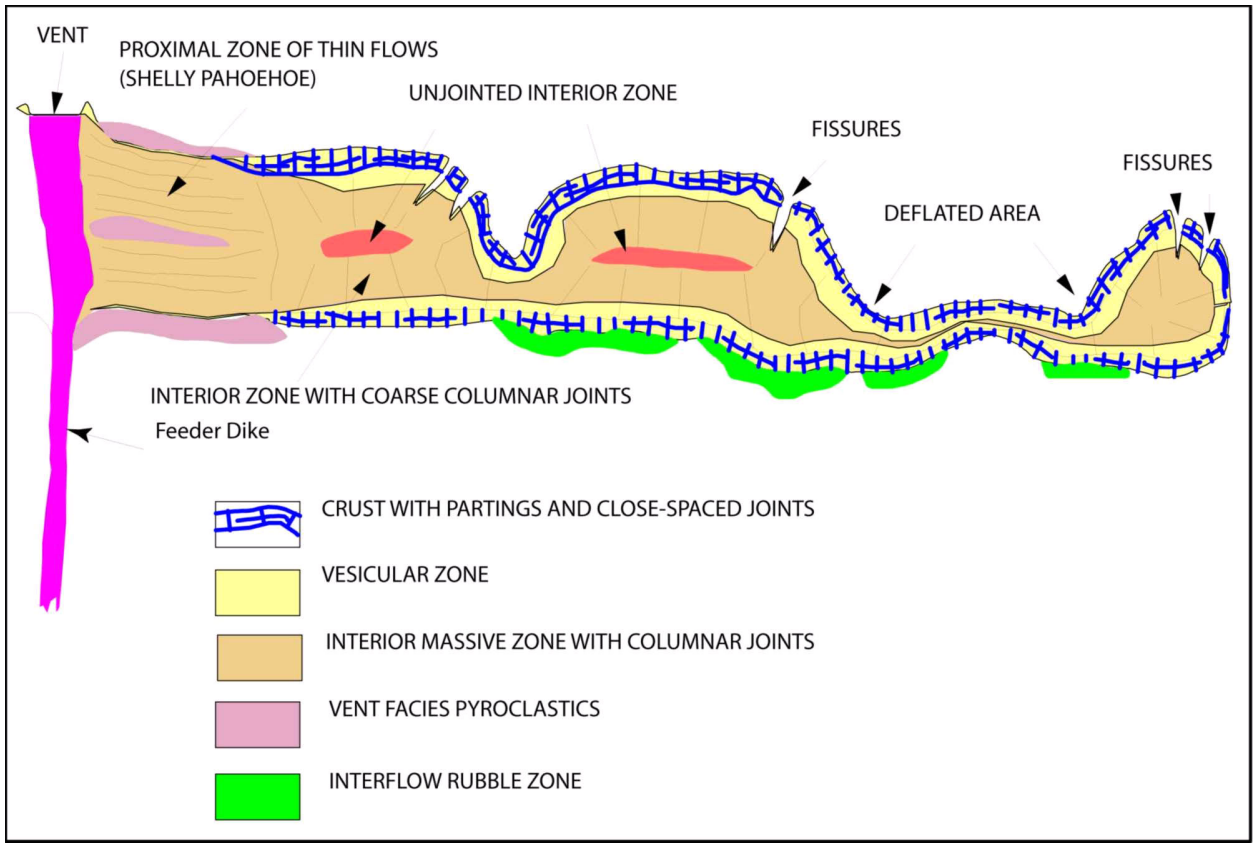

Figure 4-13. The proximal to distal structure of a pahoehoe basalt flow. Fractures and rubble zones can be preferred paths of travel for groundwater. Massive flow interiors and fracture zones closed by infiltrating sediment or alteration act as aquitards (adapted from Knutson et al. 1992).

The SRPA is characterized by extreme heterogeneity in hydraulic properties. Heterogeneity at the scale of an individual flow is attributed to flow features, including rubbly interflow zones, fissures, deflation areas, and massive, unjointed flow interiors. Within the active thickness of the SRPA, hydraulic properties are closely associated with the thickness of individual flows, number of interflow zones, and presence of sedimentary interbeds.

4.2.1.2.2 Sedimentary Interbeds—Sedimentary interbeds within the SRPA locally and regionally affect groundwater flow, because they occupy interflow zones and typically reduce the permeability of those zones. These units accumulated on the ancestral land surface of the ESRP for extended lengths of time between volcanic eruptions (Anderson and Liszewski 1997, p. 11). These units are as much as 50 ft thick and consist of well to poorly sorted fluvial, alluvial, and lacustrine clay, silt, sand, and gravel. During subsequent eruptive sequences, these units were covered by younger basalt flows. The continuing process of subsidence and concurrent aggradation gradually moved this sequence of basalt flows and sedimentary interbeds downward in the stratigraphic section. Groundwater flow and contaminant transport in the vicinity of the INEEL are controlled, in part, by the vertical and areal distribution of these sedimentary interbeds.

Deposition of sediments across the ESRP was contingent on the location of surface-water drainages. Surface-water flows from the Big Lost River basin have historically drained eastward and then northward onto the ESRP, because those stream flows were diverted by continuing rift-zone volcanic activity to the south (Arnett and Smith 2001). This extended period of drainage diversion resulted in

accumulation of numerous sedimentary interbeds within the stratigraphic sequence in the area identified as the BLT (Figure 4-5). Arnett and Smith (2001) note that numerous interbeds occur beneath the current channel and become less numerous and decrease in thickness away from the channel. Within the northern part of the area represented by the OU 10-08 model domain, extensive, thick, lacustrine sediments were deposited in ancestral Lake Terreton.

Many of the interbeds within the SRPA that have been identified in INEEL wells are of limited extent and cannot be correlated over large distances. Several interbeds are more areally distributed and might play an important role in subregional groundwater flow and contaminant migration. Two such extensive interbeds occur at TAN and in the INTEC vicinity.

A sedimentary interbed, identified by Anderson and Bowers (1995) as the QR interbed, occurs within the SRPA at TAN. Based on borehole data from at least 26 wells, this interbed is areally extensive and dips to the south. The QR interbed is considered to effectively restrict contaminants to the upper several hundred feet of saturation (Wymore et al. 2000).

The HI interbed identified by Anderson (1991) and overlying the I basalt flow group near INTEC is a key lithologic surface for the WAG 3 conceptual model (Arnett and Smith 2001). Arnett and Smith note that this interbed can affect groundwater flow locally. The HI interbed dips to the southeast from INTEC, where it thickens and is more continuous. Geophysical logs from the Special Excursion Power Reactor Test No. 4 well and Site-09 well (southeast of INTEC) indicate the HI interbed thickness can exceed 80 ft in some areas. The nature and thickness of the HI interbed and the vertical hydraulic gradient across the interbed indicate that it might control the vertical penetration of contaminants released near the surface of the aquifer at INTEC (DOE-ID 2000). The general effects of the HI interbed on groundwater flow and contaminant migration in the area represented by the OU 10-08 model domain are less significant than at the OU 3-13 model scale.

4.2.1.2.3 Volcanic Rift Zones—Rift zone features associated with tectonic extension on the ESRP might affect the movement of groundwater and contaminants. On the ESRP, rift zones have typically provided avenues for basaltic eruptions. Several southeast-trending volcanic rift zones occur within the OU 10-08 model domain (Kuntz et al. 1992). These rift zones include the Arco-Big Southern Butte volcanic rift zone and the Great Rift, both located southwest of the INEEL, and the Lava Ridge-Hells Half Acre rift zone (Figure 4-2). Each of these rift zones is characterized by numerous fissures, dikes, and past volcanic eruptions.

The distribution of numerous volcanic features associated with these rift zones might affect the distribution of hydraulic properties (Anderson et al. 1999). Areas near volcanic vents might provide localized, preferential pathways for groundwater flow. Dikes might impede flow and reduce the hydraulic conductivity (Meyer and Souza 1995; Hughes et al. 1997). Anderson and Liszewski (1997) note that hydraulic gradient changes in the vicinity of the Arco-Big Southern Butte volcanic rift zone might be associated with these features.

Arnett and Smith (2001) observe that volcanic rift zones in the area represented by the OU 10-08 model domain are perpendicular to the axis of the ESRP and might locally influence the direction of groundwater flow. Garabedian (1992) similarly notes that large-scale fractures in rift zones perpendicular to the axis of the ESRP might result in anisotropy of flow over broad areas.

At the facility scale, heterogeneities in the distribution of hydraulic properties associated with rift zone features might affect the distribution and migration of contaminants in groundwater. At TAN, the trichloroethene (TCE) contaminant plume in groundwater is oriented approximately 90^{o} from the southwest direction of subregional groundwater flow expected from water level data and approximately

parallel to the orientation of rift zone features (Hughes et al. 1997). Similarly, Kuntz et al. (2002) observe that low hydraulic conductivities and distortions in the distribution of strontium-90 concentrations in groundwater south of INTEC might be associated with a concealed rift zone feature. At the subregional scale, Anderson et al. (1999) suggest that the hydraulic complexities associated with rift zone features might affect the dispersion of tritium and other contaminants in groundwater.

4.2.1.2.4 Silicic Volcanic Features—Silicic volcanic features include four rhyolitic domes located along the southern INEEL boundary. These domes tower above the ESRP and have been identified as laccoliths (rhyolitic igneous intrusions with underlying dike-like feeders). Based on water level data, these features do not significantly modify the direction or gradient of groundwater flow. This apparent lack of effect on the groundwater flow field indicates that these intrusive features might, for the most part, lie above the water table (with the exception of the feeder dikes). However, the limited extent of water level data near these features and the relatively large permeability of basalts in the SRPA might preclude evaluation of subtle changes in gradient.

Based on temperature contours (Figure 4-11), groundwater temperatures are elevated in proximity to these silicic volcanic features. Elevated temperatures near the intrusive features might indicate that groundwater flow is impeded locally or that heat flow is sufficient locally to modify the heat capacity of the groundwater flow system. These elevated temperatures are particularly apparent near Middle and East buttes. In the vicinity of Big Southern Butte, temperature variations likely are masked by an influx of cold water from the INEEL spreading areas and by limited deep-well temperature data.

4.2.1.3 Known Aquifer Hydraulic Properties. Hydraulic properties of the SRPA include its capability to transmit and store water. The subsections below describe hydraulic properties of the SRPA. Table 4-1 summarizes these properties.

4.2.1.3.1 Capability of the SRPA to Transmit Water—Water moves through the basaltic SRPA primarily within the highly permeable interflow zones between basalt flows. The capability of the SRPA to transmit water is defined by the horizontal and vertical hydraulic conductivity and is measured in this report in feet per day (ft/day).

4.2.1.3.1.1 Horizontal Hydraulic Conductivity—Horizontal hydraulic conductivity is typically estimated from aquifer tests conducted in wells. Single-well aquifer tests were conducted in 114 SRPA wells at and near the INEEL. These tests resulted in a six order-of-magnitude range of hydraulic conductivity (1.0×10^{-2} to 3.2×10^{4} ft/day) for basalt and interbedded sediment (Table 4-1) (Ackerman 1991; Anderson et al. 1999). This range of hydraulic conductivity is a bulk property that is attributed mainly to the physical characteristics and distribution of basalt flows and related volcanic features.

Anderson et al. (1999) identified three broad categories of hydraulic conductivity corresponding to six general types of geologic controls that can be inferred from the distribution of wells and vent corridors. The geologic controls defining Category 1 correspond to the contacts, rubble zones, and cooling fractures of thin, tube-fed, pahoehoe flows and the numerous voids present in shelly pahoehoe and slab pahoehoe flows and bedded scoria, spatter, and ash near volcanic vents. Hydraulic conductivity estimates for Category 1 basalts range from 1.0×10^{2} to 3.2×10^{4} ft/day. Estimates greater than 100 ft/day are principally associated with interflow zones of thin flows. Smaller estimates locally might be associated with postulated dikes or dike swarms. The geologic controls defining Category 2 correspond to relatively thick, tube-fed, pahoehoe flows that might be ponded in topographic depressions and to thin, tube-fed, pahoehoe flows cut by discontinuous dikes. Hydraulic conductivity estimates for Category 2 basalts range from 1.0×10^{0} to 1.0×10^{2} ft/day. The geologic controls defining Category 3 correspond to

localized dike swarms and thick, tube-fed, pahoehoe flows cut by discontinuous dikes. Hydraulic conductivity estimates for Category 3 basalts range from 1.0×10^{-2} to 1.0×10^{0} ft/day.

Table 4-1. Summary of intrinsic hydraulic properties and groundwater flow parameters of the SRPA in the OU 10-08 model domain.

Property	Value/Range	Source
Horizontal hydraulic conductivity (ft/day)	1.0×10^{-2} to 3.2×10^{4}	Anderson et al. (1999)
Vertical hydraulic conductivity (ft/day)	0.001	K_v of sediments from Mann (1986)
Total porosity (dimensionless)	0.06 to 0.37	Johnson (1965) (laboratory tests)
Effective porosity (n_e) (dimensionless)	0.04 to 0.22	Johnson (1965) (laboratory tests)
	0.05 to 0.25	Ackerman et al.[a]
	0.03 to 0.05	Arnett and Smith (2001)
	0.001 to 0.02	Arnett (2003)
Horizontal hydraulic gradient (ft/mi)	<5 to 25	Barraclough et al. (1966) 1999 potentiometric map (Figure 4-15)
Vertical hydraulic gradient (ft/ft)	0.071	Upward gradient measured in INEL-1, Mann (1986)
Horizontal flow velocity (ft/day)	<6 to 17	Based on travel times from Ackerman (1995)
	5 to 20	Robertson et al. (1974)
	4 to 5	Barraclough et al. (1981)
	At least 6	Mann and Beasley (1994)
	At least 10	Cecil et al. (2000)
	0.07 to 0.49	Arnett (2002)

a. Ackerman, D. J., S. R. Anderson, L. C. Davis, B. R. Orr, G. W. Rattray, and J. P. Rousseau, 2001, *A Conceptual Model of Flow in the Snake River Plain Aquifer at and near the Idaho National Engineering and Environmental Laboratory with Implications for Contaminant Transport*, U.S. Geological Survey Draft Report.

The thick, tube-fed, basalt flows included in Category 2 and 3 hydraulic conductivity ranges are typically unfractured with few interflow zones. The hydraulic conductivity of Category 2 and 3 thick, tube-fed, basalt flows is difficult to evaluate, because few estimates are available (Anderson et al. 1999). Measurements are important, because these basalts might occur within the active part of the SRPA.

In addition, observed increases in the cumulative thickness of sedimentary interbeds related to the coalescing depocenters of the Big Lost River, the Little Lost River, Birch Creek, Camas Creek, and Mud Lake (BLT) (Figure 4-5) might affect the capability of the SRPA to transmit water. In places where sedimentary interbeds occupy interflow zones, permeability might be decreased. Elsewhere, the high permeability of the interflow zones might be retained.

The hydraulic conductivity of rocks below the active thickness of the aquifer is considered to be significantly smaller than that of the rocks within the aquifer. Mann (1986) noted that the hydraulic conductivity of rocks in the interval from 200 to 800 ft generally ranged from 1 to 100 ft/day. The

hydraulic conductivity of rocks below a depth of 1,500 ft in well INEL-1 ranged from 0.002 to 0.03 ft/day, from two to five orders of magnitude smaller.

4.2.1.3.1.2 Vertical Hydraulic Conductivity—Vertical hydraulic conductivity of the active SRPA is considered to be much smaller than horizontal conductivity because of the layered character of basalts, relatively horizontal deposition of sedimentary interbeds, and preferential flow in the horizontally to subhorizontally oriented interflow zones (Garabedian 1992). Frederick and Johnson (1996) noted that the vertical hydraulic conductivity of the SRPA is substantially less than the horizontal hydraulic conductivity. Mann (1986) estimated that the vertical hydraulic conductivity of sediments in the upper section of well INEL-1 is on the order of 0.001 ft/day.

4.2.1.3.2 Capability of the SRPA to Store Water—The capability of the aquifer to store water is measured by the storage coefficient (storativity), a unitless parameter defined as the volume of water that an aquifer takes into storage or releases from storage per unit aquifer surface area per unit change in hydraulic head. The unconfined storage coefficient represents changes in storage in an unconfined (water-table) aquifer and is derived from the volume of drainage of water from the aquifer. The confined storage coefficient represents changes in storage in a confined (artesian) aquifer and is derived primarily from the compressibility of water. Robertson (1974) estimated the unconfined storage coefficient of the SRPA to be 0.10. The total porosity is the void space in a rock volume divided by the total rock volume. The effective porosity is a measure of the volume of interconnected voids divided by the rock volume. Laboratory determinations of total and effective porosity made from basalt cores at the INEEL ranged from 0.06 to 0.37 and 0.04 to 0.22, respectively (Johnson 1965). The unconfined storage coefficient in the SRPA essentially is represented by the specific yield, because most of the water is released from gravity drainage and very little water is released from aquifer compression and expansion of water. The specific yield is a measure of the amount of water that drains from gravity from interconnected voids. In the current USGS conceptual model of the INEEL subregion, the specific yield of fractured basalt is estimated to range from 0.05 to 0.25. The specific yield of dense basalt is probably at the lower end of this range.[a] Facility-scale investigations at the INEEL indicate that the average specific yield of the SRPA ranges from less than 3 to 5%.

Johnson and Frederick (1997), in an analysis of straddle-packer aquifer tests in four wells near INTEC, noted that the aquifer at depth responds immediately to short-term pumpage as a confined system with subsequent delayed vertical leakage from underlying and overlying units. The composite storativity of this local system was estimated to be 7×10^{-6} (Frederick and Johnson 1996). Leaky confined responses to groundwater stresses at depth in the OU 10-08 model domain are attributed to the presence of massive, low-permeability basalts and, in some places, extensive sedimentary deposits within the SRPA.

4.2.2 Inflows and Outflows

Major components of groundwater inflow to the area represented by the OU 10-08 model domain include regional underflow across the northeast boundary of the area, tributary basin underflow, recharge from precipitation, infiltration from surface-water features, and groundwater flow across the base of the aquifer. Outflow occurs primarily from underflow across the southwestern boundary of the area. Table 4-2 summarizes inflow and outflow components.

4.2.2.1 Recharge from Regional Underflow. Regional underflow into the area represented by the OU 10-08 conceptual model is derived from the northern part of the ESRP (Arnett and Smith 2001). This underflow is based on groundwater flux that was estimated from a numerical modeling study (Spinazola 1994). Spinazola estimated underflow to the southwest out of the Mud Lake subregion to be 938,000 acre-ft/year (1,298 cubic feet per second [cfs]) (Table 4-2).

Table 4-2. Summary of inflows and outflows to the SRPA in the OU 10-08 model domain.

Flow Component		Value (cfs)	Reference
Inflows			
Regional underflow into the model domain		1,298	Spinazola (1994)
Tributary basin underflow	Northern streams	40–80	Garabedian (1992), Arnett and Smith (2001)
	Birch Creek valley	80–140	Garabedian (1992), Arnett and Smith (2001)
	Little Lost River valley	160–270	Garabedian (1992), Arnett and Smith (2001)
	Big Lost River valley	315–535	Garabedian (1992), Arnett and Smith (2001)
Infiltration of areal precipitation		30–100	Extrapolated from Cecil et al. (1992)
Infiltration of stream flow	Big Lost River[a]	97	USGS stream flow records (1946–present)
Inflow from underlying rocks		67	Extrapolated from Mann (1986)
Wastewater disposal (ponds, wells)[b]		—	
Outflows			
Regional underflow out of the model domain		2,000–3,000[c]	
Groundwater pumpage	INEEL[b]	—	
	Non-INEEL[d]	—	

a. Infiltration from other streams is combined with underflow estimates. The Big Lost River estimate includes spreading areas.

b. Disposal of wastewater to infiltration ponds approximately compensated by INEEL pumpage.

c. Estimated from summation of inflows.

d. Partially compensated by infiltration of applied irrigation water.

4.2.2.2 Recharge from Tributary Underflow. The SRPA is recharged along the northwestern edge by groundwater underflow from tributary valley aquifers. A limited amount of recharge might also enter the SRPA as direct runoff from the mountain ranges. Underflow estimates reported by Garabedian (1992) were used in the 1994 WAG 10 model. Careful review of the basin-yield analyses for the Big and Little Lost rivers results in an uncertainty of about 25% and perhaps more for tributary basin estimates.

The earlier WAG 10 model (McCarthy et al. 1995) incorporated underflows estimated by Garabedian (1992). WAG 10 conceptual modeling activities have included a review of various sources of tributary underflow estimates (Arnett and Smith 2001). This review concluded that Garabedian's (1992) estimates are reasonable, with an uncertainty of about 25%, and that the average underflows range from 315 to 535 cfs for the Big Lost River basin, 160 to 270 cfs for the Little Lost River, and 80 to 140 cfs for Birch Creek (Table 4-3). The WAG 10 conceptual model also includes underflow estimates of 40 to 70 cfs for Medicine Lodge Creek. Table 4-3 tabulates Garabedian's tributary underflow estimates and a range of estimates using an uncertainty of 25%.

Table 4-3. Proposed range of mean tributary underflow rates.

Basin Name	Garabedian's (1992) Estimate of Mean Underflow (cfs)	Estimated Mean Underflow Range (cfs)
Big Lost River	408	315–535
Little Lost River	214	160–270
Birch Creek	108	80–140
Warm Springs and Deep creeks	42	31–53
Medicine Lodge Creek	13	9–17

4.2.2.3 Recharge from Precipitation on the ESRP. The average precipitation at the INEEL portion of the ESRP is approximately 8 in./year. Precipitation largely occurs as winter snowfall. Much of this precipitation is returned to the atmosphere by evaporation and plant transpiration. The terrain over most of the area represented by the OU 10-08 model domain is poorly drained, with few well-developed stream channels. Locally, water from snowmelt and intermittent rainfall flows to low areas, forms ponds, and infiltrates as locally focused recharge.

Net recharge to the aquifer from direct precipitation was estimated from chlorine-36 and tritium data to be 2 to 5% of average annual precipitation, ranging from 0.012 to 0.036 ft/year at the INEEL (Cecil et al. 1992). This estimated range of infiltration from direct precipitation might provide a diffuse contribution to the groundwater system of approximately 200 to 600 cfs over the entire area represented by the 3,000-mi^2 OU 10-08 model domain (Table 4-3). This source of recharge, because it is distributed over the entire area, does not significantly affect local groundwater flow and contaminant migration in the SRPA.

The estimates from Cecil et al (1992) are based on a vegetated site with a thick soil profile over the underlying basalt. In locations where basalt or gravels are exposed at land surface, the infiltration is likely greater because of more rapid infiltration and less chance for subsequent evaporation to remove water held in storage near the surface. This infiltration rate could approach the annual average precipitation. This likelihood is addressed below as a sensitivity issue.

4.2.2.4 Recharge from Surface Water. The Snake River and its main-stem tributaries do not directly affect transient groundwater flow in the area represented by the OU 10-08 model domain, but the river and its tributaries do collectively act as the most significant single surface-water feature on the ESRP and provide the regional context for flow in the SRPA. Surface-water features that are pertinent to the OU 10-08 conceptual model area consist of the streams that flow onto the ESRP on or near the INEEL and those that directly affect the subregional water budget.

4.2.2.4.1 Snake River and its Direct Tributaries—The Snake River includes the Henry's Fork and South Fork. The Henry's Fork flows onto the ESRP from the Island Park Caldera. The South Fork originates in Wyoming and flows onto the ESRP from the Basin and Range mountains to the east. The two streams join north of Idaho Falls, Idaho, and the Snake River continues to the southwest and west along the southeast margin of the ESRP. The Snake River leaves the ESRP at King Hill.

The Snake River and its associated reservoirs and irrigation systems are the principal sources of recharge to the SRPA. Historically, development of the reservoir system and changes in irrigation application have affected regional water levels. Before the early 1900s, recharge to the SRPA was seasonal, occurring primarily in response to spring runoff cycles. With the development of reservoir systems, runoff and recharge were attenuated throughout the year. Development of an extensive network

of leaky irrigation canals and expanded flood-irrigation practices throughout the first half of the 20th century increased net recharge, raised regional groundwater water levels, and increased regional discharge to large springs near Twin Falls, Idaho. During the second half of the 20th century, regional groundwater levels began to decline in response to changes in irrigation practices, including lined canals to minimize leakage, development of irrigation wells, and introduction of sprinkler irrigation. All of these factors have affected long-term water level changes in the area represented by the OU 10-08 model domain.

4.2.2.4.2 Streams Pertinent to the INEEL—The part of the ESRP that includes the INEEL is a closed topographic drainage, with all streams terminating in playas and sinks. Stream flow onto the area represented by the OU 10-08 model domain is ephemeral and derived primarily from precipitation on the mountains and valleys to the north and northwest. Streams contributing surface water to the north and east of the INEEL consist of Beaver Creek, Camas Creek, Medicine Lodge Creek, Deep Creek, and Warm Springs Creek (Figure 4-9). Birch Creek and the Big Lost River intermittently flow onto the INEEL. The Little Lost River flows toward the INEEL but infiltrates into the ground before reaching the INEEL boundary. Figure 4-9 shows the locations of selected USGS stream flow gaging stations with at least 10 years of stream flow record beyond 1970. Records from these stations allow estimates of the mean annual flow and the range of annual flow in the tributaries.

Beaver and Camas creeks converge at the northeastern boundary of the OU 10-08 area at Camas, Idaho, to discharge into Mud Lake northeast and upgradient of the INEEL. Infiltration from these streams is taken into account in regional underflow estimates obtained from Spinazola's (1994) numerical modeling study of the Mud Lake area. Medicine Lodge Creek, Warm Springs Creek, and Deep Creek drain into the area northeast of the INEEL boundary. Their flows are included in tributary basin underflow estimates (Table 4-3).

4.2.2.4.2.1 Birch Creek—The drainage area for Birch Creek where it enters the ESRP exceeds 400 mi^2. Stream flows in Birch Creek are largely sustained by spring flows in the upper reaches. Historic stream flow data are available for two stream gaging stations operated by the USGS on Birch Creek (http://nwis.waterdata.usgs.gov/id/nwis/). Average flow for Birch Creek near Blue Dome (period of record April 1967 to March 1991) was 74 cfs. This gaging station monitors discharge from a 380-mi^2 area. Average flow for Birch Creek at Eight Mile Canyon Road (period of record June 1967 through December 1987) was 56 cfs (400-mi^2 area). This station was located approximately 9 mi upstream from the point that Birch Creek flows onto the ESRP.

Most stream flow in Birch Creek is diverted near the point where it flows onto the ESRP; this diverted water flows to an electrical power plant located at the southern extent of the Beaverhead Mountains. Wastewater from this plant is discharged to a canal that drains back onto the northern part of the INEEL. Most of this diverted water infiltrates along the canal. Because of diversions and unknown channel losses downstream from historic gaging stations, estimated stream flow contributions from Birch Creek to the SRPA are combined with estimates of tributary underflow, as described in Subsection 4.2.2.2.

4.2.2.4.2.2 Little Lost River—The Little Lost River has a contributing drainage area in the Lost River and Lemhi ranges of 703 mi^2. The average discharge for the gaging station near Howe (Figure 4-9) was 77 cfs for 44 years of record (1941 through 1989) (http://nwis.waterdata.usgs.gov/id/nwis/). Average annual flow during this period ranged from 49 to 106 cfs. All flow in the river is diverted or infiltrates before reaching the ESRP. Stream flow contributions to the SRPA are included in tributary underflow estimates (Subsection 4.2.2.2).

4.2.2.4.2.3 Big Lost River—Stream flow data are available for nine USGS gaging stations on the Big Lost River (Figure 4-9) (http://nwis.waterdata.usgs.gov/id/nwis/). The gaging station for the Big Lost River near Arco, Idaho, monitors flow onto the ESRP. The contributing drainage basin for this station encompasses 1,410 mi^2 of mountainous terrain of the Lost River and Pioneer ranges. The river flows ephemerally southeast onto the ESRP from Arco onto the INEEL. The river then flows to the northeast, terminating at playas east of Howe and south of TAN. Major features include the INEEL diversion and spreading areas near the RWMC, the Big Lost River Sinks north of the Naval Reactors Facility, and the playas.

The Big Lost River flows onto the ESRP during periods of high runoff. Flow typically occurs during the spring and early summer but has been known to continue into the fall. At other times, the stream channel characteristically is dry. During periods of low precipitation, little or no flow is in these reaches throughout the entire year.

Stream flow data from a series of stream gaging stations on the Big Lost River provide long-term information about channel losses and stream flow contributions to the SRPA from the river and from diversions to the INEEL spreading areas (http://nwis.waterdata.usgs.gov/id/nwis/). Much of the water from these flows infiltrates rapidly with some losses to evaporation or plant transpiration.

The average flow in the Big Lost River at Arco for the 48-year period of record (1946 through 1960, 1967 through 1979, and 1983 to the present) is 97 cfs (Table 4-3). The maximum annual average flow was 488 cfs in 1984; annual flow was zero from 1989 though 1992 and 2001 through 2003. Flow in the Big Lost River was increased for several years after the Borah Peak earthquake of October 1983 (Figure 4-14). These increased flows provided substantial recharge along the channel of the Big Lost River, spreading areas, Big Lost Sinks, and terminal playas. This recharge resulted in elevated water levels in proximity to those surface-water features.

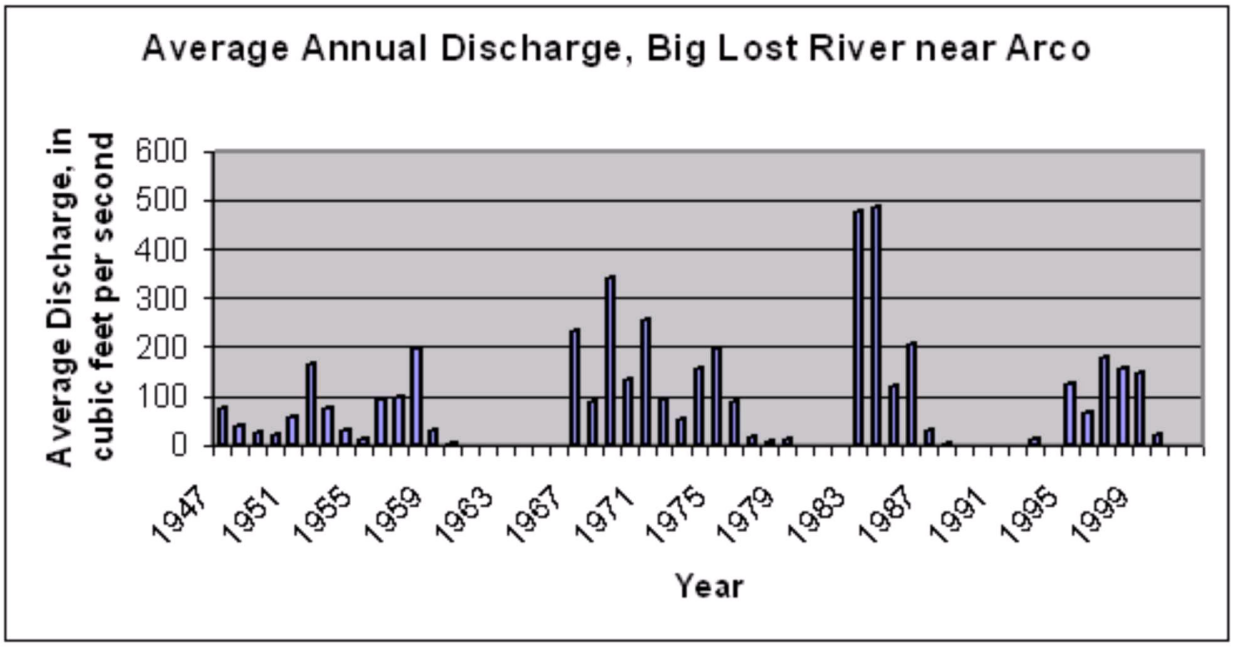

Figure 4-14. Average annual discharge for the Big Lost River near Arco, 1947 through 2002.

Bennett (1990) conducted a seepage study on the Big Lost River to evaluate channel infiltration losses. In this study, losses from Arco to the Big Lost River Sinks generally ranged from 1 to 2 cfs/channel mile at stream flows less than 100 cfs. Within the Big Lost River Sinks, channel losses increased to 7 to 12 cfs/channel mile. Channel losses also increased with discharge. A measured channel loss of 28 cfs/channel mile was measured in the Big Lost River Sinks at a discharge of 372 cfs.

4.2.2.5 Recharge across the Base of the Aquifer. Arnett and Smith (2001) noted that the hydraulic conductivity at the base of the aquifer is greatly reduced compared to the overlying aquifer. This reduction in hydraulic conductivity probably restricts aquifer recharge from deeper rocks. A small upward flow probably occurs across the bottom of the aquifer. Locally, these flows might be larger, as evidenced by higher temperatures. Geochemical evidence for upwelling deep thermal waters includes diagenetic phases in well cores and high heat flows (McLing et al. 2001). This evidence is supported by the absence of geothermal springs on the ESRP and the large number of geothermal springs around its periphery.

In the INEL-1 test hole, the hydraulic head increased with depth across the estimated base of the aquifer. If conditions observed in the INEL-1 test hole persist over the OU 10-08 model domain, the deep, low-permeability rocks might contribute an upward component of flow to the SRPA (Mann 1986). Mann estimated a flow of approximately 20 cfs across the INEEL. This rate of upward flow, if extended to the 3,000-mi^2 OU 10-08 model domain, would be about 67 cfs (Table 4-2).

4.2.2.6 Regional Underflow out of the Area Represented by the OU 10-08 Model Domain. No direct measurement of underflow out of the area represented by the OU 10-08 model domain exists. The range of underflow is estimated from cumulative inflows minus cumulative outflows to be approximately 2,000 to 3,000 cfs, depending on the uncertainties associated with the water budget (Table 4-3). Available information about underflow out of the area is restricted to limited water level data from a few wells because of the large depth to water.

4.2.2.7 Other Inflows and Outflows. Other outflows from the area represented by the OU 10-08 model domain include groundwater pumpage for irrigation and water supply. Inflows include recharge from infiltrating irrigation water and wastewater disposal. Pumping withdrawals for irrigation that occurs northeast of the INEEL are included in underflow estimates from Spinazola (1994), or are partially balanced by infiltrating applied irrigation water, and are far enough from areas of interest at the INEEL that their effect on contaminant migration is insignificant. Withdrawals from INEEL production wells are nearly balanced by local disposal to infiltration ponds.

4.2.3 Characteristics of the Field of Flow

The distribution of groundwater flow is determined by the characteristics of the geohydrologic framework and groundwater inflows and outflows to the system. The following subsections describe horizontal and vertical groundwater flow within the area represented by the OU 10-08 model domain, temporal changes in the groundwater flow field, and the response of the conceptual model of the groundwater flow system to stresses.

4.2.3.1 Horizontal Groundwater Flow. Groundwater flow within the SRPA is predominantly horizontal. Horizontal groundwater flow is defined by the distribution of hydraulic head, the gradient and groundwater flow direction, and the estimated flow velocity.

4.2.3.1.1 Distribution of Hydraulic Head, Gradient, and Direction of Groundwater Flow—A potentiometric map of the OU 10-08 model domain was constructed using June 2004 water level data (Figure 4-15). The June 2004 data set is thorough and represents a good choice

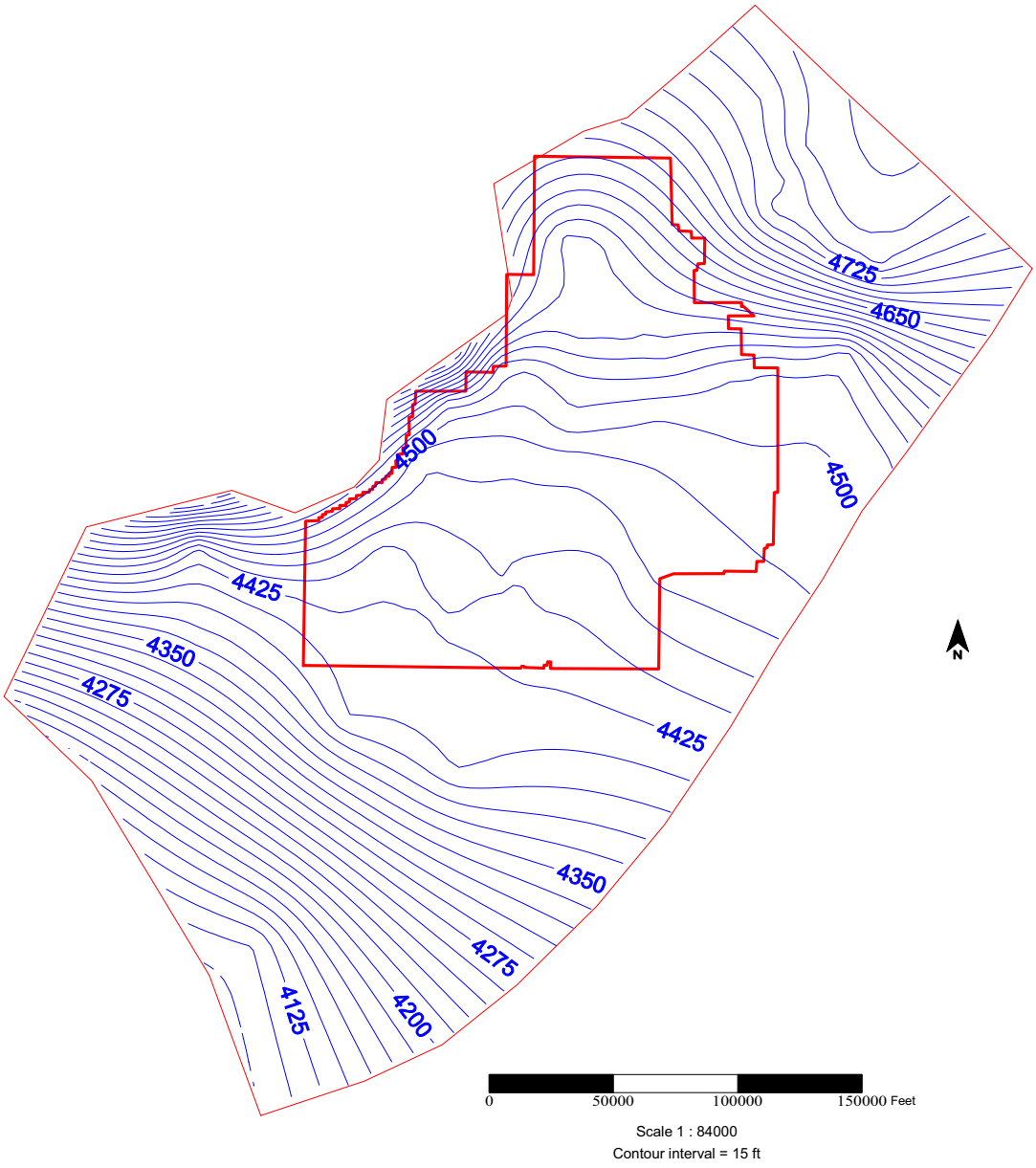

Figure 4-15. Water table elevations and contours for June 2004 within the OU 10-08 model domain.

for use in this model. Ideally, water table contour maps are developed from data that have been collected during the same timeframe. The June 2004 data set includes water levels from 237 aquifer wells measured from June 7 through June 10, 2004. Flow lines constructed on the potentiometric surface show that flow is generally from the northeast to the southwest across the model domain.

To the north of the INEEL, groundwater flow is to the west at a gradient of about 25 ft/mi, with a southeastward component of flow originating from Birch Creek underflow (Figure 4-15). East of TAN, groundwater flow generally is to the south, again at a gradient of about 25 ft/mi. Steep gradients are attributed to the presence of sediments deposited from ancestral Lake Terreton. In the vicinity of TAN, groundwater flow is generally to the south, and the hydraulic gradient is about 8 ft/mi.

Groundwater flow across most of the INEEL south of TAN is generally to the southwest, with gradients less than 5 ft/mi (Figure 4-15). The relatively flat regional gradient locally shows some variation, as is expected in a complex fractured rock system. Steeper gradients and some southward groundwater flow across the central part of the INEEL are attributed to reduced permeability resulting from the occurrence of sedimentary interbeds in the area of the BLT and to groundwater flow contributions from tributary underflow of the Little Lost River valley.

South of the INEEL, groundwater flow is to the southwest, and the hydraulic gradient is approximately 10 ft/mi (Figure 4-15). This steepening hydraulic gradient is attributed to decreasing permeability associated with volcanic features of the Arco Rift (Figure 4-2). An apparent steep hydraulic gradient is present in the vicinity of Arco, west of the INEEL, where relatively shallow tributary groundwater flow in the Big Lost River valley alluvium joins the deeper SRPA.

4.2.3.1.2 Estimates of Groundwater Flow Velocity—Ackerman (1995) applied a particle-tracking technique to Garabedian's (1992) regional numerical groundwater flow model. In this study, estimated travel times for particles originating from the OU 10-08 model domain to regional points of discharge ranged from 100 to more than 300 years. Based on these regional estimates, the average velocity along flow paths that extend across the model domain could range from less than 6 ft/day to as much as 17 ft/day.

Tracer studies conducted by Robertson et al. (1974) indicated that groundwater flow velocity at the INEEL ranges from 5 to 20 ft/day. Barraclough et al. (1981) used tritium concentration changes in groundwater to estimate a flow velocity of 4 to 5 ft/day. Mann and Beasley (1994) estimated groundwater flow velocity using first-arrival detections of iodine-129. The average groundwater velocity calculated from these data was at least 6 ft/day. Cecil et al. (2000) used chlorine-36 first-arrival times in wells south of the INEEL to estimate a groundwater flow velocity of at least 10 ft/day, while Wymore et al. (2000) reported groundwater velocities, determined from tracer tests at TAN, of less than 0.5 ft/day. Diverse estimates of velocity support the concept of preferential flow and heterogeneities associated with changes in basalt flow thickness, number of interflow zones, presence of sedimentary interbeds, and proximity to volcanic rift zone features.

Recent geochemical studies have indicated that groundwater flow might occur preferentially across the OU 10-08 model domain. Luo et al. (2000) used uranium and thorium decay disequilibria to model migration of radionuclides within the SRPA. Transit times ranged from approximately one year in the northern part of the INEEL to approximately 100 years in the central part of the INEEL. Roback et al. (2001) used isotopic composition and concentration of uranium and strontium to evaluate geochemical evolution and flow pathways in the SRPA. Johnson et al. (2000) evaluated preferential flow using radiogenic isotope ratios in groundwater. These studies indicated the occurrence of narrow channels of preferential flow across the INEEL.

4.2.3.2 Vertical Groundwater Flow. Hydraulic head increases with depth throughout most of the area represented by the OU 10-08 model domain. However, the occurrence of massive, unfractured basalt-flow interiors and sedimentary interbeds restricts significant vertical movement of water. Groundwater flow takes place predominantly through the horizontally to subhorizontally oriented interflow rubble zones between basalt flows.

4.2.3.3 Temporal Changes in the Flow Field. The field of groundwater flow in the area represented by the OU 10-08 model domain is affected by short-, intermediate-, and long-term stresses. Short-term stresses include production-well pumping cycles, episodic recharge from local streams, changes in wastewater disposal practices, and seasonal meteorological changes and irrigation of farmland; the effect of these stresses on groundwater levels is typically on the order of days to months. Intermediate-term stresses include climatological cycles. The effect of these stresses is typically on the order of several years. Long-term stresses include effects on water levels from regional changes in water use (irrigation practices), and the effects are typically observed over much longer periods (decades).

Figure 4-16 shows water level hydrographs for two INEEL wells near the mouth of the Big Lost River tributary stream basin from 1970 through 2000. Short-term stresses are reflected in these wells as small water level fluctuations (less than 1 ft). Intermediate-term drought cycles are reflected in these wells as approximately 14-year fluctuations with water level fluctuations of less than 10 ft. Long-term cycles are reflected in the continually declining low water level of the drought cycle (seen in 1981 and 1994).

Hydrologic conditions in 1980 are considered to have been relatively stable, with minimal intermediate- and short-term stresses and fluctuations in groundwater levels. The period from 1983 through 1985 is considered to be a time of large stress to the SRPA, with significant recharge from water released from storage by the Borah Peak earthquake and substantial runoff from snowmelt. The period from 1986 through 1994 was characterized by minimal stream flow onto the ESRP and continuing intermediate-term water level declines in response to decreased recharge and pumping overdraft. The period from 1995 through 1999 was characterized by increased precipitation as snow and rain, subsequent runoff and recharge, and gradually increasing groundwater levels. Since 1999, drought conditions have prevailed, recharge has been minimal, and regional groundwater levels have gradually declined.

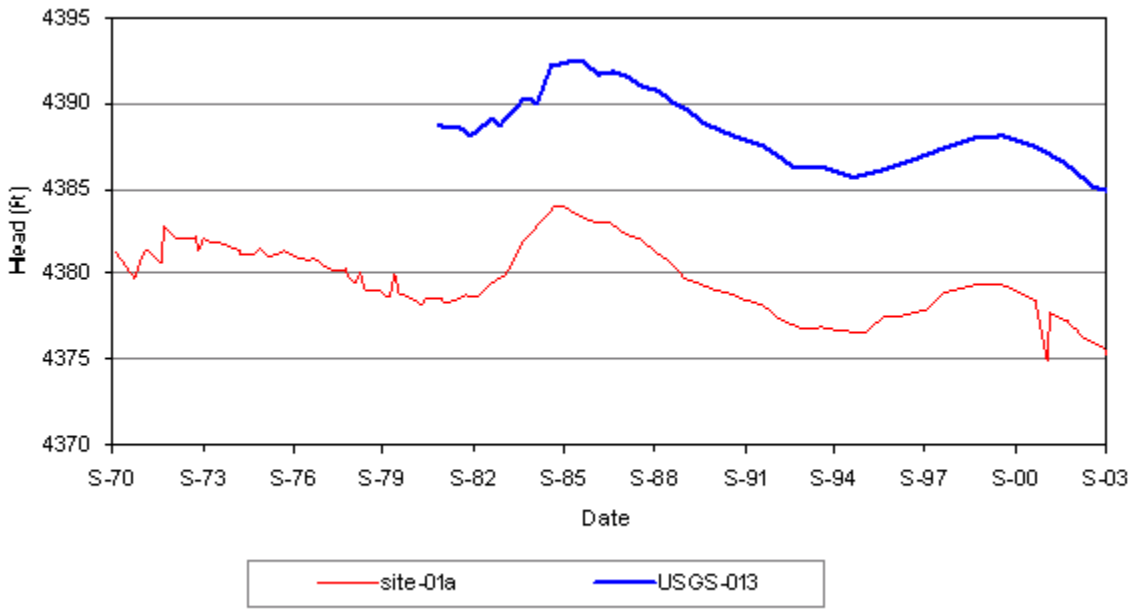

Figure 4-16. Water level changes in three USGS monitoring wells located near the mouth of the Big Lost River.

4.2.3.4 *Groundwater Flow System Response to Stresses.*

At the scale of the SRPA, researchers consider that groundwater flow is laminar and the Darcian flow is applicable (Garabedian 1992). At the scale of the INEEL, water level responses to large-scale stresses indicate that flow through the fractured SRPA behaves as flow through an effective porous medium. At more local scales, hydraulic gradient studies (Rohe 2002) indicate that response from the hydrologic system might be dominated by fracture flow at scales less than 7 mi.

Frederick and Johnson (1996) noted that the SRPA, at depth, might respond to stresses as a leaky confined system, with contributions to flow in individual fracture zones from both above and beneath. This leaky confined response is attributed to the layered system of highly permeable interflow zones, massive low-permeability flow interiors, and sedimentary interbeds.

The groundwater flow system at the subregional scale is affected by heterogeneous distribution of hydraulic properties. These heterogeneities are attributed to complexities associated with thickness and extent of individual flows, distance from eruptive vents, thickness and extent of interbeds, and volcanic rift zone features.

4.3 Geochemistry

4.3.1 Natural Geochemistry

Since the earliest studies of the SRPA, researchers have recognized that temperature and the chemical signature of groundwater are useful tools that can be combined with other hydrologic information to evaluate the aquifer flow system (Olmsted 1965; Nace et al. 1956). In 1997, a series of investigations was conducted in and around the INEEL to characterize groundwater flow in the context of the regional geologic framework. These studies evaluated subsurface temperature distribution to define the active aquifer thickness, and they utilized natural isotope chemistry to delineate groundwater flow paths. These studies demonstrated that areas of the ESRP are characterized by major geothermal input from depth. Temperature data also allowed a determination of aquifer thickness variations and helped in tracing plumes of cold, rapidly moving recharge water across the INEEL. Groundwater isotope signatures revealed that isotope ratios persist southward from the mouths of Birch Creek and the Little Lost River. These features have been interpreted as zones of preferential flow adjoined by zones of slower flow.

4.3.1.1 *Recharge and Aquifer Source Water.*

Regionally, water in the SRPA flows southwest beneath the INEEL from the Yellowstone Plateau on the northeast (Wood and Low 1986). Because of the INEEL's proximity to the northern boundary of the ESRP, a number of sources and types of water contribute recharge to the system. While most of the water in the SRPA has its origins in the highlands proximal to the Yellowstone Plateau, the drainage basins to the north and west of the INEEL contribute significantly to the water budget at the INEEL (Table 4-3). These sources include infiltrated irrigation water and tributary contributions from the Big Lost River valley, the Little Lost River valley, the Birch Creek valley, the Mud Lake basin, and the Crooked Creek basin. Another possible source of water for the SRPA at the INEEL is from upwelling of thermal water emanating from deep in the ESRP (McLing et al. 2001; Mann 1986). These recharge waters can be used as natural tracers to elucidate regional groundwater flow because of their distinct chemical and isotopic signature.

4.3.1.2 *Tracer Studies.*

Beginning in 1997, a series of studies was undertaken to characterize the geochemistry of the SRPA beneath the INEEL. The studies addressed the primary concern that long-range (tens to hundreds of miles) "fast flow paths" (interconnected zones of high conductivity in the SRPA at the INEEL) might occur and could transport contaminants downgradient faster than expected. These studies used chemical (i.e., isotopes, cation, and anions) and other (temperature) tracers to identify potential flow corridors within the SRPA.

4.3.1.2.1 Isotope Tracers—Naturally occurring chemical isotopes were derived from recharge areas. These isotopes were used to evaluate flow in the SRPA. They included isotopes of uranium, thorium, and strontium.

***4.3.1.2.1.1 Uranium* Isotopes—**Isotopes of heavy elements such as those in the uranium series can be powerful tools to evaluate in situ physical, chemical, geologic, and hydrologic variables of groundwater flow systems. Because of the high atomic mass of these elements, they do not fractionate in groundwater. To avoid any anthropogenic influences, the ratio of uranium-234 to uranium-238 is used to track groundwater flow. These isotopes are very useful, because the ratio of uranium-234/uranium-238 is generally close to the secular equilibrium value of 5.49×10^{-5} (54.9 parts per million) in rocks older than a few hundred thousand years. However, in recently recharged groundwater, uranium-234 is typically enriched relative to uranium-238 by factors most commonly ranging from 1.5 to 10 because of preferential dissolution of uranium-234 from crystallographic defects created by alpha recoil and because of direct injection of uranium-234 into groundwater by recoil (Osmond and Cowart 1992). Variations of uranium-234/-238 in short-residence (tens of years to 200 years) waters such as those in the SRPA reflect the competing effects of aquifer resident time and host rock dissolution. The longer that recharged water with an elevated uranium-234/-238 ratio is in contact with the aquifer host rock the more equilibrated (in secular equilibrium) the water becomes.

4.3.1.2.1.2 Strontium-87/-86 Ratios—Strontium-87/-86 and uranium-234/-238 ratios in groundwater reflect the water-rock reaction histories and flow pathways. Groundwater strontium-87/-86 ratios are inherited from soil or rock through which the water passes. Both strontium-87 and strontium-86 are stable isotopes, but because strontium-87 is produced by radioactive decay of rubidium-87 ($t_{1/2} = 4.8 \times 10^{10}$ y), the strontium-87/-86 ratios of rocks and soils depend on their original rubidium concentrations and their ages. Strontium isotopes are useful as groundwater tracers in systems such as the SRPA, because the rock types in the recharge regions are dramatically different from those in the aquifer. In this case, the strontium isotope ratio inherited from the recharge region will evolve toward isotopic equilibrium with the aquifer host rock. The rate at which this equilibration occurs is largely a function of the amount of time that the groundwater is in contact with the aquifer host rock. Therefore, the groundwater entering the SRPA can be tracked as it moves through the aquifer system.

4.3.1.2.1.3 Isotope-delineated Flow Paths—Contour plots of uranium and strontium isotope ratios (Figure 4-17) show that water entering the SRPA from the river valleys to the north have high strontium-87/-86 (>0.71100) and high uranium-234/-238 (>160 parts per million) values. Water entering the SRPA from the Birch Creek and Little Lost River valleys to the north has high strontium-87/-86 (>0.71100) and high uranium-234/-238 (160 parts per million) relative to waters originating east of the INEEL. Recharge waters with distinct high isotope ratios persist 12 to 19 mi into the SRPA (Figure 4-17) along zones of preferential flow. In contrast, two zones at the INEEL have relatively low strontium-87/-86 and uranium-234/-238; one of these is in the center of the INEEL near the toe of the Lemhi Range, and the other is near the western boundary of the INEEL site and the toe of the Lost River Range.

Preferential flow of groundwater through the high-ratio zones, and the relatively long residence time or slow flow through the low-ratio zones, can readily produce the observed isotope ratio pattern. In this scenario, the high-ratio zones are fast-flow zones where high strontium-87/-86 and uranium-234/-238 ratios in groundwater north of the INEEL persist far into the regional aquifer system, because the groundwater in these preferential flow corridors is less reactive and has less time to react with the aquifer host rock. In contrast, groundwater in the low-isotope ratio evolves closer to the isotopic composition of the host rock—strontium-87/-86 = 0.7070 ± 0.0003 (Leeman and Manton 1971; Morse and McCurry 1997) and uranium-234/-238 ~ 5.49×10^{-5} (Roback et al. 2001)—due to slower groundwater flow, higher

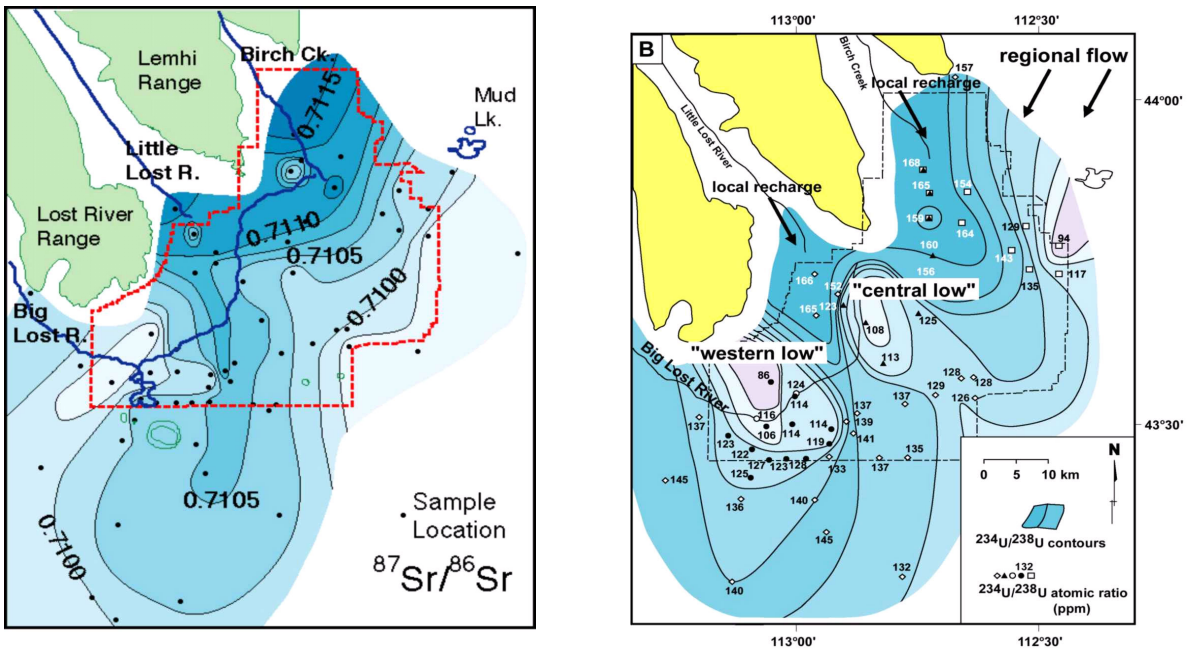

Figure 4-17. Strontium-87/-86 and uranium-234/-238 isotope contours.

residence times, and subsequent dissolution of the basalt host rock. Geochemical modeling and temperature profiles indicate that groundwater located at the toes of the Lost River and Lemhi ranges is moving slower relative to the rest of the SRPA (Luo et al. 2000), with calculated residence times for waters in these "stagnant" zones being two to 10 times longer than in the high-isotope ratio zones (Figure 4-18).

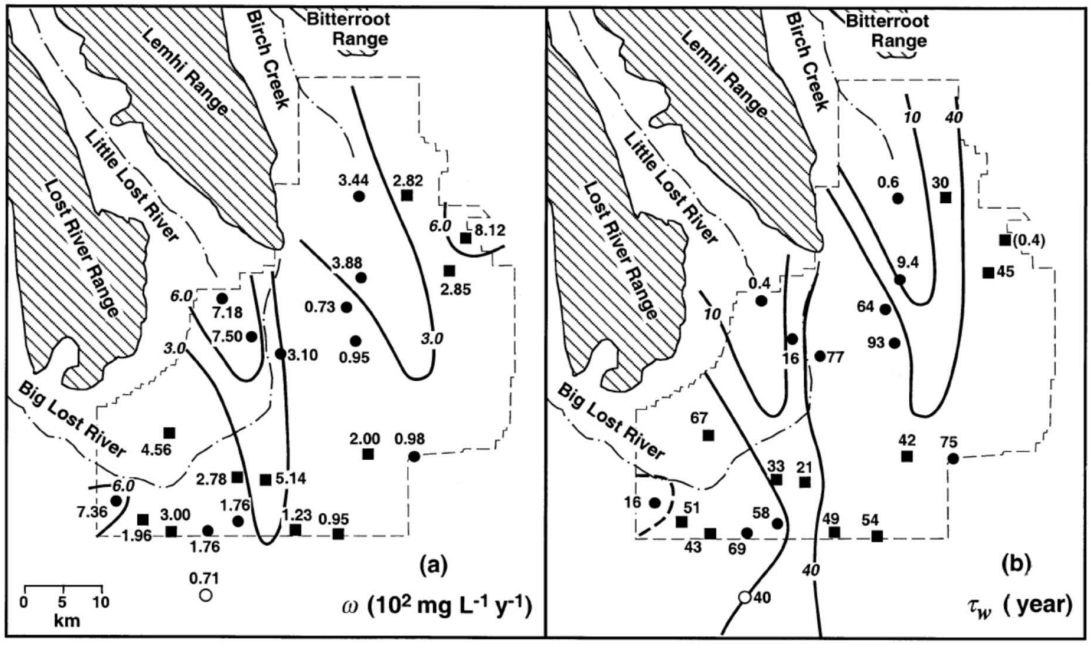

Figure 4-18. Variations of (a) rock dissolution rate (ω) and (b) groundwater residence time (τ_W) (Luo et al. 2000).

4.3.1.2.2 *Groundwater Temperature as a Tracer*—

Groundwater temperatures and borehole temperature profiles provide unique insight not only into the geometry and thickness of the SRPA but also into the flow of water through the aquifer. The distribution of groundwater temperature at the top of the SRPA beneath the INEEL is shown in Figure 4-19. Temperatures range from less than 8°C to more than 18°C, with colder water generally occurring to the east and north and in the vicinity of the INEEL spreading areas. This distribution generally supports the conclusions of the isotope-preferred flow path studies conducted by Roback et al. (2001), Johnson et al. (2000), and Luo et al. (2000).

The coldest water generally correlates with the preferential flow corridors identified by Roback et al. (2001) and is associated with areas where cold-water recharge appears to move most rapidly through the system. In contrast, regions where water temperature is warmer generally correlate with the slower flow regions identified in the previous studies.

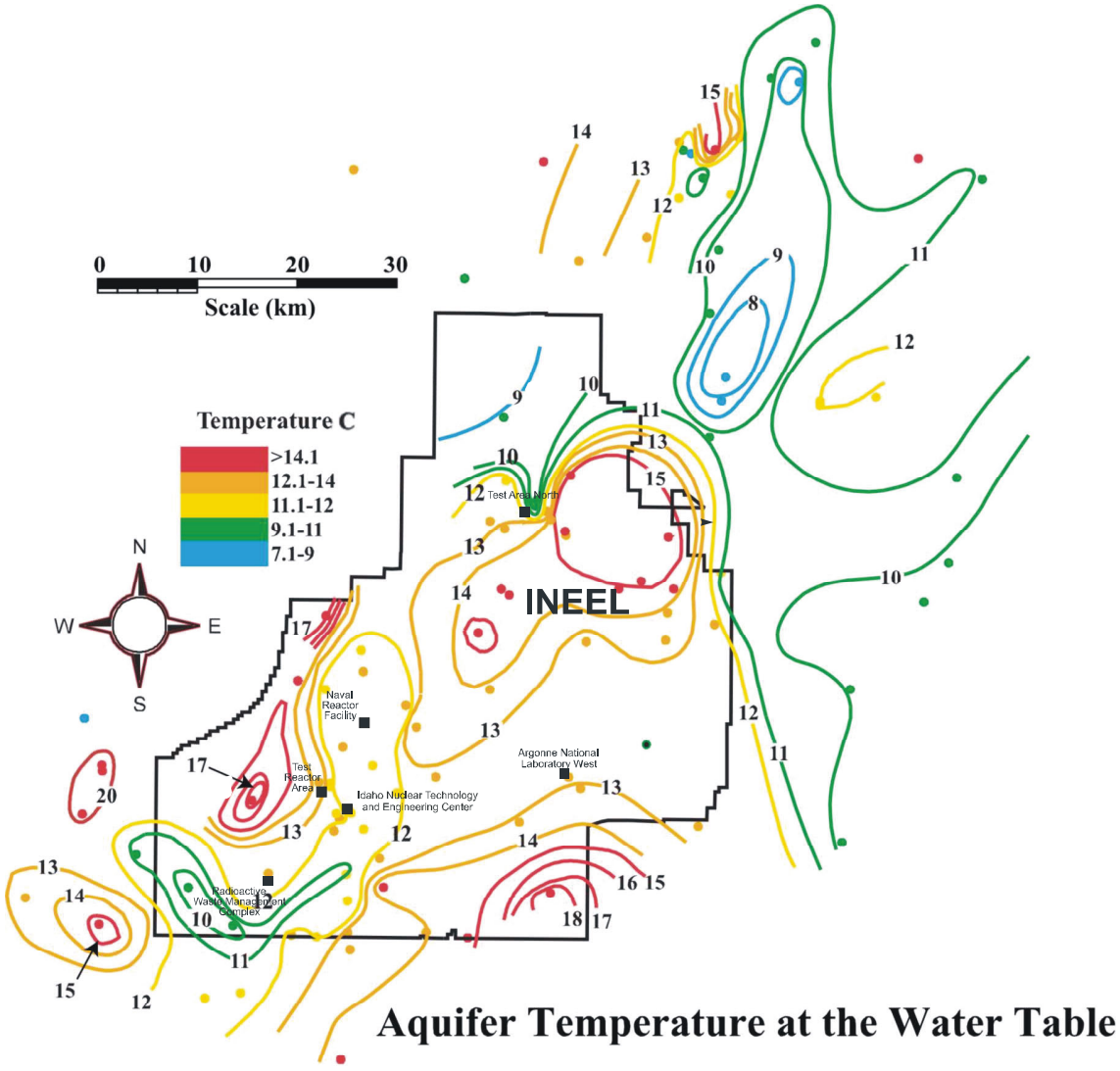

Figure 4-19. Groundwater temperature distribution at the water table in the vicinity of the INEEL.

The chemical and temperature data sets support similar interpretations of groundwater flow paths throughout much of the OU 10-08 model domain. However, these interpretations differ in several areas. For example, temperature data (13°C isopleths) support the occurrence of an apparent deep trough of relatively cold water extending west across the INEEL north of Argonne National Laboratory-West (ANL-W), turning southwest, and leaving the INEEL south of the RWMC (11°C isopleth). In contrast, the flow paths defined by isotope data indicate that groundwater east of ANL-W does not mix with water south of INTEC (Figure 4-17). These contrasting interpretations represent a significant data gap in an area of the INEEL where multiple contaminant plumes have been identified in the groundwater.

Although the interface between these two systems might not always be sharply defined, changes in geothermal gradients can be used generally to delineate the two systems. Temperature profiles in seven deep wells (Figure 4-10) show a distinct break in slope from the steep regional gradient to a shallow conductive gradient. Ackerman et al.[1] have determined that this break in slope defines the base of the upper active part of the aquifer. Drill cores from these deep wells show that this break in slope corresponds to hydrothermal alteration and secondary mineralization of basalts (Morse and McCurry 2002). Hydrothermal alteration seals otherwise conductive fractures and channels, decreasing permeability and permitting the thermal gradient to dominate aquifer temperature. Using these breaks in slope as a guide, the active aquifer thickness in the study area probably ranges from near 0 to about 1,300 ft (see Subsection 4.2.1.1).

Based on groundwater temperatures (Figure 4-19), regions of relatively cold temperatures probably correspond to the thickest sections of the aquifer and are characterized by deep "channels" of relatively cold groundwater with very sharp inflection to the regional thermal gradient. Regions of relatively warm groundwater in the SRPA correspond to areas geochemically characterized as slower-moving flow systems with longer residence time and increased water/rock interaction (McLing et al. 2001).

4.3.1.2.3 Apparent Differences between Geochemically Defined Groundwater Flow Paths and Hydraulic Head Distribution—

Since the SRPA was first characterized in the middle 1900s, little has changed with respect to the generally accepted concept of regional groundwater flow to the southwest across the INEEL, as defined by hydraulic head data (Figure 4-15). However, as additional wells have been drilled and more studies have been conducted, it has become apparent that the regional potentiometric surface does not necessarily reveal subtle gradients that would define preferential flow paths delineated in recent geochemical studies. In places, the regional hydraulic gradient is almost perpendicular to geochemically identified flow paths (Roback et al. 2001; Johnson et al. 2000; Luo et al. 2000). Isotope-delineated flow pathways are generally orientated in a northwest-to-southeast direction. This indicates a strong, geologically based hydraulic anisotropy in the SRPA and is consistent with the orientation of primary volcanic features on the plain (Rodgers et al. 1990). This orientation is also consistent with the predictions of preferred northwest-to-southeast hydraulic conductivity made by Welhan and Reed (1997). However, because of the assumptions made in the definition of the preferential flow corridors (i.e., water samples are representative of the entire thickness of the aquifer, and well density is sufficient to define flow corridors), definitive statements about the cause or exact boundaries of the preferential flow corridors are not currently possible.

Because of the limitations of the current generation of geochemical modeling codes and the lack of appropriate thermal dynamic data for the rocks of the ESRP, the current accepted practice to predict long-term contaminant migration is to use partitioning coefficient (K_d) models. Although geochemical modeling codes have rapidly evolved over the past decade, these codes still lack the ability to be fully incorporated into a GMS-type hydrologic model. Additionally, the use of K_d models to describe the transport of contaminants through the aquifer represents an oversimplified conservative approach to the problem in the absence of appropriate thermodynamic-based models. To address this limitation, the SWGM will calibrate groundwater flow to empirically based observations of the natural system (i.e., fast-

flow paths, aquifer thickness, and aquifer temperature). While this approach will make the model more responsive to currently understood aquifer chemistry, it assumes that the processes controlling the fast-flow paths, aquifer thickness, and aquifer temperature are well understood and that some unrecognized process is not responsible for the patterns on which the observations are based. The SWGM needs to be capable of incorporating advanced geochemical approaches that will continue to become available as models and data availability continue to evolve.

4.3.1.2.4 Limitations of Data—Although the use of natural flow indicators (e.g., chemistry, isotopes, and temperature) provides powerful tools for the interrogation of aquifer flow properties, one limitation of this type of data is the lack of spatially distributed data. Within the OU 10-08 model domain, most of the wells available for sampling are located near major facilities and in the uppermost part of the aquifer. The same types of problems are encountered using anthropogenic contaminants as tracers. This artifact of the INEEL aquifer monitoring system creates a data set with a high density of wells in some areas and a paucity of wells in others. As a result, flow fields or pathways based on nonanthropogenic and anthropogenic flow indicators commonly require that significant smoothing or extrapolation be made on the distal or edge portions of the data set. In some places, this generates significant discrepancies between anthropogenic plume geometries and naturally occurring isopleths. Potential solutions to this problem include more spatially located sampling wells and wells that sample more than just the top of the aquifer. New wells are planned for fiscal year 2005 to help address lack of spatially distributed data. The specific data gaps being addressed are identified in Subsection 6.5, and a task to prioritize the locations for drilling new wells is identified in Subsection 8.1.1. Additionally, integration of the natural and anthropogenic data sets would be beneficial such that each set of conclusions is considered in the context of short-term (<60 years) contaminant migration and long-term (>60 years) natural chemical tracers.

4.3.2 Distribution of Contaminants in Groundwater at the INEEL

Contamination of the aquifer at the INEEL has resulted from past practices, including disposal of wastewater to injection wells, land disposal of waste and wastewater, and spills. A summary of the contaminant plumes in the SRPA with concentrations that exceeded an established maximum contaminant level (MCL) in 2003 is shown on Figure 4-20. At TAN, TCE was the primary constituent exceeding its MCL, but cis-1,2-dichloroethene (-DCE), trans-1,2-DCE, and tetrachloroethene (PCE) also exceeded their respective MCLs. Strontium-90, technetium-99, and gross alpha exceeded their respective MCLs at and near INTEC. Chromium exceeded its MCL in water in two wells south of TRA. Nitrate exceeded its MCL in two wells south of the Central Facilities Area (CFA). Carbon tetrachloride exceeded its MCL in groundwater beneath the RWMC.

The following subsections describe the distribution of SRPA contaminants that originate from specific facilities at the INEEL. Also discussed is the potential for commingling plumes across the area represented by the OU 10-08 model domain. The discussion of commingling plumes is critical to the evaluation of the cumulative OU 10-08 risk.

4.3.2.1 Distribution of Contaminants by INEEL Facility. The following subsections describe the distribution in groundwater of selected contaminants that have been derived from waste-disposal practices at INEEL facilities. These distributions, based on groundwater monitoring data collected in 2003, will be used in subsequent model calibrations. Contaminant distribution is briefly summarized by facility for TAN, INTEC, TRA, CFA, and the RWMC. References to more thorough discussions of contaminant distribution are provided.

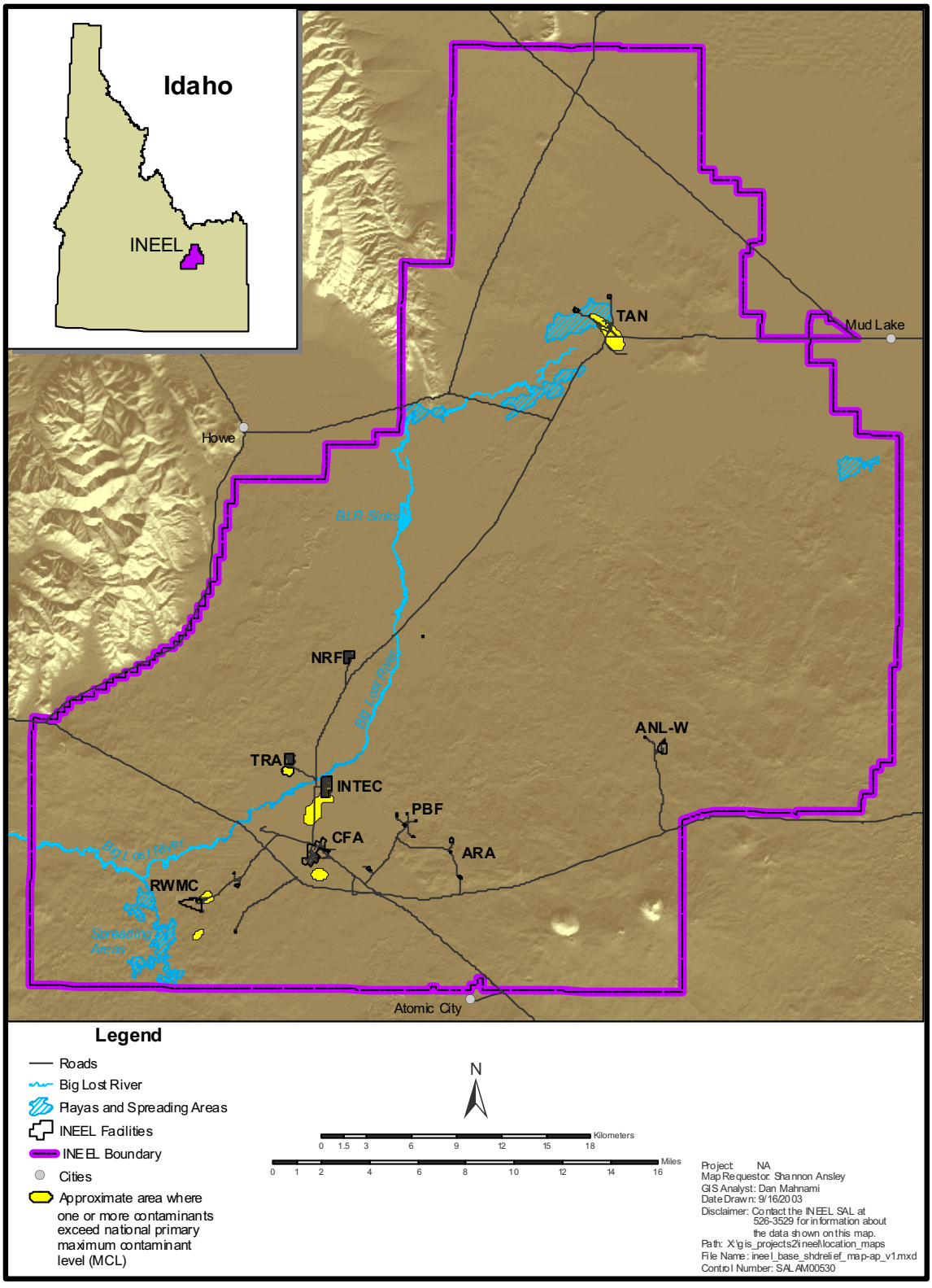

Figure 4-20. Contaminant plumes in groundwater with concentrations exceeding established or derived MCLs at the INEEL in 2003.

4.3.2.1.1 TAN—Wastewater containing volatile organic compounds (VOCs) and radionuclides was disposed of directly to the SRPA via the TSF-05 injection well from 1953 to 1972. A groundwater contaminant plume that formed from these disposal practices extends approximately 3 mi downgradient from the injection well. TCE and its degradation products (cis-1,2-DCE and trans-1,2,-DCE) are the primary organic contaminants in this contaminant plume. PCE also is present. The distribution of TCE in the SRPA at TAN is shown on Figure 4-21.

Based on TCE concentration data and other data related to TCE degradation, the remedial action objectives for the TCE plume will be achieved through in situ bioremediation and monitored natural attenuation (DOE-ID 2004a). Groundwater monitoring data indicate that the TCE plume has not expanded (DOE-ID 2004a). Continued monitoring that is intended to track the progress of the VOC remedial actions at TAN OU-1-07B is outlined in the remedial action work plans for in situ bioremediation (DOE-ID 2004b), the New Pump and Treat Facility (NPTF) (DOE-ID 2003a), and monitored natural attenuation (MNA) (DOE-ID 2003b).

Groundwater monitoring data for fiscal year 2003 indicated that radionuclide concentrations in groundwater at TAN continued to decrease through sorption and decay, as defined in the MNA remedial action work plan (DOE-ID 2003b), for selected radionuclides that include tritium, cesium-137, strontium-90, and uranium-234. All observed tritium concentrations were below the MCL of 20,000 pCi/L and were decreasing. Cesium-137 was present in the residual source area but was not detected outside of the residual source area. Uranium-234 was below the MCL in all wells. Strontium-90 concentrations decreased with distance from the source area (DOE-ID 2003b). Radionuclide concentrations have not increased unexpectedly, and future groundwater monitoring, as outlined in the MNA operations, monitoring, and maintenance plan (DOE-ID 2003c), is considered sufficient to track the progress of the MNA remedy for radionuclides at TAN OU 1-07B.

4.3.2.1.2 INTEC—Groundwater contamination at INTEC occurred primarily from disposal of service wastewater to the former INTEC injection well. Other contaminant sources included unlined service-waste percolation ponds and soil-contamination sites associated with the INTEC tank farm.

The INTEC injection well was used routinely from 1952 to 1984 to dispose of service wastewater from INTEC operations directly to the SRPA. This wastewater contained elevated concentrations of sodium, chloride, and other inorganic constituents. Before 1992, the service wastewater also contained small concentrations of radionuclides. The principal radionuclides of environmental significance discharged to the injection well were tritium, iodine-129, strontium-90, and cesium-137. The service-waste percolation ponds were constructed in 1984 to dispose of INTEC service wastewater. They remained in operation until 2002, when a new set of infiltration ponds 2 mi west of INTEC began operation. Wastewater sent to these ponds contained small concentrations of nitrate, tritium, strontium-90, technetium-99, calcium, sodium, and chloride (INEEL 2003). (Soil contamination sites at the INTEC tank farm have been identified as a contaminant source for technetium-99.)

A dilute plume of tritium in the SRPA extends downgradient from INTEC (Figure 4-22) as a result of disposals to the INTEC injection well. The approximate extent of this plume and other plumes, shown on Figures 4-22 and 4-23, is a function of the concentration used to define the edge of the plume and the location/density of wells available for sampling and is based on sampling results from 2003.

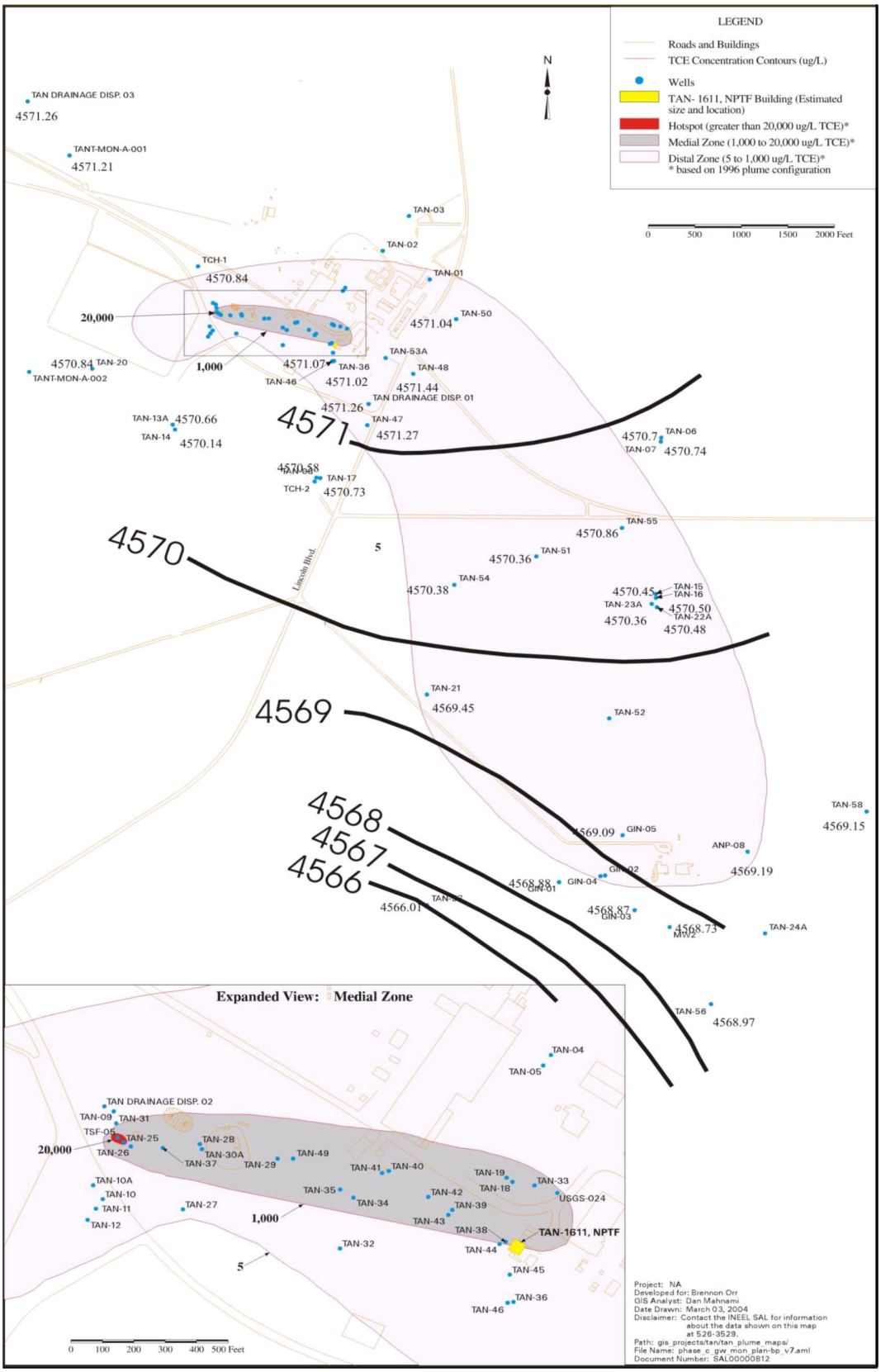

Figure 4-21. Distribution of TCE in groundwater at TAN in 2003.

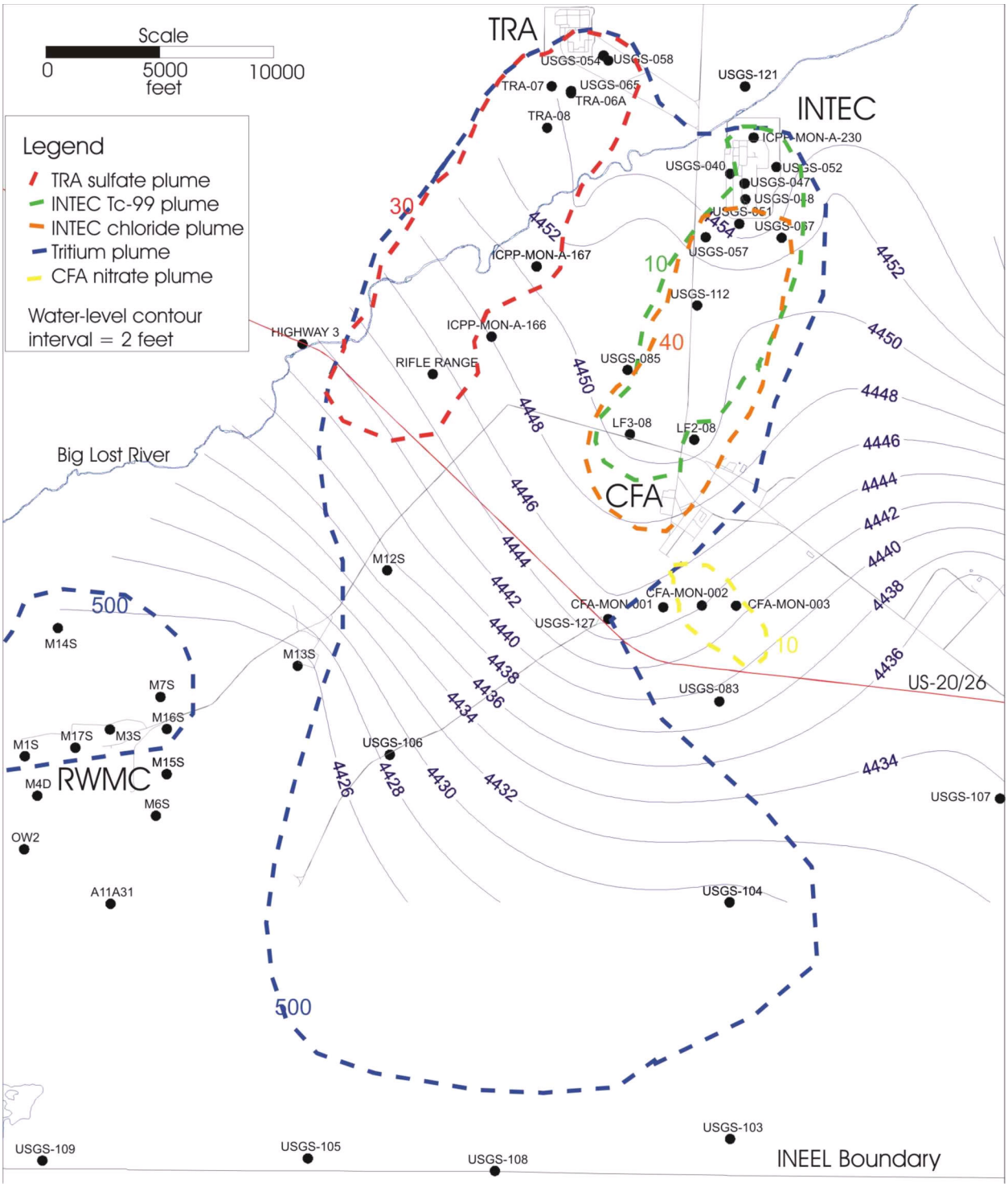

Figure 4-22. Approximate distribution of selected contaminants in groundwater at INTEC, TRA, and CFA in 2003.

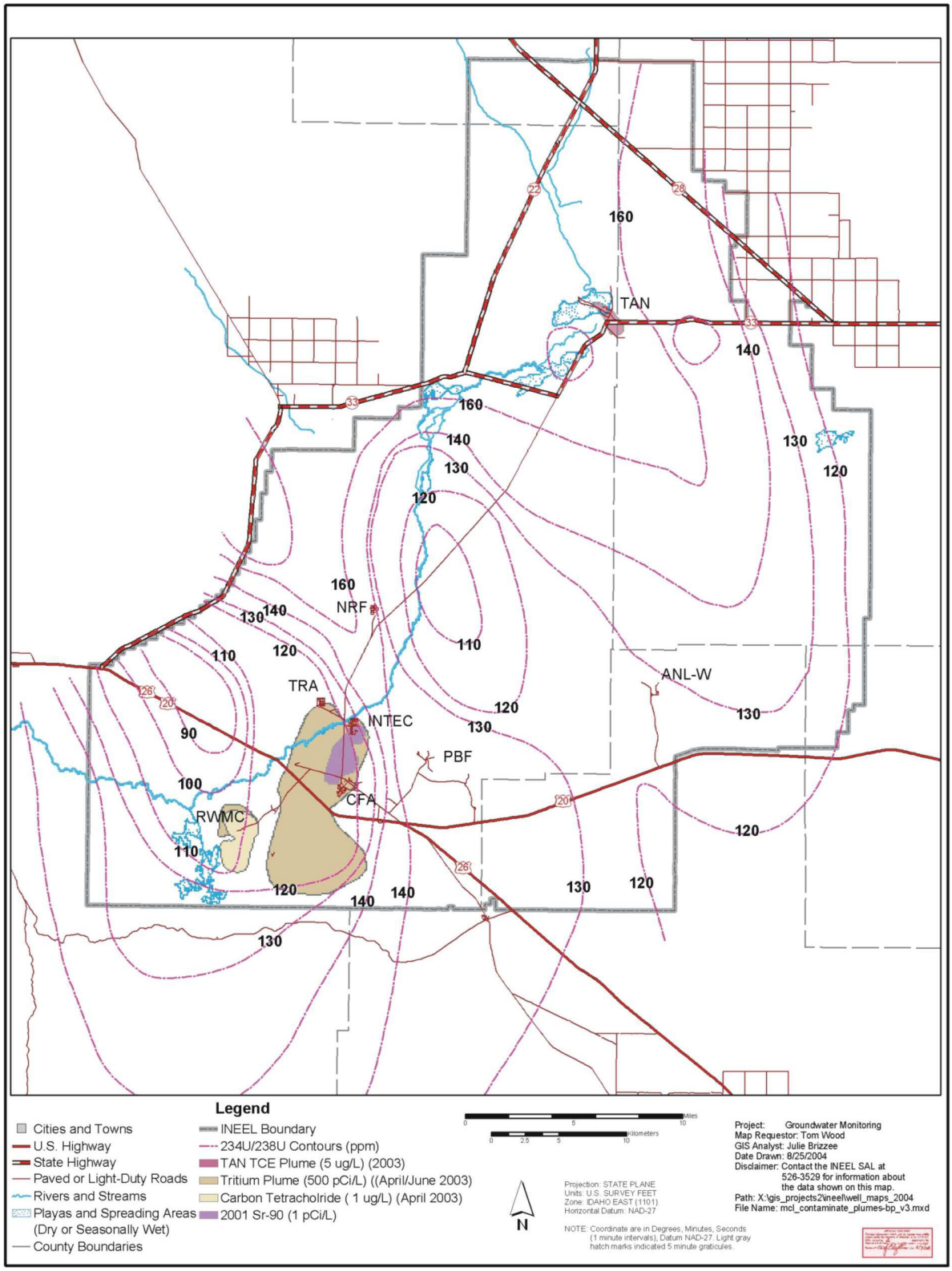

Figure 4-23. Selected contaminant plumes and distribution of uranium-234/-238 in groundwater in the vicinity of the INEEL in 2003.

This plume joined with a tritium plume originating from TRA. The combined plume, with concentrations above a detection level of 500 pCi/L, extended approximately 8 mi downgradient in 2003. No tritium concentrations in groundwater within this plume exceeded the MCL of 20,000 pCi/L in 2003. Tritium concentrations in water within the plume continue to decrease in response to radioactive decay and cessation of disposal (DOE-ID 2003d).

A strontium-90 plume extends downgradient from INTEC; the extent of the plume exceeding the MCL of 8 pCi/L is shown in Figure 4-20. In 2001, the strontium-90 plume above a derived concentration of 8 pCi/L (calculated to achieve a 4-millirem drinking water exposure) extended nearly to CFA, which is approximately 3 mi south of INTEC.

A dilute plume of technetium-99 exceeding 10 pCi/L extends from the northern part of INTEC downgradient into CFA (Figure 4-20). The primary source of this dilute plume is attributed to previous technetium-99 releases to the INTEC injection well (ICP 2004a). Concentrations of technetium-99 exceed the MCL of 900 pCi/L in only one well (i.e., ICPP-MON-A-230) located near the INTEC tank farm. The principal source of this concentration above the MCL is considered to be from liquid releases at the tank farm.

USGS studies using low-detection analytical methods have shown that very dilute concentrations of technetium-99 and iodine-129 originate from INTEC and extend downgradient beyond the southern boundaries of the INEEL (Mann and Beasley 1994; Beasley et al. 1998). These concentrations were orders of magnitude smaller than the MCL but above expected background concentrations.

A plume of dissolved chloride, with concentrations exceeding 40 mg/L, extends from the vicinity of the INTEC service-waste percolation ponds downgradient to CFA. This plume is attributed largely to previous disposal of chloride-enriched service wastewater.

Sampling results for 2003 confirmed that dissolved concentrations of tritium, iodine-129, and strontium-90 continue to decrease at and downgradient of INTEC (DOE-ID 2003e). In contrast, technetium-99 concentrations in the SRPA increased slightly at several locations within and south of INTEC, although the lack of historical data makes this conclusion tenuous.

The vertical distribution of contaminants in groundwater at INTEC has been evaluated using vertical profile packer sampling studies in several wells. In 2002, packer sampling was conducted at four locations south of INTEC, with the sampling results reported in the WAG 3 Group 5 monitoring report/decision summary (DOE-ID 2004c). The packer sampling indicated that the contaminants are present predominantly above the HI interbed.

The INEEL Environmental Data Warehouse contains extensive tritium and strontium-90 data sets dating from the early 1960s for several wells near INTEC. These are the best data sets for model calibration; more limited data sets exist for iodine-129 and technetium-99.

4.3.2.1.3 TRA—Historically at TRA, contaminants entered the SRPA in wastewater through direct injection from the TRA-05 injection well or through vadose zone infiltration from the TRA disposal ponds. Wastewater disposed of through the TRA-05 injection well contained hexavalent chromium. Wastewater disposed of in the ponds contained tritium, chromium, sulfate, and sodium.

Chromium currently exceeds the MCL of 100 μg/L in two wells (i.e., USGS-65 and TRA-07). Chromium concentrations continue to decrease, and the WAG 2 ROD model predicts they will decrease below the MCL in 2012 (DOE-ID 2003d). No other contaminants exceed their respective MCLs in groundwater at TRA. In the past, tritium exceeded the MCL of 20,000 pCi/L. Concentrations have decreased to levels below the MCL from radioactive decay, disposal cessation, and dilution. The resulting

dilute tritium groundwater plume that originated from disposals to the TRA ponds merged with the plume that originated from INTEC.

The INEEL Environmental Data Warehouse contains tritium data from the early 1960s for some wells at TRA, and these data could be used for model calibration.

In addition to chromium, concentrations of sulfate, calcium, magnesium, potassium, and, to a lesser extent, chloride were higher in wells downgradient from TRA than in upgradient wells TRA-03 and USGS-121. Data for inorganic constituents in USGS-121 were used to evaluate which inorganic analytes are elevated downgradient of TRA in 2003. The concentrations of inorganic constituents in USGS-121 are similar to those for TRA-03 located upgradient (based on water levels) of TRA.

The distribution of sulfate concentrations exceeding 30 mg/L in groundwater near TRA is shown on Figure 4-22. The elevated sulfate concentration is from the disposal ponds at TRA. The elevated sulfate concentrations in infiltration from the cold-waste ponds at TRA provide a possible tracer that could be used to distinguish sources of tritium contamination in groundwater, because tritium from INTEC is associated with elevated chloride concentrations.

4.3.2.1.4 CFA—Nitrate is the only analyte that has been consistently detected at CFA above the MCL (10 mg/L as nitrogen). Nitrate concentrations in wells CFA-MON-A-002 and CFA-MON-A003 ranged from 16 to 22 mg/L and 9 to 11 mg/L-N, respectively. The nitrate concentrations in these wells have remained relatively steady over time (INEEL 2003; ICP 2004b). Distribution of nitrate (as nitrogen exceeding 10 mg/L) in groundwater at CFA is shown in Figure 4-22.

Water samples from the two wells contaminated with nitrate also contained enriched concentrations of calcium, chloride, magnesium, potassium, and sodium compared to probable background concentrations for the SRPA (Knobel et al. 1999) and other wells in the immediate vicinity. Only a limited amount of historical data exists for these two wells, because they were first sampled in 1995. Data for the CFA wells is contained in the five-year review and the subsequent annual monitoring reports (DOE-ID 2002b; INEEL 2003; ICP 2004b).

Nitrogen and oxygen isotope ratios for nitrate indicate a non-sewage source (ICP 2004b). These isotope data suggest that the CFA-04 dry pond is a more likely candidate than the former CFA-08 sewage drainfield as the source of the nitrate contamination in wells CFA-MON-A-002 and CFA-MON-A-003. This conclusion supports the groundwater flow paths, as indicated by water level data (Figure 4-22).

4.3.2.1.5 RWMC—A wide variety of potential contaminants has been buried in the Subsurface Disposal Area (SDA) at the RWMC, but the contaminants that are consistently detected in the aquifer include carbon tetrachloride, tritium, and anomalous concentrations of chloride and sulfate. Carbon tetrachloride and TCE disposed of in the SDA have migrated through the vadose zone to the SRPA. Carbon tetrachloride is the only analyte that has been consistently detected at RWMC above the MCL of 5 μg/L. The distribution of carbon tetrachloride in the SRPA as delineated by 1 μg/L concentration is shown on Figure 4-24.

Tritium concentrations exceeding the detection limit of 500 pCi/L occur in water from several wells on the northern and eastern sides of the RWMC (Figure 4-24). Based on the distribution of tritium in the SRPA (Figure 4-23), tritium in groundwater beneath the RWMC appears to be separate from the tritium plume originating from INTEC and TRA. Whether the apparent separation can be attributed to the aerial and vertical distribution of sampling points or whether measured concentrations reflect separate tritium sources is uncertain.

An area characterized by increased chloride and sulfate concentrations occurs south of the RWMC (Figure 4-24). The exact cause of these increased concentrations is uncertain but might be attributable to dust-suppressing brine applied to the roads at the RWMC in the 1980s and early 1990s or to infiltration of precipitation through wastes in the SDA.

Other contaminants in addition to carbon tetrachloride, TCE, tritium, and selected anions are detected in the aquifer sporadically above background concentrations. Aluminum, iron, chromium, lead, and zinc are above background concentrations in some water samples from RWMC wells. Increased aluminum and iron concentrations might be derived from suspended particulates. The increased lead might be derived from corrosion of galvanized well casing.

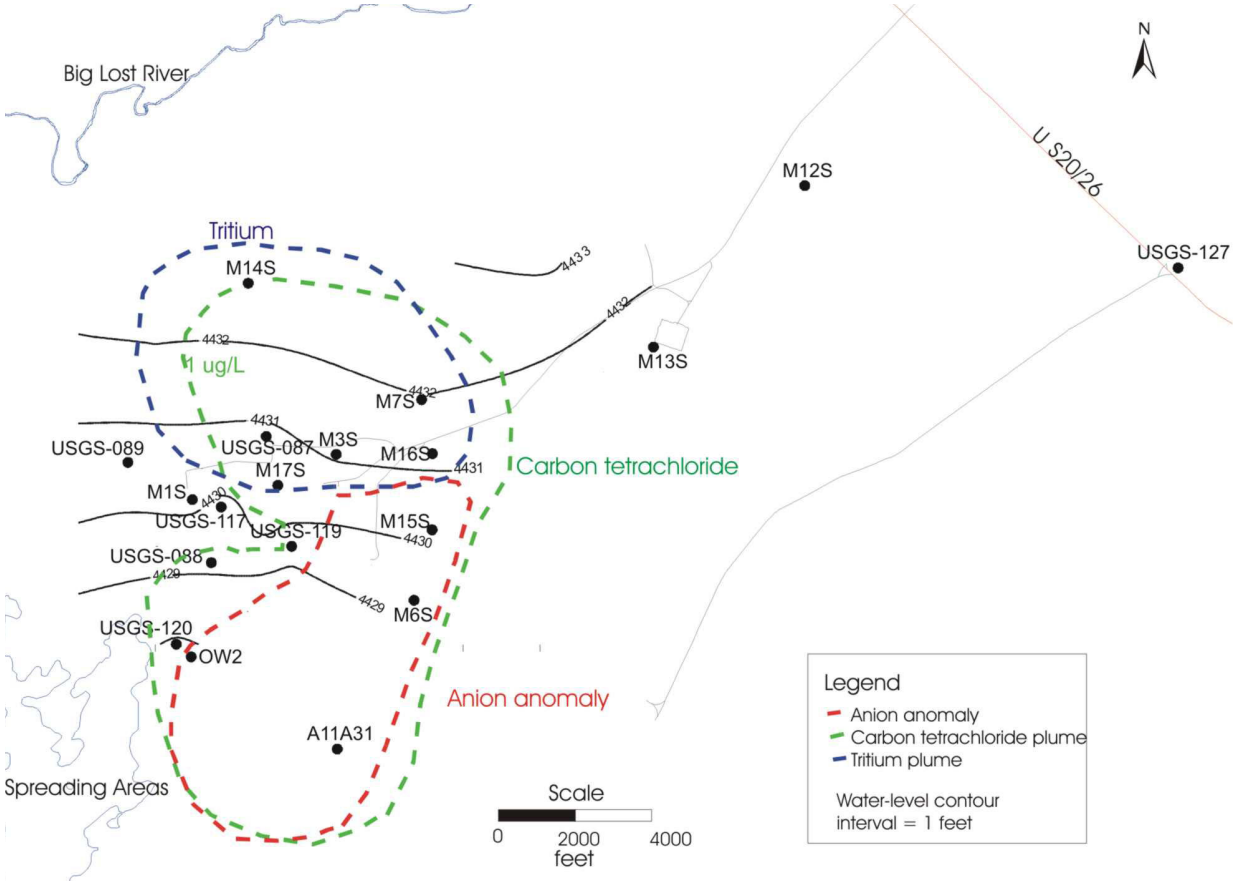

Figure 4-24. Approximate distribution of selected contaminants in groundwater beneath the RWMC in 2003.

4.3.2.2 Commingling Plumes. The potential for commingling plumes exists in INEEL areas, including INTEC, TRA, CFA, and the RWMC. Figure 4-23 shows the approximate extent of tritium contamination in the SRPA based on the data from 2003. A combined tritium plume originates from INTEC and TRA. Tritium concentrations near the RWMC potentially originate from the RWMC, but the source of tritium is uncertain.

The contaminants in the CFA nitrate plume could be commingling with contaminants originating from INTEC. The occurrence of tritium and elevated chloride concentrations would support commingling. However, these plumes could still be separate. The case for commingling is somewhat

difficult to evaluate because of the lack of wells in the southern part of the CFA and because the water supply for the CFA is affected by INTEC plume constituents.

Based on 100-year plume projections, the potential exists for plumes to overlap in the future (Figure 4-25). As more information becomes available on source terms, contaminant distributions in the SRPA, and/or aquifer hydraulic parameters, the new data could be used to evaluate the potential for commingling plumes.

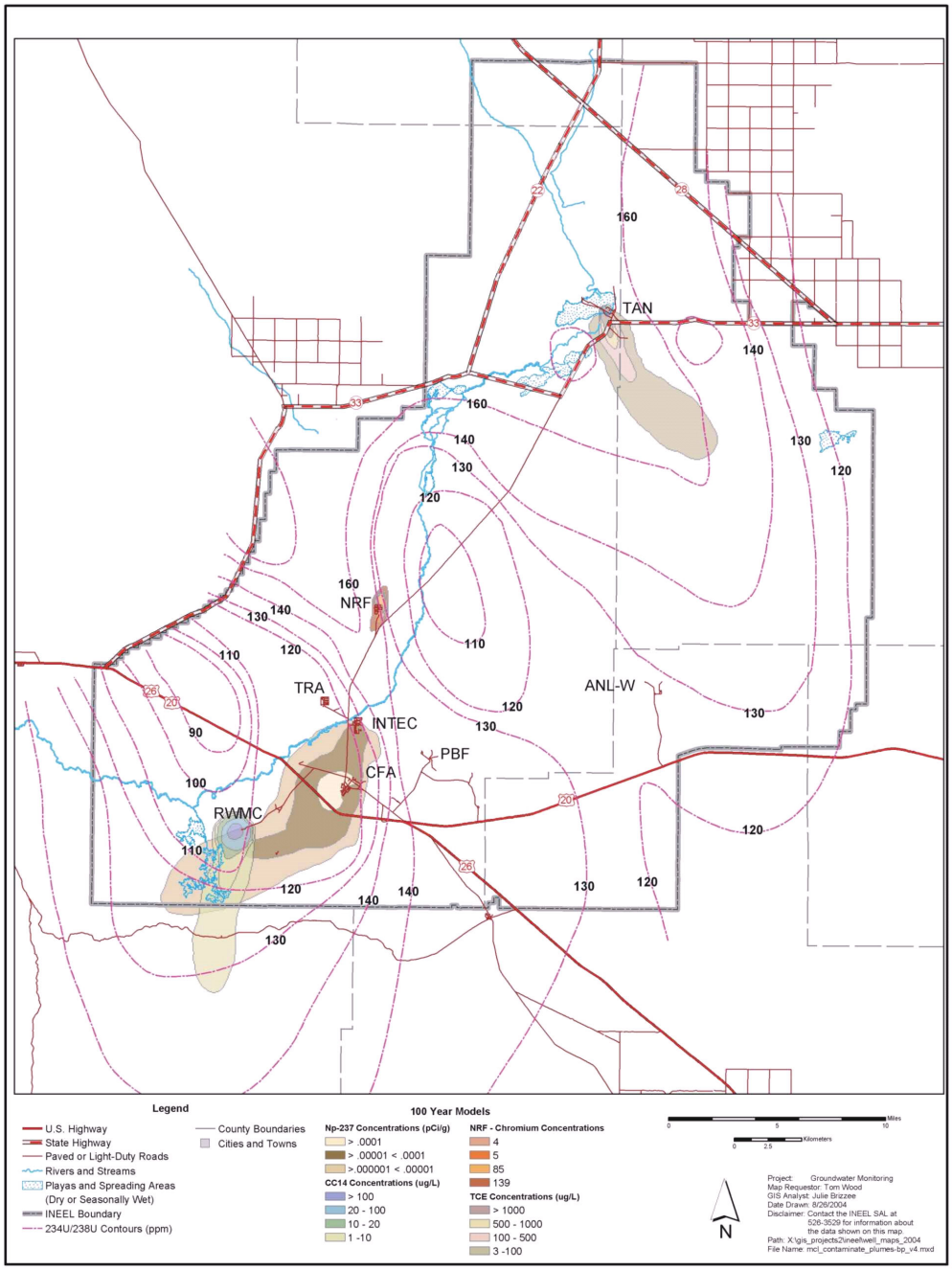

Figure 4-25. Projected 100-year distribution of selected contaminant plumes and distribution of uranium-234/-238 in groundwater in the vicinity of the INEEL.

5. NUMERICAL MODELING APPROACH

The first step in generating the numerical model is to convert the conceptual model to a form suitable for computer modeling. This step includes selecting an appropriate modeling code, designing a model grid, selecting boundary and initial conditions, and selecting initial aquifer parameter values.

5.1 Mathematical Model

The goal in converting the conceptual model to a numerical model is to simulate groundwater flow and contaminant transport and to predict contaminant concentration at selected locations and future times. Modeling distributions of temperature and natural geochemistry in addition will enhance understanding of the movement of groundwater and improve predictions of contaminant concentrations in the aquifer.

Typically, a contaminant transport model consists of two submodels: one to solve the groundwater flow equation and another to solve the contaminant transport equation. The solution to the groundwater flow equation provides a distribution of hydraulic head. From this distribution of head, one can calculate the groundwater velocity field. Groundwater velocities can then be used as input for the transport model, and the transport model will determine contaminant concentration as a function of space and time.

For the flow submodel, two approaches can be taken. The aquifer viewpoint is based on concepts of confined and unconfined aquifers, where flow is horizontal through aquifers and vertical through confining beds. The approach is used to simulate two-dimensional horizontal flow in confined and unconfined aquifers. Leaky confined aquifers can be simulated using a quasi-three-dimensional approach in which vertical flow is through confining layers in a vertical direction only.

Alternatively, the flow system viewpoint models the three-dimensional distribution of heads, hydraulic conductivities, and storage properties everywhere in the system. This flow system viewpoint allows for both vertical and horizontal components of flow throughout the system. The aquifer viewpoint has the advantage of neglecting true vertical flow simulation by using a leakage term; the result is computationally more efficient. However, true vertical flow simulation might be required in this modeling application, because there is some evidence of vertical hydraulic gradients.

For the transport submodel, the current model assumes that contaminant geochemistry can be described using adsorption isotherms (i.e., using K_d). This assumption stipulates that laboratory experiments to measure these isotherms accurately replicate all of the processes active in the subsurface at the site of interest. This assumption is problematic, because it is rooted in current standard practice. However, the relative paucity of geochemical characterization data and lack of a GMS-based code that can accommodate advanced geochemical calculations currently prevent the adoption of a more advanced geochemical model. Consequently, we adopted the isotherm approach while highlighting the need to improve our ability to accurately describe the operative geochemical processes.

Additionally, it is well known among geologists that the Earth has a thermal regime involving the flow of heat from deep layers of the planet up toward the surface. The natural, background geothermal gradient averages approximately 1°C increase in temperature with every 130 ft of depth. However, this gradient is often non-uniform. Anomalous geothermal gradients can arise due to variations in thermal conductivity between geological formations, response to geologically recent volcanic or intrusive sources of heat production at depth, or spatial redistribution of heat by flowing groundwater.

5.1.1 Governing Equations

A general form of the governing equation of groundwater flow in an aquifer via the flow system viewpoint, which includes transient flow, is as follows:

$$\frac{\partial}{\partial x}\left(K_x \frac{\partial h}{\partial x}\right)+\frac{\partial}{\partial y}\left(K_y \frac{\partial h}{\partial y}\right)+\frac{\partial}{\partial z}\left(K_z \frac{\partial h}{\partial z}\right)=S_s \frac{\partial h}{\partial t}-R^* \tag{5-1}$$

where

K_x, K_y, K_z = components of the hydraulic conductivity tensor

S_s = the specific storage

R^* = a general sink or source term

h = hydraulic head

x, y, z = principal axes of a rectilinear coordinate system

t = time.

When combined with boundary and initial conditions, equation (5-1) describes transient three-dimensional groundwater flow in a heterogeneous and anisotropic medium, provided that the principal axes of hydraulic conductivity are aligned with the coordinate directions.

The governing equation for solute transport, a partial differential equation known as the advection-dispersion equation, describes a given contaminant species concentration in a transient three-dimensional groundwater flow system that can be written as follows:

$$\frac{\partial(\theta C)}{\partial t}=\frac{\partial}{\partial x_i}\left(\theta D_{ij}\frac{\partial C}{\partial x_j}\right)-\frac{\partial}{\partial x_i}(\theta v_i C)+q_s C_s+\sum R_n \tag{5-2}$$

where

θ = porosity of the subsurface medium

C = contaminant species concentration

t = time

x_i , x_j = distance along the respective Cartesian coordinate axis

D_{ij} = hydrodynamic dispersion coefficient tensor

v_i = seepage or linear pore water velocity

q_s = volumetric flow rate per unit volume of aquifer, both sources and sinks

C_s = source or sink flux concentration

$\sum R_n$ = chemical reaction term, including radioactive decay.

The general chemical reaction term includes the effects of biochemical and geochemical reactions. Two basic types of reactions should be considered: aqueous-solid surface reaction (sorption) and first-order rate reactions. With such, equation (5-2) can be rewritten as a mass balance statement, wherein the change in the mass storage of both dissolved and sorbed phases at any given time is equal to the difference in the mass inflow and outflow due to dispersion, advection, sinks/sources, and chemical reactions. With the assumption of local equilibrium for the various sorption processes, the general governing transport equation can be written as follows:

$$R_d\theta\frac{\partial C}{\partial t}=\frac{\partial}{\partial x_i}\left(\theta D_{ij}\frac{\partial C}{\partial x_j}\right)-\frac{\partial}{\partial x_i}(\theta v_i C)+q_s C_s-q'_s\,C-\lambda_1\theta C-\lambda_2\rho_b C_s \tag{5-3}$$

Here, R_d is a retardation factor defined as follows:

$$R_d=1+\frac{\rho_b}{\theta}\frac{\partial C_s}{\partial C} \tag{5-4}$$

where (for both equations)

ρ_b = porous medium bulk density

λ_1, λ_2 = first-order chemical reaction rates for dissolved and sorbed phases, respectively

C_s = concentration of contaminant sorbed onto subsurface solids

q'_s = time rate of change in transient groundwater storage.

The governing equation for contaminant transport is linked to the groundwater flow equation via Darcy's law:

$$q_i=-K_i\left(\frac{\partial h}{\partial x_i}\right) \tag{5-5}$$

where

q_i = volumetric flow rate per unit area in a given direction

K_i = hydraulic conductivity for that direction

$\partial h/\partial x_i$ = change in hydraulic head per unit length in this direction.

From Darcy's law, the seepage velocity, v_i, can be obtained ($v_i = q_i/\theta$). As with the flow equation, certain boundary conditions must be specified to obtain a meaningful solution.

There are analogous equations describing the transport of heat in materials (indeed, the equations describing fluid flow of groundwater are based on early heat transport equations). The transport of heat is by both conduction and convection. Conductive transport can occur even in static groundwater. It is controlled by the thermal conductivity of geological formations and pore water. On the other hand, convective or advective heat transport occurs only in moving groundwater. It is the heat that is entrained

along with flowing groundwater. In most flowing groundwater systems, convective transport of heat dominates conductive transport.

The advective heat transport equation is discussed in detail in model code manuals such as the manual for HST3D (Kipp 1987), a USGS heat and solute three-dimensional transport code. The advective heat transport equation in an energy conservation form is based on the conservation of enthalpy in both the fluid and solid phases of a modeled region. Enthalpy is a measure of total system energy and includes the product of temperature and heat capacity. In the following equation, enthalpy is a derived property that contains both internal energy and flow energy with temperature as a dependent variable:

$$\frac{\partial}{\partial t}\left[\left(\theta\rho_f c_f + (1-\theta)\rho_s c_s\right)T\right] = \frac{\partial}{\partial x_i}\left[\left(\theta K_f + (1-\theta)K_s\right)\frac{\partial T}{\partial x_i}\right] + \frac{\partial}{\partial x_i}\left(\theta A_{ij}\frac{\partial T}{\partial x_j}\right) - \frac{\partial}{\partial x_i}\left(\theta\rho_f \cdot v_i T\right) + q_H + q^*\rho^* c_f T^* \quad (5\text{-}6)$$

where

T = the fluid and porous media temperature

T^* = source fluid temperature

ρ_s = solid phase density

ρ_f = liquid phase density

ρ^* = source fluid density

c_f = fluid phase heat capacity at constant pressure

c_s = constant pressure solid phase heat capacity

K_f = thermal conductivity of the fluid phase

K_s = thermal conductivity of the solid phase

A_{ij} = thermal-mechanical dispersion

q_H = heat source rate intensity

q^* = source fluid flow rate intensity.

This equation keeps temperature as a dependent variable and relates a variety of changes to system enthalpy: rates of change of fluid and solid enthalpy; net advective, conductive, and dispersive enthalpy fluxes; and heat and fluid sources. The equation is linked to the flow model through temperature, on which fluid density is dependent, as in the following relationship:

$$\rho_f = \rho_o - \rho_o\beta_T\left(T - T_o\right) \quad (5\text{-}7)$$

where

ρ_o = fluid density at a standard reference temperature (T_o) and pressure

β_T = fluid thermal expansion coefficient.

Because the fluid density is now considered a function of temperature, a new governing equation describing fluid flow is in order. The following groundwater flow equation incorporates the temperature dependence of fluid density by breaking down the hydraulic conductivity coefficient into its basic components of fluid density, viscosity, and formation permeability:

$$\frac{\partial}{\partial t}(\theta\rho_f) = \frac{\partial}{\partial x_i}\left[\rho_f \frac{k_{ij}}{\mu}\left(\frac{\partial P}{\partial x_j} + \rho_f g \delta_{i3}\right)\right] + q\rho^* \tag{5-8}$$

where

ρ_f = fluid density

ρ^* = source fluid density

q = source fluid flow rate

g = gravitational constant

μ = fluid viscosity

P = pressure

k_{ij} = formation permeability

δ_{i3} = Dirac delta function.

This, in turn, yields a new formula for describing the velocity, required in determining contaminant transport:

$$v_i = -\frac{k_{ij}}{\theta\mu}\left(\frac{\partial P}{\partial x_i} + \rho_f g \delta_{i3}\right) \tag{5-9}$$

This equation is based on Darcy's law provided in equation (5-5).

5.1.2 Key Assumptions

The SRPA is usually considered an unconfined aquifer, i.e., a free water table surface with no overlying confining layer. The governing equation for groundwater flow listed above applies to unconfined aquifers only if Dupuit assumptions are made. These Dupuit assumptions require that all flow lines are horizontal, all equipotential lines are vertical, the hydraulic gradient is equal to the slope of the water table surface, and this gradient is constant with depth (Anderson and Woessner 1992).

By assuming that the transmissivity in the x and y directions can be defined as $T_x = K_x h$ and $T_y = K_y h$, where h is the saturated thickness, the governing equation listed above can be simplified for unconfined aquifer application. The result is a nonlinear expression known as the Boussinesq equation:

$$\frac{\partial}{\partial x}\left(K_x h \frac{\partial h}{\partial x}\right) + \frac{\partial}{\partial y}\left(K_y h \frac{\partial h}{\partial y}\right) = S_y \frac{\partial h}{\partial t} - R \tag{5-10}$$

Here, S_y is a storage coefficient called specific yield, and R is a general source/sink term. During computer simulation, the equation is solved using the current time step's value for the saturated thickness (i.e., hydraulic head) in order to make the equation effectively linear, which is the approach taken in the USGS code for saturated groundwater flow, MODFLOW (Harbaugh et al. 2000). Use of the Dupuit assumptions mandates horizontal flow by requiring that there is no change in head with depth, effectively turning the three-dimensional problem into a two-dimensional problem.

However, two-dimensional profile or full three-dimensional models are required in order to simulate unconfined aquifers when vertical head gradients are important. In the SRPA, vertical gradients have been observed in several nested piezometer wells that have multiple completed intervals at various depths. As such, it is anticipated that the SWGM will eventually be a full three-dimensional model.

The contaminant transport equation currently requires assumptions regarding solute sorption processes. Specifically, it is assumed that contaminant geochemistry can be described using adsorption isotherms and that the laboratory experiments used to measure these isotherms accurately replicate all of the processes active in the subsurface at the site of interest. Furthermore, the geothermal transport equation assumes the following:

- Thermal dispersive transport takes place with a mechanism analogous to solute-dispersive transport.
- Fluid kinetic energy, radiant energy transport, and the thermal effects of chemical reactions are negligible. The thermal expansion of the porous medium is negligible.
- Heat capacities and thermal conductivities are not functions of temperature or solute concentration. Thermal equilibrium exists between the fluid and solid phases.

5.1.3 Approximation Methods

A computer program or code solves a set of algebraic equations that are generated from discretizing the partial differential equations that govern the groundwater flow and chemical transport. The finite-difference and finite-element methods are the two most often used discretization techniques. These convert the mathematical model into numerical approximations that result in a set of algebraic equations that can be solved by a computer. The set of algebraic equations produced in this way can be expressed easily in matrix form.

There is a fundamental difference between the two methods. Finite-difference methods compute a value for the head at the node, which is also the average head for the entire cell that surrounds the node. This allows no head variation within the cell. Finite elements, however, precisely define the variation of head within an element by means of interpolation, or basis, functions. Heads are calculated at the nodes but are also defined everywhere by means of these basis functions.

The finite-difference method is easier to understand and program. Fewer input data are needed to construct a finite-difference grid. However, finite elements are better able to approximate irregularly shaped boundaries than standard finite differences. Finite elements are also better at handling internal boundaries such as fault zones and can simulate point sources and sinks, seepage faces, and moving water tables better than finite differences (Anderson and Woessner 1992).

Both finite-difference and finite-element models are able to simulate aquifers in profile, but movement of the water table is more easily handled with a finite-element model. Irregularities of the model boundaries, fractures, and other features might warrant use of a finite-element method.

For the finite-difference method, there are also grid types. The block-centered grid approach models flux boundaries as always being located at the edge of a block. The mesh-centered grid approach models boundaries at the node. A code such as the USGS saturated groundwater flow code, MODFLOW, uses the block-centered finite-difference approach.

5.1.4 Code Selection

The initial code selection process for the previous WAG 10 modeling effort (Arnett et al. 1993) identified a set of mathematical model characteristics required to adequately model regional flow. The following is a list of essential code capabilities from the initial WAG 10 code selection effort:

- Saturated porous media
- Unconfined flow
- Variable aquifer thickness
- Heterogeneous hydraulic conductivity and storage coefficient
- Anisotropic hydraulic conductivity
- Transient flow
- Transient-point, line, and areal recharge
- Transient-point and line discharge
- Transient-head and flux-boundary conditions.

These are all desirable features, but few modeling codes can satisfy all of them. It is also important to note that the initial code selection was in support of a regional, two-dimensional model. The current conceptual model is a three-dimensional representation of the aquifer and limited to a subregional domain.

Furthermore, the SWGM is anticipated to support cumulative risk assessment, i.e., predict groundwater contaminant concentrations that result from the possible commingling of contaminant plumes from various individual WAGs. This will necessitate use of a suitable transport code. An additional criterion imposed in this work plan is that the selected model be able to reasonably run the fate and transport simulations with a discretization that duplicates the current minimum aquifer grid block size used in the OU 7-13/14 and OU 3-14 aquifer models. This will prevent arbitrarily reducing simulated concentrations at those facilities by averaging over larger grid blocks.

The following capabilities were identified for the transport code during the initial code selection process:

- Advection
- Dispersion (mechanical and diffusive)
- Retardation
- Radioactive decay
- Transient-point and areally distributed contaminant sources to the aquifer.

Despite their limitations, the USGS saturated groundwater flow code, MODFLOW, and the USGS transport code, MT3D, were identified in the initial code selection document as the best codes for OU 10-08 simulations based on the above selection criteria. MODFLOW is a modular, three-dimensional, finite-difference, groundwater-flow modeling code where the various modules of the code deal with different aspects of the simulation. MT3D is a modular, three-dimensional, transport-modeling code compatible with MODFLOW.

The primary weaknesses of MODFLOW are its (a) limited flexibility with the spatial grid design because of its finite-difference approximation approach and (b) inability to simulate flow in fractures. Fracture flow is believed to be an important component of flow at the INEEL at the local scale (Arnett and Springer 1993). At smaller scales, if an equivalent porous media approach cannot explain observations in the aquifer, a fracture flow model might be necessary to improve the model. Ideally, the selected flow code should be able to simulate fracture flow. However, fractured media are often treated as effective porous media, and the Darcian flow assumption is used in most field applications—even in the finite-element-based method. The MT3D code does have the option to use dual porosity for chemical transport in a fractured medium.

An improved transport code is MT3DMS, which is a three-dimensional, multi-species transport simulator for advection, dispersion, and chemical reactions of contaminants in a groundwater system. Improvements include schemes for minimizing numerical dispersion, schemes for improving the stability of time-step sizes, and packages for nonequilibrium sorption and add-on chemical reactions. MT3DMS uses the output flow field from MODFLOW as the input of the transport model. These codes do allow prediction of commingled plume concentration predictions.

Additionally, modelers generally require either an easily modified code to support changes in input and output formats or some form of a user interface to facilitate code programming. Recent OU 10-08 modeling has focused on the graphical user interface system, GMS, that was developed by the U.S. Army Corps of Engineers for a consortium of federal agencies, including the DOE (BYU 2002). As such, contractors supporting DOE groundwater modeling have access to GMS.

This user interface allows easy conversions of conceptual models to numeric models, allows quick updates that result from conceptual model changes, prepares model input files, and processes output. GMS supports several finite-difference and finite-element groundwater flow or transport codes, such as MODFLOW, MT3DMS (an improvement over MT3D), and FEMWATER. Unless major flaws are identified with this approach, the SWGM will be developed using GMS and most likely MODFLOW and MT3DMS.

However, it is important to note that codes such as MODFLOW cannot be used to model heat transport. The simulation of heat transport must be accomplished through a separate but coupled model using another modeling code such as PORFLO, SUTRA, TOUGH2, or TETRAD.

5.1.5 Model Coupling

It is commonly recommended that geochemical data, if available, be used to strengthen the conceptual model. Water geochemistry can be used to infer flow directions, identify and quantify sources of recharge, estimate groundwater flow rates, and define local, intermediate, and regional flow systems (Anderson and Woessner 1992). Typical geochemical analyses include major cations and anions, temperature, and stable and radiogenic isotopes.

It might be possible to model geochemistry using a mixing model approach oriented along primary streamlines, as described in the literature (Dahan et al. 2004), to define preferential pathways and guide the development of the numerical flow model. Recent INEEL geochemistry analyses are described in detail in Section 4.

A regional application of heat transport concepts is seen in the definition of the effective base of the SRPA; the effective base is currently defined through a combination of observed phenomena, including the change from a convective-dominated heat transport to a purely conductive heat transport regime (Smith 2002). Smith (2002) used vertical temperature profile data from six deep wells at the INEEL that penetrate the entire thickness of the active portion of the aquifer. An additional deep well, Middle-1823, has been drilled since then and also logged for vertical temperature data. Smith (2002) also incorporated thermal profile data from seven other shallower aquifer wells to help define aquifer thickness.

Indeed, an abundance of ESRP water table temperature and water well thermal profile data have been collected over the past 40 or more years by researchers from the USGS, the INEEL, and various academic institutions. Temperature vertical profile data for use in a complementary SWGM thermal model include information on 87 wells at or near the INEEL. Thermal profile data for another 38 wells located on the ESRP, but outside the INEEL boundaries, are also available. Most of these 125 wells do not penetrate the entire aquifer thickness, and the dates of their temperature logs range from 1960 to 2003.

Additionally, almost all wells within the proposed OU 10-08 model domain that have been logged or sampled in some manner by the USGS have some representative water table temperature value associated with them. Water table temperature data are available for more than 800 wells in the general vicinity of the proposed model domain.

The observed spatial variation in temperature helps define significant flow field differences. Therefore, modeling the thermal effects as heat transport analogous to solute transport will be beneficial. Most model codes for groundwater flow, however, ignore the contribution of thermal gradient to groundwater flow. Still, the thermal contribution might be significant for a comprehensive flow and transport set of models. For example, it is well known that mineral dissolution rates increase with increasing temperature. Modeling the temperature dependence of mineral dissolution rates to generate the observed geochemically defined fast-flow paths might prove very useful.

5.2 Discretization of Space and Time

An important part of the conversion of a conceptual model to a numerical model is the discretization of space and time. How grid layouts, node spacing, boundary locations and types, and time-stepping are selected greatly influences simulation outcomes.

5.2.1 Model Type

Models can be either transient or steady state, confined or unconfined, and consider one, two, or three spatial dimensions. Two-dimensional areal and quasi-three-dimensional models assume the aquifer viewpoint, while full three-dimensional models use the flow system viewpoint. It is anticipated that the SWGM will be a full three-dimensional model.

Transient effects in a groundwater flow system are the temporal changes in heads or flow directions induced by time-dependent stresses to the system, such as seasonal variations in recharge or groundwater pumping. For contaminant transport modeling, steady-state models, which do not include transient stresses, are applicable where flow directions, and therefore solute transport, are little affected by the transients that invariably occur. This might be because the transients are essentially negligible, they are of sufficiently short duration that they have little impact on long-term average transport directions, or the water level changes occur almost uniformly across the region so that there is little impact on long-term average transport directions. The modeling process thus requires that the magnitude of system transients and the impact of those transients on contaminant transport be assessed to determine whether the transport processes must be included in the simulations to accurately predict long-term fate and transport behavior. So, although the SWGM will initially be defined as a steady-state system, the final flow model may incorporate transient effects if the modeling process indicates that is necessary.

5.2.2 Domain Size

The domain, or area extent, of the SWGM should represent an area that extends beyond the institutional boundaries of the INEEL to include regional flow effects and to ensure that risk assessment studies will be adequately supported by a model domain extended sufficiently downgradient of the INEEL southern boundary. This will allow incorporation in the model of important regional physical features and processes that affect groundwater flow in contaminated INEEL areas. It is important that the boundaries of the model be located far enough to prevent them from affecting the flow field in the areas of interest.

However, the domain should not attempt to represent the entire ESRP. Including simulation of complex surface-water features such as the Snake River is impractical. It is also important to control the overall model domain size. It is necessary to provide sufficient grid resolution at individual WAG scales while keeping the total grid cell count to a size compatible with a manageable computational burden.

Figure 5-1 shows the current configuration of the model domain. This domain covers nearly 3,000 mi^2, as proposed initially in the OU 10-08 modeling strategy report (Arnett and Smith 2001). The domain is approximately 89 mi along the general direction of groundwater flow, between 27 and 38 mi in the transverse direction, and oriented along the principal axes of the Snake River Plain. Figure 5-1 depicts model boundaries, INEEL institutional boundaries, and locations of other important model features.

5.2.3 Boundary and Initial Conditions

The boundaries of the model play an important role in the model output, and care should be used in their selection. For numerical models, there are three possible boundary types referred to as Types 1, 2, and 3.

Type 1 boundary conditions are specified head boundaries, also known as Dirichlet conditions, for which head is always specified and fixed (Anderson and Woessner 1992). The prescribed head (Dirichlet) boundary conditions are as follows:

$$h = \bar{h}(x, y, z, t) \tag{5-11}$$

where $\bar{h}(x, y, z, t)$ defines the value of the prescribed head boundary conditions in space and time. The head can be prescribed within the domain as well as on the boundary.

Type 2 boundary conditions are specified flow boundaries, known as Neumann conditions, for which the derivative of head (flux) across the boundary is specified. A no-flow boundary condition is set by specifying the flux to be zero. The flux (Neumann) boundary conditions are as follows:

$$-K_i\left[\frac{\partial h}{\partial x_i}\right]n_i = q_i \tag{5-12}$$

where

K_i = conductivity

n_i = components (x, y, z) of the outward unit vector normal to the boundary

q_i = i^{th} component of the water flux across the boundary.

Type 3 boundaries are head-dependent flow boundaries, also called Cauchy or mixed boundary conditions, for which flux across the boundary is calculated based on a boundary head value. It is anticipated that the SWGM will accommodate only the first two boundary types (Types 1 and 2) listed above.

As shown in Figure 5-1, the OU 10-08 model domain is bounded to the north and south by Type 1 (specified-head) boundaries. The eastern boundary is a Type 2 (specified-flux) boundary that corresponds to an estimated groundwater flow line. The western boundary is also a Type 2 (specified-flux) boundary that represents the mountain ranges and the mouths of important tributary streams. The base of the aquifer model corresponds to a Type 2 (specified-flux) boundary along an undulating surface, while the top surface of the model corresponds to the surface of the free water table and is modeled as a Type 2 (specified-flux) boundary.

5.2.3.1 Type 1 Specified Head Boundaries. The north and south boundaries of the OU 10-08 model domain are currently considered Type 1 (specified-head) boundaries. The model will simulate groundwater flowing into the model domain through the north boundary and exiting from the domain through the southern boundary. Hydraulic head values will be specified along these boundaries. For the steady-state portion of the SWGM, these will be interpolated using aquifer water levels measured in wells during June 2004. A contour map of the June 2004 water table configuration will support assignment of fixed-head boundary conditions; this map is shown in Figure 4-15. From this map of observed irregularly spaced values, fixed-head values at nodes along prescribed head boundaries can be interpolated. Various interpolation schemes, such as bilinear interpolation, are available to determine hydraulic head values at precise grid node locations.

The southern specified-head boundary is positioned far enough away from the INEEL that it will not affect flow conditions at important locations within the INEEL, i.e., individual WAG model boundaries. It is expected that hydraulic heads interpolated from observed heads in the area will be specified along the boundary. This boundary is currently 37.7 mi long.

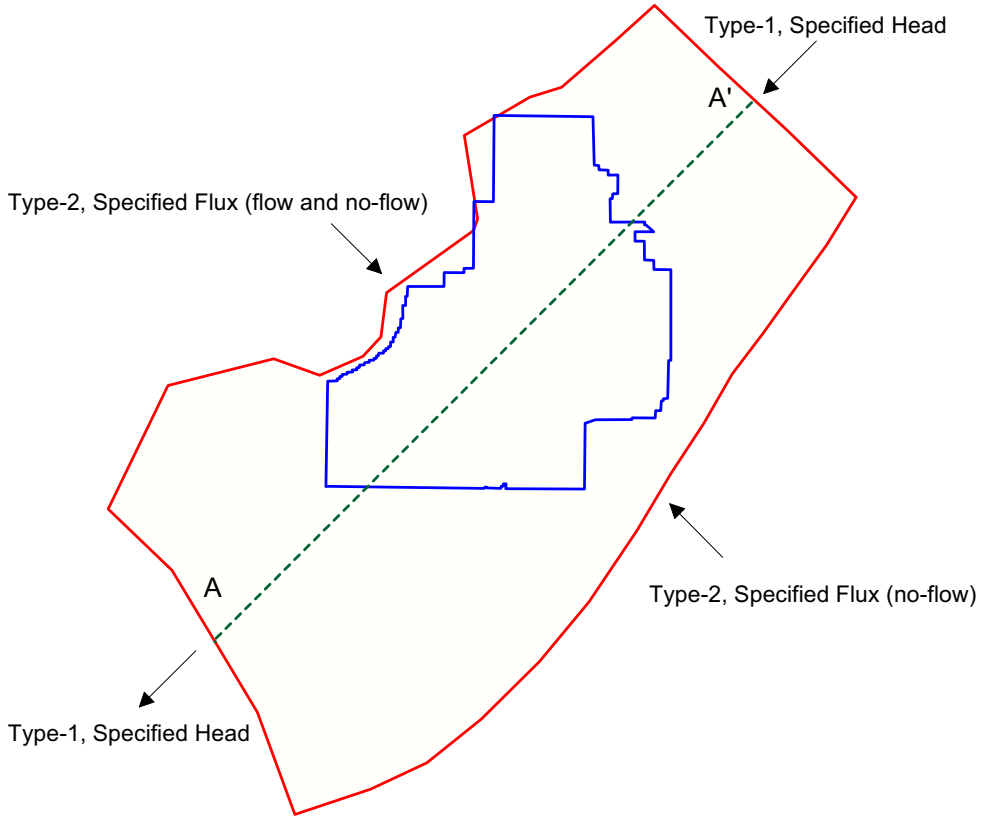

a) plan view

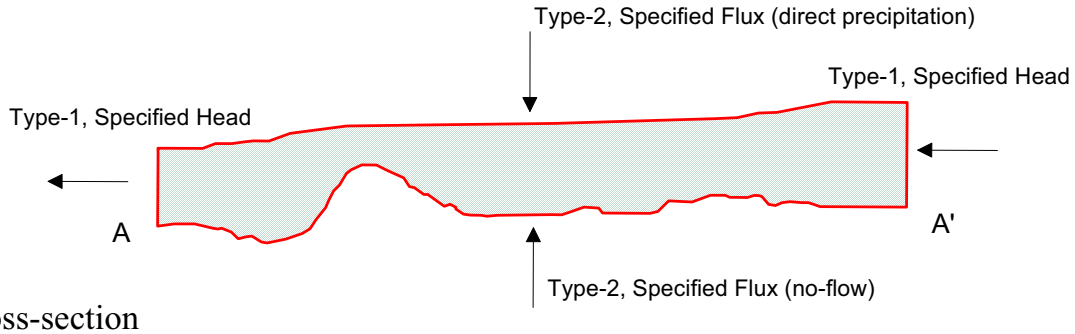

b) cross-section

Figure 5-1. Depiction of model domain and boundary conditions in (a) plan view and (b) cross section.

The northern boundary of the SWGM is oriented such that it corresponds to the transverse direction of the USGS Mud Lake model (Spinazola 1994). That boundary is approximately 29 mi long and is angled perpendicular to the general south-southwest direction of regional groundwater flow. Because long-term records of head are available along that boundary but the flux across it is only poorly known, a

specified-head condition is the logical choice of boundary type for that segment of the domain. The flux across the boundary is then constrained by the requirements that reasonable conductivities be applied in the hydrostratigraphic description and that downstream heads match observed heads. A specified-flux condition, in contrast, assumes that both the head gradient and the aquifer conductivity are well known.

There are, however, some constraints on the flux through the northern boundary that might be used to test alternative models. The USGS estimated the underflow exiting its Mud Lake model as part of an overall, detailed water balance (Spinazola 1994), and flux through the southern boundary of that model could be used as specified flux for the northern boundary of the SWGM. If review of that water balance suggests that flux through the northern boundary is adequately constrained, that change may be incorporated in the final SWGM. Even if the northern boundary remains as a specified-head boundary, the flux entering the simulation domain across this boundary will be compared against that from the Spinazola (1994) model to look for possible discrepancies between the two models. At a minimum, the sensitivity of the modeling results to the two different boundary conditions will be assessed.

5.2.3.2 Type 2 Specified-flux Boundaries. The eastern boundary of the proposed OU 10-08 model domain extends in a northeast-to-southwest direction and corresponds to an estimated groundwater flow line across which there is no groundwater flow. The assumption of a Type 2 specified flux (here, zero flux) limits the size of the model domain and was selected to avoid the requirement to include direct interactions of the aquifer with the Snake River, which lies farther to the east. The current eastern boundary is approximately 88.7 mi long.

The preliminary model domain is bounded on the west by a Type 2 boundary (part no-flow and part specified-flux) that represents the mountain ranges and the mouths of important tributary streams. The total length of this boundary is approximately 88.8 mi. The toes of mountain ranges (Lost River, Lemhi, and Beaverhead ranges) are assumed to prevent groundwater movement in and out of the model domain and will, therefore, be modeled as no-flow (zero-flux) boundaries. Between these locations, estimates from the USGS regional aquifer model (Garabedian 1992) will be used as preliminary estimates of groundwater flux from tributary valleys.

Currently, the western boundary includes specified fluxes due to tributary underflow from the Big Lost River, Little Lost River, and Birch Creek, for which Garabedian (1992) estimates of underflow across the western boundary are available and listed in Section 4. Typically, surface-water streams entering the model domain can be expected to have a component of underflow beneath the land surface. These are only included in this boundary if the underflow enters the model domain at the water table. There are other surface streams along this boundary, such as Warm Springs Creek and Deep Creek, but their underflow contributions are very minimal compared to the other three tributary valleys along this boundary. Other nearby creeks, such as Medicine Lodge, Beaver, and Camas creeks, are not included in boundary conditions; they have been included in the USGS Mud Lake model and might make a contribution as underflow to the SWGM if the northern model boundary is made a Type 2 specified-flux boundary with input from the USGS Mud Lake model.

Other boundaries requiring specification during the model construction phase include the upper and lower horizontal surfaces of the model. The upper surface of the model conforms to the free water table surface, as defined in the steady state by the June 2004 water table contour map in Figure 4-15. If MODFLOW is used to construct the numerical model, then the upper surface will extend somewhat beyond the June 2004 water table elevation in order to contain within the model domain any simulated high-water conditions. Regardless, the upper surface boundary comprises a Type 2 specified-flux boundary with only a minor influx contributed through the unsaturated zone throughout most of the domain. Significant fluxes across the upper boundary of the model will likely exist only in areas that lie directly beneath significant surface water within the model domain.

The bottom boundary of the SWGM corresponds to the base of the active aquifer, as currently defined by Smith (2002). This is not a horizontal surface, and its location is not well defined throughout much of the domain. Therefore, additional studies to better constrain the location of the bottom boundary of the aquifer have been included in this work plan. Currently, the base of the active aquifer is defined through an analysis of temperature profiles and electrical resistivity data, which describe an undulating surface of temperature gradient and resistivity changes. The surface is believed to reflect a strong decrease in permeability, below which horizontal flow is comparatively negligible. This boundary will therefore be approximated as a Type 2 specified-flux boundary with zero flux , unless further study indicates that fluxes through the bottom boundary are a more significant control on groundwater flow directions than has been estimated previously.

The model domain and boundary conditions for the heat flow model will be chosen to reflect our best understanding of that system. The model domain will likely be larger in order to extend the northern and southern boundaries to areas with significantly different temperature profiles, such as the cold-water recharge area associated with mountain-front runoff from the Yellowstone Plateau. Geothermal heat flux estimates from previous geothermal studies (Blackwell 1983; Ziagos and Blackwell 1986) in the region will be used to define a Type 2 boundary for the bottom of the aquifer, which will coincide with the bottom of the groundwater flow model. Flux in the heat transport model is defined as energy per unit time per unit area, or power per unit area. The land surface will be used as the upper boundary for the heat transport model, with a Type 1 boundary condition defined by average annual temperatures. The model will be run to steady state using these boundary conditions to match observed temperature profiles in the region.

5.2.3.3 Initial Conditions. In addition to boundary conditions, transient simulations require that initial conditions be specified. Transient simulations are those that include a change of some parameter with time, i.e., some non-constant stress is applied to the system. Initial conditions describe the head distribution throughout the model system at the beginning of the simulation and are, therefore, boundary conditions in time.

Transient flow simulations will prove useful for the OU 10-08 cumulative risk assessment process. Previous researchers (Robertson 1974; Goode and Konikow 1990) have recognized that transient recharge conditions might significantly affect solute dispersion in the aquifer. However, both studies were indeterminate regarding the need to include transient flow conditions when simulating transport. Transient flow simulations would also allow development of a predictive capability for assessing whether future water resources will meet critical INEEL mission requirements, such as cooling water for new reactors.

In the SWGM effort, initial conditions for transient simulations will be generated from a steady-state head solution from the calibrated flow model. For steady-state conditions, the head distribution will be calibrated against the June 2004 water level data set. The transient solution will also be used to generate dynamic conditions consisting of a set of heads that represent observed water level fluctuations occurring at differing time scales.

5.2.4 Grid Layout

The size of the nodal spacing in the horizontal dimension is a function of the expected curvature in the water table or potentiometric surface (Anderson and Woessner 1992). Finer nodal spacing is required for highly undulated water tables. Spatial variation of the hydraulic parameter should also be considered in the selection of node spacing. Currently, the minimum base node spacing used in any of the three existing individual WAG models is 1,000 ft in the WAG 7 groundwater model, but each WAG model also has local refinements with smaller node spacing. For instance, the WAG 7 model is refined near the

SDA with a grid spacing of 500 ft. The WAG 3 groundwater model has a base grid spacing of 1,312 ft and is refined to 656 ft within facility boundaries. The WAG 1 groundwater model has a 5,249-ft base grid spacing and an 82-ft refined spacing resulting from a six-layer telescopic refinement scheme.

Some optimization will be required to find the ideal grid spacing; spacing that is too coarse will fail to capture groundwater flow, but spacing that is too fine will result in an unwieldy number of grid cells and reduced computational efficiency. It is anticipated that a variable grid spacing scheme will be required. Toward the margins of the model, the grid spacing will be largest; flow directions in those areas have little impact on the required contaminant transport predictions. Local refinements will be made at the portions of the model corresponding to the individual WAGs. This might be important in revisiting the initial code selection; MODFLOW uses a structured grid discretization. As a result, local refinements made at individual WAGs must be carried throughout the model in both grid alignment directions.

5.2.5 Time Steps

Selection of the time step is usually a critical decision in model design, because the discretization of time in the model greatly affects numerical results (Anderson and Woessner 1992). Model accuracy and computational efficiency must be balanced. It is best to use small nodal spacing and small time steps to better approximate the partial differential equation; however, the sensitivity of the solution to both space and time-step size should be evaluated. The size of the time step can be allowed to increase as the simulation progresses, but the size should not increase at a rate more than 1.5, although MODFLOW offers a user-specified multiplier to increase the size of the time step as a geometric progression (Harbaugh et al. 2000).

5.3 Hydrologic Property Distribution

The distribution of hydraulic properties within the modeled domain must balance the practicality of a simplified subregional conceptual model with the local-scale effects modeled by individual WAG groundwater simulations. The complex aquifer matrix resulting from thin basalt layers of varying permeability extruded from somewhat aligned vent sources and separated by sedimentary layers might yield anisotropic conditions as well.

Recent geochemical studies reveal flow patterns that are not entirely in agreement with potentiometric surface maps. Subregional-scale potentiometric surface isocontours indicate a general southwest gradient direction consistent with regional flow direction that is parallel to the longitudinal axis of the Snake River Plain. However, isotope studies delineate flow pathways that are generally northwest to southeast, which is in orientation with primary volcanic features and preferred hydraulic conductivity predictions (see Section 4). Yet practical limitations in the detail that can be included in this model might exist.

5.3.1 Conductivity Zones

Initial hydraulic conductivity field assignments will be based on a zonation approach adopted from the USGS model (Garabedian 1992) and modified in the previous OU 10-08 modeling effort (McCarthy et al. 1995). These are depicted in Figure 5-2 for the OU 10-08 model domain. The Parameter Estimation (PEST) modeling package will be used to support parameter adjustments. PEST is a model-independent, nonlinear-parameter-estimation package that automates the adjustment of parameters to match calibration targets. This initial conductivity field in the OU 10-08 model will be adjusted using PEST during the calibration process described in Section 7. This process will also estimate the coefficient of variation (CV) for each zone where the CV is the standard deviation divided by the estimated value. High CV values would indicate potentially beneficial locations for additional wells. More importantly,

however, the selection of locations for additional wells will have to consider the impact of the uncertainty in hydrologic properties and water levels at those locations on predicted concentration and risk at hypothetical receptor locations.

Average values at the subregional scale have not been estimated because of heterogeneity attributed to the complex stratigraphy of basalt and the effects of volcanic rift zones on hydraulic properties. Tests suggest that vertical hydraulic conductivity is substantially less than horizontal hydraulic conductivity (Johnson and Frederick 1997). Conductivities may be modified by constant multiplier factors for different layers beneath the top layer of the three-dimensional aquifer model.

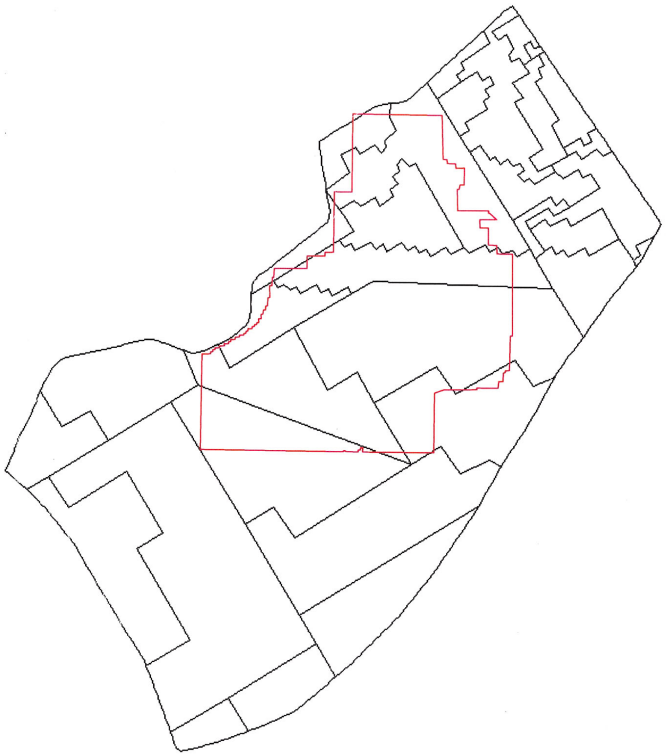

Figure 5-2. Initial hydraulic conductivity zones, as modified from Garabedian (1992), Spinazola (1994), and McCarthy et al. (1995).

5.3.2 Hydrostratigraphic Layering and Aquifer Thickness

The upper vertical extent of the modeled system will be limited by the configuration of the water table, because the SWGM is expected to be a completely saturated model (i.e., no vadose zone representation). The surface will contain some local variations but otherwise is a relatively flat upper boundary. Conversely, the bottom surface of the conceptual model is believed to be highly variable; this surface determines aquifer thickness, which has a significant impact on the resulting groundwater flow field.

Hydrostratigraphic units that will "lump" detailed information about the stratigraphy and lithology in the numerical model will need to be defined; this will require a good understanding of the geology and hydraulic properties of these features before designing the layering and property distributions in the initial conceptual and numerical models. Thus, more work needs to be done to identify and delineate key stratigraphic and lithologic features so that assignment of hydraulic properties can be made to a few (less

than 10) stratigraphic units. Until the OU 10-08 hydrostratigraphic evaluation is complete, the proposed conceptual model will consist of seven layers that are consistent with the USGS condensed model layering.[1] The OU 10-08 conceptual model will use hydrostratigraphic units based on stratigraphic data, geophysics, pumping tests, and hydrogeologic interpretations. Upper fractured basalt is represented by several layers equivalent to one of the important composite hydrostratigraphic units of the USGS conceptual model.

The OU 10-08 conceptual model includes another composite layer that is also equivalent to a unit in the current USGS conceptual model. This unit underlies the upper units and represents a section of thick, dense, basalt flows and interbedded sediments. This composite layer represents several different layers and intersects the water table (upper boundary of the OU 10-08 model) south of the INEEL. It is not perceived to be a flow barrier. The lower extent of this layer determines aquifer thickness. The thick aquifer and thin aquifer alternative interpretations described in Subsection 4.2 are equally likely, and both will be considered in the SWGM. Some issues persist with portions of the current interpretations of aquifer thickness and how to incorporate these in the numerical model. For instance, preliminary two-dimensional modeling, with a single model layer but a variable grid thickness, has indicated that potential incompatibilities exist between interpreted thickness and underflow estimates along the western boundary of the OU 10-08 domain. Unusually high head buildup in this portion of the preliminary model suggests that underflow estimates are too high or thickness estimates are too low.

5.3.3 Transport Properties

A logical assignment of transport properties is required to satisfactorily simulate observed contaminant concentrations. The set of transport properties—refer to equation (5-3)—includes effective porosity, dispersivities, retardation coefficients, half-lives, and source terms.

The individual WAG models will determine contaminant source terms. The output of the vadose zone models for these WAGs will be included as input to the top of the aquifer in the SWGM. Other transport parameters will vary significantly from the local to subregional scale.

Total porosity is defined as the percentage of aquifer matrix that is void space. Effective porosity is limited to the void spaces that are interconnected and not dead-end pores (Domenico and Schwartz 1990). The effective porosity range of the SRPA is discussed in detail in Section 4. The SWGM will match the effective porosities used in individual smaller-scale INEEL models, noting also the reduction in porosity expected with depth in the aquifer.

Dispersion refers to the spreading of contaminants (and, analogously, heat) caused by variation in groundwater velocity. The model derives an average linear velocity, but in reality, porous media cause the velocity to be distributed over a wide range locally. Contaminant movement is strongly influenced by the presence of local heterogeneities that cause deviations from the average linear velocity (Freeze and Cherry 1979). Dispersion includes the process of diffusion, which is complicated by electrical charge (Fetter 1988). A modification of Fick's law of diffusion captures the dispersion concept in the following expression:

$$\frac{\partial C}{\partial t} = \frac{\partial}{\partial x_i}\left(D_{ij} \frac{\partial C}{\partial x_j} \right) \tag{5-13}$$

where

D_{ij} = dispersion coefficient

C = contaminant concentration.

This dispersion coefficient is typically expressed as follows:

$$D_{ij} = \alpha_{ijmn}(v) + D_d \quad (5\text{-}14)$$

where

D_d = molecular diffusion

v = average linear velocity

α_{ijmn} = all components of dispersivity.

Dispersion is complicated by scale; dispersivities seem to increase as contaminant plumes move downgradient (Anderson and Woessner 1992). Another complication in quantifying dispersion results from channeling of contaminants along paths of high hydraulic conductivity or preferential flow paths. Dispersion also appears to be affected by transient recharge or water supply conditions that change the velocity. Historical groundwater modeling at the INEEL (Robertson 1974) required higher transverse dispersivities than longitudinal dispersivities in order to match observed chloride plume data. This is not typical of large-scale modeling and was attributed to changing velocities resulting from transient recharge (Goode and Konikow 1990).

Chemical reactions affecting transport include sorption reactions and decay. Contaminant half-lives are usually constants whether they are for radioactive decay or chemical and biochemical degradation, although local groundwater geochemistry conditions might affect these later decay rates.

Sorption reactions are simulated via retardation. Retardation describes whether a contaminant in solution with groundwater acts as a conservative tracer. Conservative tracers do not react with the aquifer matrix and move with water via advection with dispersion. Non-conservative tracers undergo various chemical reactions, including adsorption-desorption or cation exchange with the aquifer solid matrix. The retardation factor quantifies the distribution of contaminants between solid and liquid phases. This factor is a function of the solid's density and a distribution coefficient for the contaminant specific to the matrix. Typically, this distribution coefficient is determined experimentally. The retardation coefficient can also vary spatially depending on local groundwater chemistry conditions (Kehew 2000).

5.3.4 Local versus Regional Properties

The assignment of hydraulic properties within the OU 10-08 model domain corresponding to local scales at individual WAGs must be consistent with individual WAG modeling efforts. The OU 10-08 conductivity field must reflect individual WAG models' conductivity fields. For instance, the saturated portion of the WAG 7 groundwater model has horizontal hydraulic conductivity ranging from 0.42 to 195 ft/day. In addition, the Spinazola (1994) conductivity field may be used for the upper northeast portion of model domain.

Aquifer test results at INTEC support a conceptual model of an aquifer locally characterized by highly heterogeneous hydraulic properties that appear homogeneous when examined at a sufficiently large scale. With regard to storage, INTEC tests suggest that the basalts of this area respond locally as a leaky confined aquifer with a composite storage coefficient of 7E-6 (Frederick and Johnson 1996).

Geochemistry analyses discussed in Section 4 suggest that groundwater even at the subregional scale (tens to hundreds of miles) might be influenced by features such as fast flow paths, which are capable of moving contaminants downgradient much faster than other portions of the aquifer.

Temperature changes with depth observed in several deep aquifer wells at the INEEL suggest that the lower surface of the active (flowing) portion of the aquifer might be extremely varied, i.e., an undulating surface that affects overall thickness of the aquifer. These features will be incorporated in the SWGM.

Spatially variable transient changes to water table conditions should also be considered in the SWGM to provide a more realistic portrayal of the contaminant transport effects of changing overall water supply. These changes have been observed in the SRPA on various temporal scales, including seasonal (due to irrigation practices and annual recharge), decadal (due to long-term climate effects on recharge), and long-term trends (declining water table conditions occurring over the past 50 years because of the changes in irrigation efficiency and increases in water use).

5.4 Numerical Model Construction Summary

The following is a summary of tasks needing immediate attention before completing construction of the SWGM:

- Improve the definition of tributary underflow flux.
- Improve the definition of the active aquifer thickness.
- Determine the sensitivity of simulation results to changes in the boundary condition type at the northern boundary.
- Improve the definition of layering to be used in the numerical model.

6. DATA GAPS

Hydrologic research at the INEEL over the past 50 years has resulted in a large body of information about the capability of the SRPA to transmit water and contaminants. However, much of this information was collected from areas near facilities within the OU 10-08 model domain; information from other areas is limited or nonexistent. Properties used in flow and transport simulations across the INEEL site are extrapolated from this limited information. Unfilled gaps in understanding caused by insufficient data could have a significant impact on the ability to predict contaminant transport in the SWGM.

In the course of developing this work plan, specific data gaps have been identified. These data gaps have been organized into four general discipline areas: (1) geology/geophysics, (2) geochemistry, (3) hydrogeologic data, and (4) modeling. Organizing data gaps into these discipline areas helps to manage the collection of data to fill the gaps. The four categories of data gaps are discussed individually below, although many data gaps are cross-cutting discipline areas.

6.1 Geology/Geophysics

The geology/geophysics category includes data gaps primarily associated with the understanding of the geologic framework (stratigraphy) of the SRPA. Geologic understanding is based on interpretation of borehole geophysical logs, surface geologic maps, remote sensing, surface geophysical methods, well logs, collected cores, petrologic microscopy, paleomagnetics, and other remote and direct methods of subsurface interrogation.

6.1.1 Direct Evidence (Temperature, Core Description, Neutron Logs) of the Active Aquifer Thickness

Direct evidence (temperature, core description) of the active aquifer thickness is limited to nine wells in the central part of the INEEL site. Elsewhere throughout the area represented by the OU 10-08 model domain, thickness is inferred from electrical resistivity data (with significant uncertainties) and groundwater temperature in the upper part of the aquifer. Additional borehole data are needed in areas where direct evidence of the active aquifer thickness is unavailable.

Well USGS-22 was drilled in the southwestern part of the INEEL site. Geochemical, temperature, and other data from this well indicate that the SRPA in this area could be very thin. The nearest borehole is over 3 mi to the east, however, and additional boreholes are needed in this area to evaluate aquifer thickness. Drilling south of the Power Burst Facility, along the southern INEEL boundary, might significantly reduce the uncertainty over current interpretations of thick and thin aquifer scenarios.

In addition, the aquifer thickness near the tributary drainage basins, i.e., the Big Lost and Little Lost rivers, is not well defined. The two-dimensional, one-layer flow model with variable aquifer thickness reveals that the aquifer thickness near these drainage basins greatly affects the flow patterns nearby, and that different estimates of thickness result in completely different (or unreasonable) model parameters. Additional boreholes are needed in these important underflow recharge areas to more accurately estimate aquifer thickness there. Electrical resistivity surveys are also recommended in order to fill the gaps between boreholes.

6.1.2 Stratigraphy

Basalt flows of the same age do not correlate between TRA and INTEC. Basalts dated at ~414,000 to ~441,000 years old are 200 to 250 ft deeper under INTEC than under TRA. Basalts dated at ~640,000 years old are 300 to 400 ft deeper under INTEC than under TRA. These vertical discrepancies

imply a major structural change in the stratigraphy under the floodplain of the Big Lost River between TRA and INTEC. The structural change could be caused by a buried fault, a fold, or a topographic feature like a canyon wall. The exact nature of this feature and how it affects groundwater flow are unknown, because a gap exists in borehole coverage between TRA and INTEC. So additional boreholes are needed in this area to determine the cause of these large vertical discrepancies in the subsurface stratigraphy.

6.1.3 Vertical Distribution of Water Temperature within the SRPA

The spatial distribution of water temperature at the top of the SRPA indicates that locally recharged water might not be vertically mixed within the aquifer but is instead spread laterally over the upper part of the aquifer (e.g., cool water beneath the INEEL spreading areas and the Big Lost River). The effect of locally layered water on the three-dimensional geochemistry of the active aquifer is not well defined. Additional depth-integrated, water-temperature geophysical logs are needed to improve the understanding of the three-dimensional thickness and geochemical features of the SRPA. Areas of importance include those areas in proximity to identified "fast paths" and recharge areas. Flowmeter logging of open boreholes might also aid in the identification of fast-path zones in the aquifer.

6.2 Geochemistry

The geochemistry category of data gaps includes the general geochemical understanding of groundwater and geologic media beneath the ESRP. Two primary subdivisions of this category can be made: (1) naturally occurring variations in aquifer water that are caused by different sources and contact times with geologic media and (2) anthropogenic alteration (i.e., contamination) of aquifer waters.

6.2.1 Geochemical Modeling

Geochemical modeling codes have rapidly evolved over the past decade but still cannot be fully incorporated into a GMS-type hydrologic model. This represents a key gap in our groundwater/ contaminant transport modeling capability and forces the use of adsorption isotherms to describe geochemical processes. Such isotherms describe subsurface transport behavior but are based on a faulty conceptual model that contains a significant amount of unquantifiable error. Filling this capability gap is a critical long-term need. To help address these limitations, both geochemical data (i.e., fast-flow paths, aquifer thickness, and aquifer temperature data) and anthropogenic plume geometries will be used to calibrate the SWGM. This approach addresses short-term needs and will make the model more consistent with the current conceptual model for fate and transport in the SRPA. However, this approach also assumes that the processes controlling contaminant fate and transport in the SRPA are well understood, the processes can be fully emulated in a laboratory experiment, and the patterns of observations are not based on some unrecognized processes. Thus, there is a critical long-term need to build an SWGM capable of incorporating advances in geochemical science and incorporating these advances into a process-based conceptual model. Current data gaps (i.e., the lack of a detailed three-dimensional data set) alleviate this need for the short term but do not preclude it.

6.2.2 Natural Geochemical Data in the Vicinity of USGS-22

Additional geochemical data are needed in the vicinity of well USGS-22, which was drilled in the west-central part of the INEEL site to evaluate the age of water and areas of "stagnation" within the SRPA. Geochemical, temperature, and other data from this well indicate that the SRPA in this area could be very thin. Geochemical data from additional boreholes, or from the deepening of USGS-22, are needed in this area to evaluate these geochemical anomalies.

6.2.3 Three-Dimensional Natural Geochemistry

Current well completions within the OU 10-08 model domain commonly provide water samples that are representative of only the most conductive horizon in the completed interval. This "selective sampling" has resulted in the assumption that the aquifer is chemically homogeneous. Additional information is needed to define the three-dimensional distribution of geochemical data in the SRPA and to assess possible preferential flow paths. This information will require depth-integrated sampling in selected wells.

"Fast" or preferential groundwater flow paths within the SRPA have been identified from isotopic data. These paths have tentatively been associated with rift zone features, but other competing hypotheses such as collapse structures or gravel-rich sands (river channel deposits) have equal merit. Locally, these preferential flow paths are not in agreement with the regional hydraulic head-based flow paths, indicating that water level data might not be sufficient to delineate local flow paths. Most wells providing groundwater geochemistry information in the OU 10-08 model domain are completed in the upper part of the active aquifer. These data are being used to evaluate flow paths and contaminant migration in groundwater. Additional work is needed to refine our understanding of preferential flow, its effect on contaminant migration, and the relationship between geochemical and hydraulic data.

6.2.4 Determination of Anthropogenic Contaminant Sources

Until recently, the distribution of tritium in groundwater was attributed primarily to waste-disposal practices at INTEC and TRA. Water chemistry data from additional wells drilled east and northeast of the RWMC have since indicated that a discrete tritium plume might originate from the RWMC. However, this potential source and the actual distribution of tritium are not well identified. Evaluation of potential sources of contaminants will require additional geochemical analyses based on existing conservative geochemical tracers that were present with tritium in the source areas.

6.2.5 Partitioning Coefficients for Anthropogenic Contaminants

Partitioning coefficients (K_ds) have been estimated from laboratory tests for several non-conservative contaminants. These K_ds lump a number of factors that affect sorption of dissolved contaminants to basalts and sediments. Characteristically, the factors that contribute to these K_ds are not well understood. The primary modeling approach outlined in this work plan continues to utilize the large-scale lumped-property K_d approach.

A parallel approach will also be pursued in which the appropriateness of the use of K_ds is evaluated. Simulating or predicting the transport of solutes at the INEEL site has relied on empirical solute partition parameters for each individual solute of interest in each distinct geochemical regime in the conceptual model for the subsurface. The partition parameters are conventional K_d parameters—simple ratios of adsorbed mass of solute per mass of solid to the dissolved concentration. Limitations to K_d parameters have been discussed extensively in the scientific literature, but describing solute retardation using a K_d has several advantages and can be valid as long as a number of critical criteria are met, e.g., Davis et al. (2004). The uncertainties in K_d parameters, and controversies over the validity of K_d parameters, generally focus on the set of basis assumptions and criteria for use, which are frequently overlooked. The INEEL has a responsibility to defend the conceptual model for contaminant transport. OU 10-08 will analyze critical assumptions behind the use of K_d parameters at the INEEL site and how values are assigned.

Defense of the K_d, and subsequently the values for individual K_ds that will be used at the INEEL, should be separated into four areas that can be treated independently:

1. The chemical equilibrium and reversibility assumption: A K_d parameter is only valid if the set of partitioning reactions are reversible and equilibrium conditions can be assumed. Further, geochemical and biologic heterogeneity, even on small scales, can impact the approach to equilibrium states depending on rates of flow and diffusion.

2. The scientific basis for K_d: The advantage of a K_d measurement is that it captures the complex nature of natural materials. There is also a fundamentally sound basis for the K_d. The main issue is whether the assumption of linearity is valid within the range of conditions expected in a contaminant plume.

3. The method of measurement: K_d parameters are determined in laboratory experiments where sample collection and alteration methods raise concerns about the types of surfaces actually accessed by solutes. Alternatively, effective K_d parameters could be derived from field data.

4. Even if all criteria for using a K_d are met, computational issues (e.g., interpolation) in incorporating K_d into the models of the geochemical reactions in flow need to be addressed.

In the OU 10-08 analysis of the K_d parameters for the INEEL site, each of these assumptions will be analyzed in order to help establish the defensibility of the contaminant transport models applied to the INEEL site.

6.3 Hydrogeologic Data

The hydrogeologic data category focuses on data gaps in our understanding of how water is transmitted and stored in geologic media beneath the ESRP and, more important, how detailed information can be simplified for use in the numerical simulation.

6.3.1 Delineation of Hydrostratigraphic Units

Although a significant amount of borehole stratigraphic data has been accumulated, hydrostratigraphic units have not been adequately defined within the OU 10-08 model domain. Delineation of these hydrostratigraphic units is required to “lump” hydraulic properties into layers for modeling. This “lumping” will require a good understanding of the geologic, geochemical, and hydraulic properties of the INEEL subsurface. Hydrogeologic data include aquifer test information, tracer tests, statistical representations, water levels, fast path controls, and plume geometries. Ideally, the conceptual understanding of the subsurface can be simplified into to a few (fewer than 10) stratigraphic units.

In some areas, boreholes providing stratigraphic data are widely spaced and correlations are uncertain. Areas most important to this effort are those in the vicinity of individual WAGs, specifically WAGs 1, 3, and 7. Distribution of hydrostratigraphic units in these areas is tentative. However, areas downgradient from the INEEL with respect to groundwater flow are of special importance from a risk-receptor point of view, and only a few wells are needed in these areas to determine the distribution of the hydrostratigraphic units. Additional borehole data are needed in these areas to better define the distribution, thickness, and hydraulic properties of hydrostratigraphic units.

6.3.2 Distribution of Hydraulic Properties (Heterogeneities)

The distribution of hydraulic properties is not well understood throughout the area represented by the OU 10-08 model domain. The extreme complexity and heterogeneity of basalts composing the SRPA is demonstrated in the observed six-orders-of-magnitude variation in hydraulic conductivity. In some areas (e.g., the southern part of the OU 10-08 domain), the absence of wells introduces significant uncertainty about the capability of the aquifer to store and transmit water. Although aquifer test data are available from more than 114 wells, most of these tests are single-well tests and provide only limited information about distribution of hydraulic conductivity in the vicinity of those wells. Additional analyses of existing well test data might be helpful when evaluating hydraulic properties.

The ratio of vertical to horizontal permeability in the SRPA is assumed to be large, based on the layered nature of interflow rubble zones and massive basalt-flow interiors. This ratio is critical in understanding vertical groundwater flow and contaminant migration. Little information is available about the ratio of vertical-to-horizontal permeability. Measured water level differences in wells completed at different depths, particularly measurements from nested piezometers such as those in well USGS-30, indicate that vertical hydraulic gradients occur with depth and that vertical flow might be important if it is not limited by a very small vertical-to-horizontal hydraulic conductivity ratio. Additional work to provide this information will include packer tests in existing wells and construction of additional nested piezometers.

Several major rift zones have been identified within OU 10-08. Indirect information (hydraulic gradient, apparent low-transmissivity zones) indicates that features associated with these rift zones (dikes and other intrusive features, rifts) might have a significant effect on contaminant transport within the SRPA. Direct information about these features is unavailable. Some rift zones might redirect contaminant transport, depending on whether they act as barriers or conduits; redirecting contaminants might shorten paths to risk receptors. Direct information includes well and geophysical studies in proximity to these features.

6.3.3 Hydraulic Head Data

Typically, water level data are used to infer groundwater flow directions. However, water level data truly represent only point measurements of head. Flow directions inferred from them generally assume that there is no refraction of flow due to conductivity contrasts or anisotropy and commonly neglect vertical flow because heads are integrated over long well screens. Water level data, whether on a regional or facility scale, are also often incomplete and can change significantly from one measurement period to the next. There is a need to capture a consistent set of water level data, i.e., data obtained at regular intervals from the same set of wells and over a relatively short collection period. Coordinating data collection with other organizations, such as the USGS, that are collecting similar data will support development of better local, facility-scale, flow-field maps and their sitewide regional counterparts. There is also a need to assemble transient water level data as an aid to developing transient flow simulations.

The SWGM will integrate hydraulic head and geochemical data to provide a new and consistent picture of local and regional groundwater flow fields. Hydraulic head data will be inspected and corrected to obtain the highest quality possible. Corrections might include adjustments for large barometric pressure fluctuations occurring across the timeframe of water level measurements used in the model, measurement device calibration, and well borehole deviation.

6.4 Modeling

The modeling category includes data gaps associated with the numerical simulation of groundwater flow and transport. This category includes how heterogeneous geologic, geophysical, geochemical, and hydrogeologic data will be simplified into the SWGM as layers, boundary conditions, and so forth; how uncertainty will be determined; and how risk will be estimated.

6.4.1 Assumption of Effective Porous Media Flow

At the scale of the INEEL, researchers generally agree that groundwater flow responds as flow through an effective porous medium. Research indicates that at local scales, groundwater flow is increasingly dominated by fracture flow. The scale at which fracture flow becomes important has not been clearly identified.

6.4.2 Modeled Thickness and Boundary Assumptions

Some resolution of active aquifer thickness where tributary underflow enters the model domain along the western edge will be required before the current estimates of tributary underflow can be used. A large degree of uncertainty exists regarding underflow. Current estimates of the active aquifer thickness are not compatible with these underflow quantities.

The model sensitivity to either a specified-head or specified-flux type boundary along the northern edge of the model domain is unknown and should be examined before final model calibration.

6.4.3 Simulation of the Effect of Hydrostratigraphic Unit Distribution on Contaminant Transport

Accumulations of sedimentary interbeds in the area of the BLT recently have been identified as having potentially large control over the direction and velocity of groundwater flow and contaminant migration. This effect is not fully understood. Also, certain interbeds might occur extensively in areas of known contaminant migration. However, limited information precludes a complete understanding of the effect of these interbeds on the retardation and distribution of contaminants in groundwater. Numerical-model sensitivity tests are needed to evaluate the potential effect of these interbeds on contaminant transport within the OU 10-08 model domain.

6.4.4 Numerical Simulation of Contaminants in Groundwater

The potential dispersion of contaminants due to transient recharge should be further examined. Long-term changes have been observed in the water supply of the OU 10-08 portion of the SRPA. These changes have resulted in non-uniformly distributed transient recharge from tributary underflow along the western edge of the INEEL and might cause hydraulic gradient shifts in both direction and magnitude.

Contaminant dispersion in the large, fractured-rock SRPA is not well defined. Previous researchers used inordinately large transverse dispersivities to simulate known plumes. Other researchers have attributed the large transverse dispersivity to spatially non-uniform transient recharge. The issue has significant importance in assessing cumulative impacts from potentially commingled contaminant plumes but is still poorly understood. The numerical model will be used to evaluate potential geohydrologic controls on contaminant dispersion within the SRPA.

WAG-specific and regional numerical models have resulted in projected contaminant plumes that are inconsistent from model to model (Figure 4-25). These inconsistent plume portrayals have resulted

from application of different boundary conditions and fluxes that might not be consistent with subregional fluxes. Work is needed to incorporate our understanding of regional flow into facility-scale models. Factors such as interpolation schemes, grid-size matching, and time-step issues need further study before the SWGM is successful in meeting the modeling goals.

6.4.5 Numerical Simulation of Temperature in Groundwater

Temperature profiles of wells and boreholes in the SRPA represent a yet unexploited means of calibrating groundwater flow models of the aquifer. Because heat is transported in essentially the same manner as solutes, a non-uniform distribution of heat sources in an aquifer produces a temperature signal that is largely defined by water movement in the aquifer. Temperature profiles can thus be used to constrain groundwater flow rates and directions, by calibrating a thermal energy transport model to observed temperature data. Thermal investigations in the Snake River plain have been conducted, and continue to be conducted, by several researchers (Brott et al. 1981; Blackwell 1983; Ziagos and Blackwell 1986). Those studies indicate that thermal sources are, indeed, non-uniform and demonstrate that temperatures from wells screened at different elevation intervals have different signatures. Temperature profiles (see Figure 4-10) thus appear to represent the fullest available three-dimensional data set for the aquifer (geochemical data also provide three-dimensional flow data for similar reasons, but the data are more expensive to obtain). Development and calibration of an integrated model of saturated groundwater flow and thermal energy transport would provide a valuable means of better constraining hydrogeologic conditions in the SRPA. This would, in turn, improve the reliability of contaminant transport predictions based on numerical modeling of the aquifer. Therefore, development and calibration of a three-dimensional thermal energy transport model is included as part of the calibration effort for the groundwater modeling task.

6.4.6 Numerical Simulation of Influence of Spatially Variable Infiltration

The standard approach in aquifer simulation for the SRPA is to assign a uniform infiltration flux as an upper surface boundary condition. As discussed previously in Subsection 4.2.2.3, infiltration varies spatially as a function of whether land surface consists of sediments, gravels, or exposed basalt. Whether this variation in infiltration substantially affects the simulation results can be considered a data gap that will be addressed via a sensitivity case. A variant of the flow and transport simulations will be conducted where infiltration rates will be assigned based on the geologic media exposed at land surface.

6.4.7 Numerical Simulation of Reactive Transport

Reactive transport simulations will be performed as an alternative approach to the standard method of lumping all geochemistry interactions into a single K_d. These simulations will initially be performed along a one-dimensional flow path and compared to existing monitoring data, most likely southward from INTEC. These simulations would use stochastically distributed physical properties that control chemical reactions. Based on the results of the one-dimensional simulation, we will determine whether more detailed geochemical modeling can or should be introduced to the SWGM to replace the use of K_ds.

6.4.8 Steady-state versus Transient Flow Simulations

The viability of selecting a quasi-steady-state condition from what is obviously a transient flow system needs to be assessed. Traditionally, steady-state conditions have been used for convenience to keep the computational burden lower. If water levels do rise and fall in an effectively uniform fashion over most of the simulation domain, then the gradients and flow velocities remain effectively constant and the use of steady-state conditions is appropriate. Whether this condition occurs in the SWGM simulation domain needs to be evaluated.

As discussed previously in Subsection 5.2.3.3, the necessity of including transient flow conditions when simulating transport is indeterminate. At a minimum, transient flow simulations need to be included as sensitivity evaluations in both the two- and three-dimensional flow modeling. These transient simulations will also be used in simulating transport where the effect on simulated concentrations at hypothetical receptor locations will be evaluated.

6.5 Filling of Data Gaps

The preceding subsections clearly identify significant data gaps, particularly with respect to the geologic framework, variability of hydraulic parameters, uneven distribution of data across the INEEL site, and sparseness of chemical data. The model development and testing efforts can provide a useful guide for additional data-collection activities and for prioritizing them. The need for additional data will be continually re-evaluated based on modeling results. The same applies to acquisition priority, but all of this needs to be done in the context of available resources. When possible and within available resources, the data gaps will be filled as modeling progresses. Table 6.1 lists the data gaps, the justification for the data needed, and the strategy for satisfying the data needs. Some data needs cannot be optimized until the model is actually used in the evaluation process.

Table 6-1. Data gaps, justification for the data needs, and strategies for satisfying the data needs.

Number	Discipline	Data Need	Justification for Data Need	Strategy to Satisfy Data Need
6.1.1	Geology/ geophysics	Direct evidence (temperature, core description, neutron logs) of the active aquifer thickness	The current understanding of aquifer thickness is based on limited data. This information is required in order to establish the geologic framework of the flow model, particularly in areas where understanding is limited (e.g., western flank of flow domain, near tributary basins, and stratigraphic discontinuity between TRA and INTEC).	Drill corehole adjacent to USGS-22, and complete the corehole as a monitoring well. Install corehole between TRA and INTEC. Develop a priority list for future drilling projects based on the need for information. Conduct modeling sensitivity test on inflows from tributary basins. To better define tributary basins, collect gravity, aeromag, and resistivity surveys. Log stock, irrigation, and domestic water wells, and evaluate well driller logs.
6.1.2	Geology/ geophysics	Stratigraphic/structural information to explain the 200- to 400-ft vertical discrepancies of dated basalts under TRA versus INTEC	The cause of the vertical discontinuity could significantly impact groundwater flow in the BLT.	Drill a deep corehole through the aquifer in the undrilled area between USGS-80, -66, and -39 on the TRA side of the floodplain and USGS-121, -43, and -57 on the INTEC side of the floodplain, and complete the corehole as a monitoring well.
6.1.3	Geology/ geophysics	Vertical distribution of water temperature within the SRPA	Delineate the vertical distribution and heterogeneity of groundwater flow; identify/confirm “fast flow paths.”	Conduct temperature logging and heat-sensitive flowmeter logging.

Table 6-1. (continued).

Number	Discipline	Data Need	Justification for Data Need	Strategy to Satisfy Data Need
6.2.1	Geochemistry	Natural geochemical data in the vicinity of USGS-22	Limited geochemical information from USGS-22 indicates that groundwater in that area has been in contact with local rocks for extended periods, flow is relatively slow, and the aquifer is thin in this area. The extent of this area is poorly defined but might extend from the base of the Big Lost Range toward INTEC and the RWMC. Additional information is needed about these zones of relatively slow-moving groundwater, their extent, and their effect on contaminant transport.	Collect geochemical information from the well to be drilled near USGS-22. Evaluate acquired water chemistry data with respect to geochemical processes associated with stagnation and fast paths.
6.2.2	Geochemistry	Three-dimensional natural geochemistry	A small but significant amount of existing data indicates that the SRPA is vertically stratified. The geochemical data set largely consists of information from wells completed in the upper part of the active aquifer, which biases the data toward the most conductive horizons in the aquifer. The three-dimensional distribution of geochemical data is needed to better define fast paths and groundwater flow systems.	Conduct straddle-packer tests in deep open boreholes. Drill new boreholes capable of characterizing the change in hydraulic head, temperature, and geochemistry with depth.

Table 6-1. (continued).

Number	Discipline	Data Need	Justification for Data Need	Strategy to Satisfy Data Need
6.2.3	Geochemistry	Determination of anthropogenic contaminant sources	Contaminant migration paths from INTEC and TRA need to be clarified to establish groundwater flow paths for model calibration and for evaluation of commingling plumes. A limited data set of water chemistry suggests that the commingled tritium plume might not extend to the RWMC and that a separate RWMC source might exist. Delineation of the commingled plumes is critical to estimating plume width and evaluating dispersivity in contaminant migration.	Sample for chlorine-36 in selected wells in the TRA/INTEC/RWMC area to trace the groundwater flow path from INTEC. Sampling will be integrated into the sampling done by the individual WAGs. Other possible natural and anthropogenic tracers will be evaluated. Based on geochemical evaluation, additional wells will be located in the area between INTEC/TRA and RWMC to further evaluate the potential for commingling plumes and possible separate sources.
6.2.4	Geochemistry	Partitioning coefficients for anthropogenic contaminants	The distribution of non-conservative contaminants in groundwater at the INEEL is controlled by a number of factors. The cumulative effect is represented by the partitioning coefficient (K_d). Consensus is needed about appropriate ranges of K_ds within the OU 10-08 model domain and at different scales.	Conduct a literature search to evaluate the current understanding of partitioning coefficients for contaminants at the INEEL. Evaluate different factors that make up K_ds from site to site. Develop consensus among INEEL researchers about appropriate ranges of K_d. Evaluate the appropriateness of assumptions necessary to apply K_ds.

Table 6-1. (continued).

Number	Discipline	Data Need	Justification for Data Need	Strategy to Satisfy Data Need
6.3.1	Hydrogeologic data	Delineation of hydrostratigraphic units	Numerous geologic units have been encountered in the SRPA beneath the INEEL site, far too many to represent each unit individually in the SWGM. The complex section of numerous basalt flows and sedimentary interbeds that makes up the SRPA within the OU 10-08 model domain must be "lumped" and simplified to support reasonable numerical modeling activities.	Assess the stratigraphic database in light of recent borehole data. Delineate hydrostratigraphic units based on common hydraulic properties. Use geostatistical techniques to extrapolate the zones between wells across the INEEL site. Identify potential drilling targets to improve the understanding of the areal extent of known hydrostratigraphic units.
6.3.2	Hydrogeologic data	Distribution of hydraulic properties (heterogeneities)	The areal distribution of hydraulic properties of the fractured basalt aquifer is based primarily on single-well tests. An improved understanding of these test data is needed to adequately simulate subregional flow and transport.	Evaluate existing aquifer tests, and include an assessment of early- and late-time data. Evaluate known hydraulic properties in light of stratigraphic, geochemical, and temperature data.

Table 6-1. (continued).

Number	Discipline	Data Need	Justification for Data Need	Strategy to Satisfy Data Need
6.3.3	Hydrogeologic data	Hydraulic head data	Water level data are the easiest to collect and the most widely available regarding the SRPA at the INEEL, and they provide good information about the flow system. However, many uncertainties are inherent in these data. The water table underlying the INEEL is relatively flat, so minor errors associated with water level data—such as inconsistent measurement methods and devices, well deviation, and temporal spacing—can have a significant effect on the calculated local, and sometimes regional, hydraulic gradients. Additionally, in a fractured flow system such as the SRPA under the INEEL site, the hydraulic gradient might not completely coincide with the direction of groundwater flow. Existing water level data must be reviewed to ensure quality and optimize future data-collection efforts. Currently, water level data sets are inconsistent and often incomplete. Problems using these data can be further exacerbated with unquantified error.	The existing water level data must be scrutinized, and the reliability of individual well water levels must be graded. Include an evaluation of the well deviations (and associated corrections), measurement timeframe and equipment, and regional climatic conditions. Local- and regional-scale water levels must be resolved with the grid size of the SWGM in mind. An evaluation of aquifer anisotropy must be conducted by comparing the hydraulic gradients calculated from the water level measurements with that predicted by other data types, such as chemical, thermal, or isotopic data. Areas where significant deviations occur will likely require further field study. Implement consistent collection activities (i.e., regularly follow water data-collection plans and methods documents). Coordinate data collection efforts with the USGS. Quantify sources of error, including error associated with measuring equipment and borehole deviation.

Table 6-1. (continued).

Number	Discipline	Data Need	Justification for Data Need	Strategy to Satisfy Data Need
6.4.1	Modeling	Assumption of effective porous media flow	Groundwater flow at the regional and subregional scale has long been assumed to behave as flow through an effective porous medium. However, scales at which the effective porous medium assumption is valid for the INEEL are unclear. At some local scale, this assumption is increasingly dominated by fracture flow. This scale also determines the finest grid cell sizes that the model can use. More data and study are required to resolve this issue.	Conduct sensitivity analyses with numerical modeling tools. Analyze the existing borehole logs. Fracture density, apertures, and orientations recorded in those logs could be used for volume averaging in order to establish representative elemental volume. The proposed new wells should have the previously mentioned fracture property records. Conduct single-well pumping tests using packers; establish vertical scales. Conduct multiple well-pumping tests; establish horizontal scale. A dual-porosity model might be used for the contaminant-transport modeling to account for the fractured nature of SRPA. Strengthen internal coordination with individual WAGs on the scale issue.

Table 6-1. (continued).

Number	Discipline	Data Need	Justification for Data Need	Strategy to Satisfy Data Need
6.4.2	Modeling	Modeled thickness and boundary assumptions	The active aquifer thickness across the OU 10-08 model domain is poorly defined. In a true three-dimensional groundwater flow model, the variations of aquifer thickness affect the flow patterns, both horizontally and vertically. Furthermore, unrealistic aquifer thickness can result in unrealistic model parameters that reduce model credibility and reliability.	Use model sensitivity to evaluate the effects of uncertainties in thickness and boundary assumptions on contaminant transport and to identify optimal data-collection strategies. Drill new deep wells. Conduct surface and inter-borehole geophysical surveys.
6.4.3	Modeling	Simulation of the effect of hydrostratigraphic unit distribution on contaminant transport	The selection and definition of hydrostratigraphic units in the SWGM will determine fluid flow and chemical transport behavior. Reduction of field and laboratory data to model layers must accurately represent SRPA conditions.	Improve the understanding of aquifer lithology distributions, based on new and existing data and through focused studies as resources allow. Design an SWGM that is flexible enough to easily accommodate new information on hydrostratigraphic units.
6.4.4	Modeling	Numerical simulation of contaminants in groundwater	Large lateral spreading of INEEL plumes might be attributed to transient surface recharge and underflow, deviation of local flow paths from the ambient flow directions, or both. Additional understanding is required to more accurately represent flow projected into the future.	Plume spreading must be correlated to transient surface and underflow recharge from the Big Lost and Little Lost rivers. Conduct a focused geochemical study on local flow paths near INTEC, TRA, and the RWMC. Perform a model-sensitivity study.
6.4.5	Modeling	Numerical simulation of temperature in groundwater	Such simulation allows incorporation of a data set of known values.	Perform numerical temperature simulation.

Table 6-1. (continued).

Number	Discipline	Data Need	Justification for Data Need	Strategy to Satisfy Data Need
6.4.6	Modeling	Influence of spatially varying infiltration on simulation results	The current approach assumes uniform distribution of the low infiltration rate.	Conduct a sensitivity simulation once the base model is developed where infiltration to the surface of the aquifer varies based on geologic media exposed at the land surface.
6.4.7	Modeling	Reactive transport simulation	There are known limitations in the current use of a simplified, lumped K_d for simulating transport.	Perform reactive transport simulations, initially along one-dimensional flow paths, using stochastically distributed properties. Compare the simulations against observed contaminant concentration histories in the aquifer to see if the simulation approach improves agreement. Expand the reactive simulation approach as appropriate, depending on one-dimensional results.
6.4.8	Modeling	Steady-state versus transient flow	The appropriateness of selecting water table elevations from single time points has not been demonstrated. The necessity of using transient flow influences when simulating transport is indeterminate.	Evaluate the appropriateness of using a quasi-steady-state water table. Perform transport simulations using transient flow simulations.

7. CALIBRATION PROCESS

The overall objective of the OU 10-08 groundwater flow and contaminant transport calibration process is to provide a set of optimal values of aquifer hydraulic properties and transport parameters. These values need to adequately reproduce the observed groundwater flow patterns and plume migration history within a pre-established range of error. The values also need to realistically represent the aquifer's physical and chemical heterogeneity patterns and be consistent with the known hydrogeological conditions within the site. The objective of the geothermal model calibration process is to provide optimal aquifer thermal transport properties that adequately reproduce the observed vertical temperature profiles and spatial spreading patterns.

7.1 Identification of Calibration Targets

Model calibration is a multi-step process. Initially, the groundwater flow model is calibrated using appropriate calibration targets. The transport model is then calibrated using the output from the calibrated flow model. The results of transport calibration might lead to refining the flow model and recalibrating in order to obtain satisfactory transport calibration. The calibration process typically includes identifying calibration targets, techniques, and measures of error.

7.1.1 Flow Model Calibration Targets

This OU 10-08 modeling study provides both regional- and local-scale groundwater flow fields for the integration of groundwater flow and transport modeling results from individual WAGs. The flow velocity is the primary parameter of importance. Typically, measured heads and head gradient are the targets used to calibrate the flow model.

The groundwater model flow calibration focuses on assigning hydraulic conductivity within the domain, estimating appropriate values that allow the model to reproduce the measured hydraulic head values at selected key observation wells.

Key wells will be chosen within the area represented by the OU 10-08 model domain to be primary locations for the calibration to ensure that the flow model adequately reproduces the gradients and flow direction through each of the nine facility-specific WAGs. The following criteria will be used to select key wells:

1. Relative spacing with respect to the WAG locations and other well locations

2. Reasonably uniform well completion for all of the key wells

3. Wells with some transient response, particularly near areas of significant infiltration such as the tributary drainage basins.

In addition to the key wells, a large number of additional hydraulic head observation wells will be chosen as secondary flow calibration targets in order to adequately reproduce the intermediate- to regional-scale groundwater flow patterns.

Water levels measured in June 2004 will help define hydraulic gradients that can be used in a steady-state flow calibration. Water levels were measured at nearly all available INEEL aquifer wells within a few days. Hydrologic conditions for the ESRP during June 2004 might not be exactly representative of steady-state conditions, but a regional drought cycle has continued for the previous

five years, and transient recharge fluxes have been minimal. As a result, water levels in the SRPA have been declining gradually in response to small recharge and pumping overdraft.

7.1.2 Contaminant Transport Model Calibration Targets

The calibrated flow model only provides Darcy flux. To predict the chemical transport in groundwater, the other aquifer properties—i.e., effective porosity, sorption partitioning coefficient (or retardation factor), and dispersivity—also need to be calibrated. Therefore, measured concentrations and observed plume movements (or travel times) will be used to calibrate the chemical transport model. Similar to the flow calibration, key wells will be chosen within the INEEL site to be the primary locations for calibration to ensure that the transport model adequately reproduces the history of plume movements near individual WAGs. More specifically, the tritium or chloride concentrations (assumed to be conservative and not retarded) will be used to estimate the effective porosity and dispersivity.

A variety of data is available for use in aquifer transport model calibration. The following are primary sources of information:

1. Distribution of contaminant plumes from the INTEC injection well

2. Distribution of contaminant plumes from the TRA injection well and wastewater disposal ponds

3. Distribution of contaminant plumes from the TAN injection well

4. Natural tracers, including ratios of stable isotopes of uranium or strontium that occur naturally in this groundwater system.

From this plume and tracer information, concentrations as a function of time will be tabulated for use as calibration targets. It is important to note that calibration targets consist of a calibration value and its associated error. Error associated with each calibration value will be assessed. Sources of error include errors in measurements, errors in scaling and averaging, and errors associated with interpolating between measurement locations and model grid node locations. Because minimizing these errors is desirable, weighting schemes will be used to provide a measure of relative confidence for each target.

7.1.3 Geothermal Model Calibration Targets

In order to predict the thermal transport—and more specifically, the temperature distributions—the aquifer thermal properties such as thermal conductivity and thermal-mechanical dispersion coefficient also need to be calibrated. Therefore, the measured temperature data within the model domain may be used to calibrate the geothermal transport model. As with the solute transport calibration, key wells will be chosen within and outside the INEEL site to be the primary locations for calibration to ensure that the simulated temperature distribution not only satisfactorily matches the measured temperatures in those key wells but also reproduces the regional geothermal distribution patterns.

The available temperature profile data for use in the geothermal model include information on 87 wells at or near the INEEL. Thermal profile data are also available from another 38 wells located on the ESRP but not near the INEEL. Most of these 125 wells do not penetrate the entire aquifer thickness, and the dates of the temperature logs range from 1960 to 2003. Vertical temperature profile data from six deep wells at the INEEL that penetrate the entire thickness of the active portion of the aquifer are also available (Smith 2002). An additional deep well, Middle-1823, has been drilled and logged for vertical temperature data. Smith (2002) incorporated these thermal profile data and data from seven other shallower aquifer wells to define the active aquifer thickness.

Additionally, almost all wells within the proposed SWGM domain that have been logged or sampled in some manner by the USGS have some representative water table temperature value associated with them. All of the temperature logs will be reviewed and tabulated. Choosing key wells for geothermal model calibration will be done in a manner similar to choosing key wells for flow model calibration and solute transport model calibration.

7.2 Calibration Procedures

With calibration targets identified, the next step will be to select a specific calibration procedure. In this study, three calibration techniques are proposed. The technique chosen will need to solve the inverse problem (i.e., fitting model to known measured values). The three proposed calibration methods are zonation with automated parameter estimation, automated parameter estimation using the "pilot point" approach, and a combination of these two methods. Each method has advantages and disadvantages. We plan to try all three methods and then choose the method that produces best results. This subsection describes the processes for (a) calibration of the OU 10-08 groundwater flow model, (b) calibration of the OU 10-08 contaminant transport model, and (c) calibration of the geothermal model.

7.2.1 Zonation Approach for Groundwater Flow Model Calibration

The zonation approach is the traditional method of calibration; this approach divides the model domain into zones of constant property value. The main steps in the process are as follows:

1. Identify the key observation wells and/or flux points to be used to calibrate the flow model. Collect all of the available hydraulic head measurements (observations) and flux information appropriate for use in calibrating the flow model.

2. Divide the model domain into zones of equal hydraulic conductivity. Each zone of hydraulic conductivity is defined by a different parameter with a constant model parameter value.

3. Make initial estimates for the hydraulic conductivity values for each zone.

4. Use MODFLOW 2000 to simulate hydraulic head values at each numerical grid in the domain and at each point that corresponds to locations of available hydraulic head measurements. Weighted differences between the measured hydraulic heads and the simulated hydraulic heads are the prediction errors (or residuals).

The weights assigned to each observation depend on the modelers' confidence in the observation and the importance to the calibration objective. The calibration objective is to find the optimal values for each zone of hydraulic conductivity such that the weighted sum of the squared simulation errors (residuals) is minimized. This objective is called the performance measure for the flow model. Initially, the flow will be calibrated manually by trial and error to reach a reasonable fit. Then the estimated conductivity values will be used as the starting values for the automated inverse package, which is outlined below:

1. The use of PEST will automatically adjust the hydraulic conductivity values of a selected set of hydraulic conductivity zones and therefore minimize the weighted sum of the squared simulation errors over all of the hydraulic head measurements. PEST is a model-independent, nonlinear-parameter-estimation package that automates the adjustment of parameters to match calibration targets. For the particular geometry of hydraulic conductivity zones chosen, the results of a PEST run consist of a set of hydraulic conductivity values that provide the "best" fit of the flow model to the hydraulic head measurements being used for calibration. PEST also calculates the parameter

sensitivities and parameter correlation (non-uniqueness) and estimates individual parameter resolution. In particular, the parameter standard deviation and CV are calculated for each hydraulic conductivity value estimated. The CV is the standard deviation divided by the estimated parameter value. The standard deviation is used to calculate the error bounds on the estimated parameters, and the CV is a measure of the uncertainty in the estimates.

2. The output from PEST will be used to modify the geometries of the hydraulic conductivity zone or modify boundary conditions and sources and sinks and better understand the aquifer behavior. The goal of the flow model calibration process is to develop an accurate aquifer model with a minimum number of parameters (hydraulic conductivity zones). By minimizing the number of parameters, the prediction reliability will be maximized; however, we might not have the best calibration fit. A tradeoff exists between more parameters and better fit to the data and fewer parameters and a more reliable prediction. Nevertheless, the final calibrated conductivity zones will be consistent with the available information on the geologic conditions and hydrogeological settings.

7.2.2 Pilot Point Approach for Groundwater Flow Model Calibration

The pilot point approach also utilizes PEST automated parameter adjustment, but instead of beginning with zones of constant parameter value, the approach uses arbitrarily positioned pilot points. The steps in this approach are as follows:

1. Identify the key observation wells and/or flux points to be used to calibrate the flow model. Collect all of the available hydraulic head measurements (observations) and flux information that are appropriate for use in calibrating the flow model.

2. Select a set of points inside the model domain as “pilot points.”

3. Assign initial estimates of hydraulic conductivity values for each pilot point.

4. Interpolate hydraulic conductivity values from the pilot points to each grid block.

5. Use PEST to automatically adjust the hydraulic conductivity values of pilot points to minimize the weighted sum of the squared simulation errors over all of the hydraulic head measurements. The results of a PEST run consist of a set of optimal hydraulic conductivity values at pilot points that provide the best fit of the flow model to the hydraulic head measurements being used for calibration. The hydraulic conductivity values of the rest of the model domain are obtained by interpolating those optimal conductivity values at pilot points.

One advantage of the pilot point approach is that it provides a smoothly varying and heterogeneous conductivity map without arbitrarily defining hydraulic conductivity zones. Another advantage is that this method can directly incorporate aquifer test data as a subset of pilot points with fixed hydraulic conductivity values inferred from those tests.

The disadvantage of the pilot point approach is that it is difficult to incorporate lithologic information when available. Therefore, we plan to use the following coupled pilot point/zonation calibration approach, which has advantages of both approaches.

7.2.3 Coupled Pilot Point/Zonation Approach for Groundwater Flow Model Calibration

The coupled pilot point/zonation calibration approach bounds upper and lower limits of possible pilot point values via the zonation approach, taking advantage of known geologic features. The steps in this method are as follows:

1. Define hydraulic conductivity zones according to available lithology and hydrostratigraphic information.

2. Select zones where additional variation within zones is desired, and set up pilot points within them. The hydraulic conductivity values at pilot points of a particular zone are bounded by the range of hydraulic conductivity appropriate for that particular zone's lithology.

3. Assign uniform hydraulic conductivity values to zones without pilot points.

4. Assign hydraulic conductivity values to pilot points.

5. Use PEST to adjust the hydraulic conductivity values of each pilot point and for zones without pilot points.

The output of PEST will be a conductivity map that consists of zones with a constant hydraulic conductivity value and zones with varying hydraulic conductivity values. This feature might be important for the transport model to reproduce the observed plume migration behaviors, because local-scale heterogeneity largely affects plume migrations. The coupled pilot point/zonation approach provides a good combination of the large-scale heterogeneity (from zone to zone) and local-scale heterogeneity (inside zone). For the OU 10-08 numerical model, we propose to start with zonation approach, followed by the pilot point and coupled pilot point/zonation approaches. The approach that is most efficient and most realistically reflects field hydrogeological settings will then be used for future calibrations.

7.2.4 Calibration Approaches for Contaminant Transport Model

Contaminant transport properties must be quantified for use in the transport simulations. These parameters include effective porosity, dispersivity, and retardation. Because of the highly heterogeneous nature of the aquifer and scale discrepancy between the laboratory and field, these transport parameters are typically obtained through the transport model calibration process.

The calibration approaches mentioned previously for the flow model also apply to the transport model. Therefore, in this subsection, only the zonation calibration approach for the transport model is discussed as an illustration of standard transport model calibration. The various steps involved in the zonation approach for transport model calibration are as follows:

1. Identify key concentration wells to be used to calibrate the transport model. Collect all available concentration measurements that are appropriate for use in calibrating the transport model. In particular, tritium and chloride concentrations will be used to estimate the effective porosities and dispersivities. The tritium and chloride are normally treated as non-sorptive (conservative) tracers in groundwater modeling practice. The measured concentrations of other sorptive contaminants are used to estimate the chemical-specific retardation factors due to adsorption.

2. Define the parameter zones in a manner similar to the method used to determine the conductivity zones. This definition is based primarily on our knowledge of the hydrogeologic settings in the area represented by the model domain and by the output results of the flow calibration process.

3. Make initial estimates for the transport parameters for each zone. The initial estimate will use the values from the previous modeling practices.

4. Use MT3DMS to simulate the plume migration and calculate the concentrations at locations corresponding to observation wells. Weighted differences between the model-simulated concentrations and measured concentrations are the prediction errors. The calibration objective is to obtain a set of optimal values of transport parameters such that the weighted sum of the squared simulation errors is minimized.

5. Use PEST to automatically adjust the values of transport parameters and to calculate the parameter sensitivities, correlations, and resolutions. The result of the PEST run is a set of transport parameter values that provides the best fit of the transport model to the observed plume migration and measured concentrations.

6. Use the information from the output of PEST to modify the zone geometries of transport parameters or modify boundary conditions and sources and sinks to better understand the flow paths and barriers.

7.2.5 Calibration Approaches for Geothermal Model

The calibration approaches mentioned previously for the contaminant transport model also apply to the geothermal transport model. So, in this subsection, only the zonation calibration approach for the geothermal model is discussed as an illustration of standard model calibration. The various steps involved in the zonation approach for geothermal model calibration are as follows:

1. Identify key wells with temperature logs to be used to calibrate the geothermal model. Collect all available temperature measurements that are appropriate for use in calibrating.

2. Define the parameter zones in a manner similar to the method used to determine the conductivity zones. This definition is based primarily on our knowledge of the hydrogeologic settings in the area represented by the model domain and by the output results of the flow calibration process.

3. Make initial estimates for the geothermal transport parameters for each zone.

4. Use a geothermal transport simulator to simulate the temperature distribution and calculate the temperature at locations corresponding to observation wells. Weighted differences between the model-simulated and measured temperatures are the prediction errors. The calibration objective is to obtain a set of optimal values of geothermal transport parameters such that the weighted sum of the squared simulation errors is minimized.

5. Use PEST to automatically adjust the values of geothermal transport parameters and to calculate the parameter sensitivities, correlations, and resolutions. The result of the PEST run is a set of geothermal transport parameter values that provides the best fit of the geothermal model to the observed plume migration and measured concentrations.

6. Use the information from the output of PEST to modify the parameter zone geometries or modify boundary conditions and sources and sinks to better understand the flow paths and barriers.

7. Note that the geothermal model is coupled with the flow model—unlike the contaminant transport model, wherein the governing equations for chemical transport and groundwater flow are not coupled together. The governing equations for geothermal transport and groundwater flow are

coupled together and can only be solved iteratively. Therefore, one should expect more complexities to calibrate the geothermal model.

7.3 Success/Failure Criteria

The results of calibration should be evaluated both qualitatively and quantitatively. Even in quantitative evaluation, the criteria for success or failure of calibration are subjective. There is no standard protocol for evaluating calibration. Quantitative measures of calibration success are typically error-quantifying statistics such as the mean error, the mean absolute error, and the root-mean squared error.

With respect to hydraulic head calibration targets, the mean error is the mean difference between measured heads and simulated heads. The mean absolute error is the mean of the absolute value of the differences in measured and simulated heads. The root-mean squared error is, like standard deviation, the average of the squared differences in measured and simulated heads.

Each of these success criteria can be applied to the other calibration targets. The following paragraphs discuss six types of calibration targets that will be used for OU 10-08 modeling: (1) hydraulic head, (2) hydraulic head gradient, (3) water budget, (4) plume data (contaminant concentrations), (5) temperature data, and (6) parameter value range.

7.3.1 Hydraulic Head

For the groundwater flow model to be considered calibrated, the areal fit to assumed steady-state hydraulic heads must be reasonable. The sitewide head measurements made in June 2004 will be used as surrogates for steady-state conditions, because hydrologic conditions in the SRPA have been relatively stable since 1999 in response to extended regional drought. McCarthy et al. (1995) chose a maximum head measurement error of ±0.33 ft as their target mean absolute value of the difference between the model-simulated and measured heads (residual), based on their head measurements after corrections for borehole deviation. Because of the heterogeneity of the system, this target is reasonable as an average residual but unreachable as a maximum residual for a regional-scale model with large-scale hydraulic conductivity zones defined. Therefore, a target of ±3.3 ft (10 times the measurement error) was used as the target maximum residual for the McCarthy et al. (1995) key head observation wells.

The same target mean head residual, ±0.33 ft, will be selected for the OU 10-08 model. The maximum head residual is chosen to be somewhere between ±0.33 and ±3.3 ft. This ensures that the model reasonably reproduces the measured head values over each of the WAGs.

In the model domain representing the area outside of the INEEL boundaries, the steady-state hydraulic gradient distribution should be similar to the observed gradient distributions used by Garabedian (1992) and Spinazola (1994). The Garabedian and Spinazola models (parameter zones and values) will be used to the extent possible to satisfy this target and to maximize the consistency between the SWGM and the USGS models. The SWGM, however, will provide a significant variation to both the Garabedian and Spinazola models; therefore, some differences will be expected and considered acceptable.

7.3.2 Hydraulic Head Gradient

For each of the individual WAG scales, the simulated steady-state hydraulic gradient should be within 10% of the measured gradient based on the key wells in the area. For the INEEL scale, the steady-

state hydraulic gradient error should be less than 1%. For a total head drop of about 340 ft over the INEEL site (Figure 4-15), this translates to a maximum residual of about 3.4 ft.

7.3.3 Water Budget

The steady-state mass balance calculated from the flow model should be less than 0.1% to ensure the numerical convergence of the simulation model.

7.3.4 Plume Data (Contaminant Concentrations)

Several plumes of contaminated groundwater, i.e., tritium, chloride, strontium-90, and nitrate, that can provide calibration targets for subregional numerical modeling have been identified in the SRPA beneath the INEEL site. Migration of tritium or other plumes can be viewed as large-scale, long-term, tracer tests. Transport model calibration can also be viewed as the interpretation of such tests. Therefore, the calibrated transport model should adequately reproduce the migration of plumes. The spatial spreading patterns of those plumes should also be accurately reproduced by the transport model.

Natural isotope ratios provide valuable information on flow paths and travel time. Such information might not be used directly as calibration targets but will be used to cross check the flow and transport model. We will ensure that the flow field simulated by the model is consistent with natural isotopes.

7.3.5 Temperature Data

Relatively abundant temperature data are available within the model domain, including both vertical temperature profile logs and horizontal spreading. Therefore, as a success/failure criterion of the calibration process, the calibrated geothermal model should adequately match the measured vertical temperature profiles. The geothermal model should also adequately reproduce spatial distribution patterns of the temperature.

7.3.6 Parameter Value Range

Garabedian (1992) defined hydraulic conductivity zones associated with various rock types and assigned the hydraulic conductivity values based on each rock type and the range of conductivities given in *Groundwater* (Freeze and Cherry 1979). The OU 10-08 model will define the target hydraulic conductivity value ranges based on the hydraulic conductivity zones defined by Garabedian (1992); however, local refinements near individual WAGs and areas with new information available will be required in order to set up the target hydraulic conductivity value ranges.

The target range for specific yield is 0.01 to 0.3, and the target range for the storage coefficient is 5×10^{-3} to 5×10^{-5} (Freeze and Cherry 1979). These values bound the values used in the past by Garabedian (1992) and Arnett and Springer (1993).

Nace et al. (1959) estimated the effective porosity for the SRPA between 0.025 and 0.05. Model-estimated values of effective porosity at the INEEL range from about 0.001 to 0.15 (Robertson 1974; Goode and Konikow 1990; Arnett and Springer 1993; Arnett 2003), suggesting that large-scale effective porosities are greater than values estimated from local hydraulic tests. Given the fact that hydraulic conductivities vary by almost six orders of magnitude, effective porosity is also probably quite variable. Typical values of effective porosity for basaltic rock are reported in McWhorter and Sunada (1977) as ranging from 0.03 to 0.35.

The effective dispersivity is normally estimated from the transport model calibration process. This approach has been used in the previous modeling studies at the INEEL (Robertson 1974; Goode and Konikow 1990; Arnett and Springer 1993). The dispersivity values obtained from those modeling studies vary significantly, depending on the model scale and grid resolution. One important issue is the transient flow direction change from the mean flow direction at the INEEL site—which could contribute to a significant transverse plume spreading. Therefore, this additional spreading must be accounted for by explicitly incorporating transient hydraulic head. Otherwise, unreasonably large transverse dispersivity has to be assigned to account for the wide transverse spreading of the plume (Robertson 1974).

Retardation for different constituents depends on the chemical and physical characteristics of the rock; hence, the retardation factor can be treated as a heterogeneous property, similar to hydraulic conductivity. Most likely, the SWGM will continue using uniform retardation factors implemented through the use of a linear reversible isotherm commonly referred to as a partitioning coefficient (K_d). For the most recent OU 7-13/14 aquifer modeling (Holdren et al. 2002), K_ds of 0.0 mL/g were used for all contaminants. This approach is still being used in current OU 7-13/14 RI/FS modeling efforts (Holdren and Broomfield 2004) and can be used because of an absence in the aquifer of consistently monitored contaminants attributable to strictly dissolved-phase reactive (undergoing sorption) transport.

OU 3-13 modeling (DOE-ID 1997) has used an approach where uniform aquifer K_ds are assigned values obtained by scaling down the estimated sediment K_d by a constant ratio. The ratio used in the OU 3-13 modeling was 25:1. Currently, for ongoing OU 3-14 modeling, this approach is undergoing a slight revision. The OU 3-14 modeling will likely continue to use the same scaling approach, but the scaling ratio might be revised by performing a more detailed inverse model of strontium-90 movement in the aquifer in response to injection in well CPP-3. This inverse-estimated K_d would be compared to the most recent estimated sediment partition coefficient of 12 mL/g for strontium-90. This recent K_d value is in the process of being documented in ongoing work for OU 3-14.

The final approach used to simulate chemical interactions between contaminants and the geologic media composing the SRPA, and the parameters used to describe the interactions, will be reached through a consensus process with the regulatory agencies.

8. SCHEDULE AND DELIVERABLES

The WAG 10 OU 10-08 RI/FS work plan (DOE 2002a) describes the enforceable milestone schedule for OU 10-08, and the reader is referred to that work plan for a detailed summary of the events controlling the final deliverable date for the OU 10-08 ROD. The 10-08 ROD is expected to be the last ROD completed at the INEEL, and the deliverable date depends on when the other WAG RODs are signed.

Currently, two major RODs remain to be finished. The planned completion date for the OU 3-14 draft ROD is December 31, 2006, and the planned completion date for the draft OU 7-13/14 ROD is December 31, 2007. When the OU 7-13/14 ROD is signed (assumed to be 6 months later), the period for completing the OU 10-08 RI/FS begins. The draft OU 10-08 RI/FS report will be due to the regulatory agencies for review within 15 months, and the draft OU 10-08 ROD will be due two years after the OU 7-13/14 ROD is signed. Assuming the OU 7-13/14 ROD is signed in June 2008, the draft OU 10-08 RI/FS report will be due September 2009, and the draft OU 10-08 ROD will be due June 2010.

This schedule is subject to change depending on the completion of other INEEL RODs. Groundwater modeling activities described in this work plan are scheduled to support the aquifer flow and transport portions of both the OU 3-13 and OU 7-13/14 RODs. The two-dimensional SWGM will be finished in time to support the OU 3-13 ROD, and the three-dimensional SWGM will be finished in time to support the OU 7-13/14 ROD.

It is critical that the OU 10-08 RI/FS activities overlap and are tied to remedial decisions across the INEEL site. All the other WAGs will be managed under WAG 10 as activities close after individual WAG RODs are signed. This will ensure a smooth and cost-effective transfer into the long-term stewardship role of WAG 10. Also, consolidation and communication of SRPA-wide concerns are needed as soon as possible because of the crucial importance of the SRPA to the population of eastern Idaho and the fact that predicted contaminant levels in the SRPA drive most selected remedies for individual WAGs. INEEL management has taken a proactive, technically acceptable approach to developing the SWGM. The following OU 10-08 actions support this approach:

1. Immediately begin data collection, interpretation, and analysis required to meet OU 10-08 objectives and ensure work is completed in time to meet the Federal Facility Agreement/Consent Order schedule (DOE-ID 1991). Many activities require more time than allowed in the 15-month schedule.

2. Develop a comprehensive and consistent numerical model of aquifer flow and transport in time to support CERCLA decisions for WAGs 3 and 7 (i.e., avoid subregional modeling that is not consistent with prior RODs).

3. Work with individual WAGs as they define their RI/FS source-term loading to the aquifer, reducing time and effort for this critically important parameter in the SWGM (i.e., in an ongoing process, gather and incorporate contaminant source-term information from individual WAGs for use in the SWGM).

4. Overlap model development with ongoing WAG 3 and 7 modeling to create an “institutional memory” that captures the codes, the understanding of programming, the modeling assumptions, and the monitoring requirements that WAG 10 can roll into long-term management of selected remedies; this will also ensure long-term compliance with selected remedies (e.g., preserve the ability to perform and, as necessary, revise modeling in the future for five-year reviews and modify model assumptions).

5. This schedule allows iteration and modeling updates using information from new wells installed in fiscal year 2005. For example, these wells will help in assessing the question of whether plumes from TRA/INTEC/CFA commingle with RWMC contaminant plumes. Phased data collection and interpretation is more cost-effective, because fewer properly sited wells are needed in order to answer the same question. The alternative solution under a shorter schedule will require more wells to ensure adequate characterization.

With the preceding discussion as the regulatory and management background, the following deliverables and schedule have been developed for the SWGM. The overall schedule for the SWGM is presented in Figure 8-1.

8.1 Fiscal Year 2005 Planning

In fiscal year 2005, the SWGM project will provide a white paper on well site selection, a white paper on numerical code selection, and the summary report on the subregional-scale preliminary two-dimensional aquifer model with flow.

8.1.1 Well Site Selection White Paper

A white paper will be prepared describing and considering various alternatives for well locations and construction approaches for drilling in fiscal year 2005. This white paper will be transmitted to DOE by December 9, 2004.

8.1.2 Numerical Code Selection White Paper

A white paper will be prepared to update and supplement the previous OU 10-08 code selection document. This white paper will evaluate off-the-shelf numerical codes that are available for the SWGM and will provide justification for selection of the preferred code. The white paper will be delivered to DOE by March 15, 2005.

8.1.3 Summary Report on the Subregional-scale, Preliminary Two-dimensional Aquifer Model

A summary report containing the subsections described below will be prepared and delivered to DOE by September 30, 2005.

8.1.3.1 Definition of INEEL Geologic Framework. The following investigations will be undertaken to better define the aquifer thickness at the subregional scale:

1. The thickness and stratigraphy of the major tributary basins will be defined based on existing data.

2. An interpretive analysis of the stratigraphic discontinuity between INTEC and TRA will be prepared using data from the new well proposed for this area. The existing geological interpretation will be expanded to include understanding gained from the proposed deep well near USGS-22.

3. Existing geophysical data (both borehole and surface) will be reviewed and recommendations made for fill-in surveys required to adequately describe aquifer thickness and hydrostratigraphic units defined during this effort.

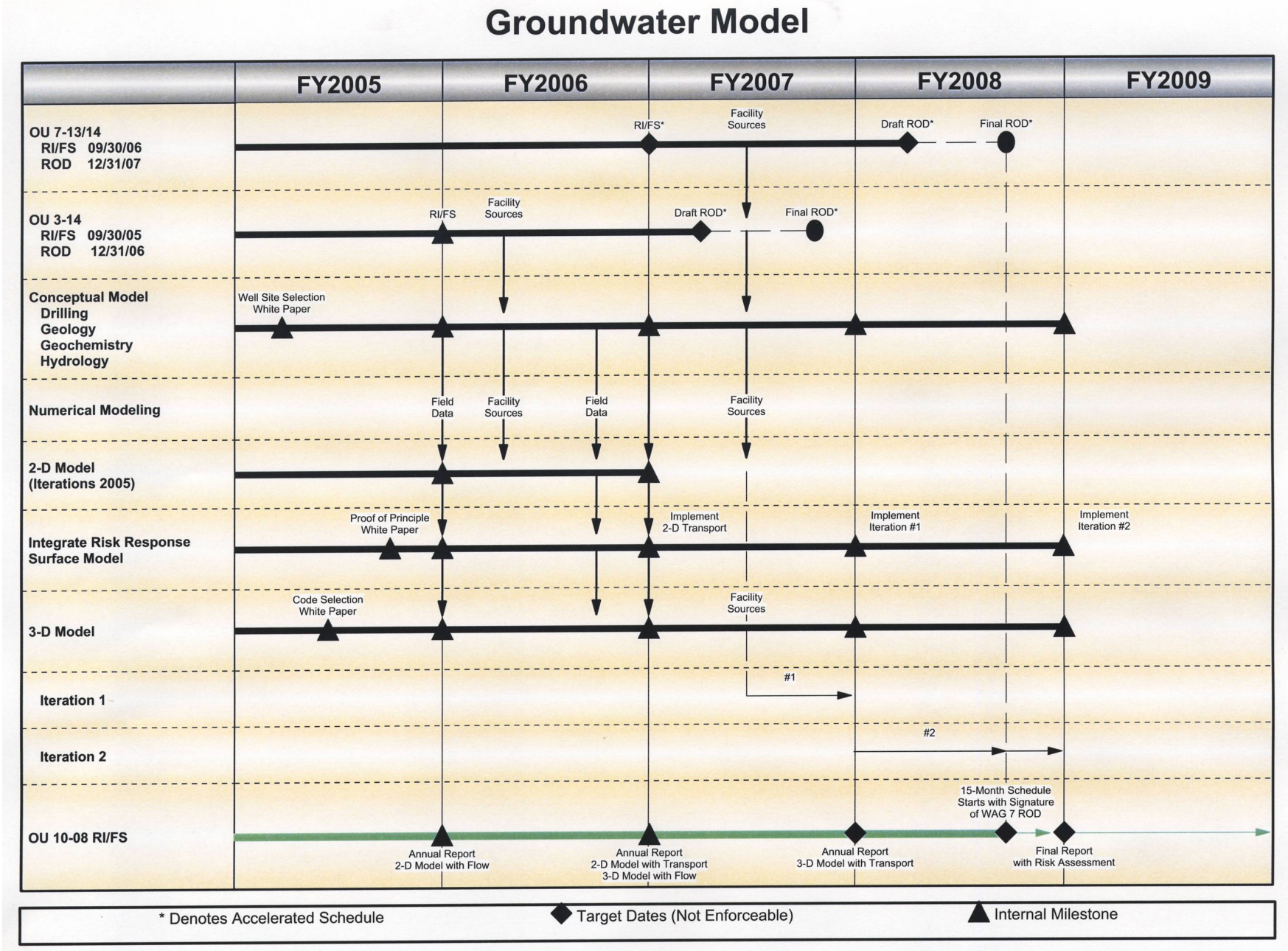

Figure 8-1. SWGM schedule.

8.1.3.2 Natural and Anthropogenic Geochemistry Flow Fields. To date, apparent discrepancies between observed contaminant plumes and aquifer "fast-flow paths" have not been resolved. Additionally, subregional aquifer transport parameters have not been defined for SWGM transport. To address these issues, the following subtasks will be undertaken:

1. Evaluate areas in the aquifer thought to have slower or "stagnant" flow relative to fast-flow paths. In particular, the significance of these zones on contaminant-plume migration will be assessed. Data from the proposed deep well near USGS-22 will help clarify the extent of the stagnant zone thought to extend to the western boundaries of WAGs 3 and 7.

2. Based on existing natural geochemistry data, a plan will be developed for sampling wells in a depth-discrete manner to define the three-dimensional aspects of aquifer flow.

3. Existing data will be reviewed to identify potential anthropogenic tracers (e.g., chlorine-36 and/or sulfate) that can be used to determine whether contaminants beneath the RWMC are locally derived or are from upgradient sources at TRA/INTEC/CFA. A plan for sampling selected wells will be developed.

4. Existing models and data will be assessed to define appropriate transport properties at the subregional scale. As appropriate, recommendations will be made to increase quality levels of existing data for defining transport parameters in the three-dimensional SWGM.

8.1.3.3 Representation of Hydrogeologic Data. As described elsewhere in this document, much work remains to done in order to reduce the complex aquifer data to a meaningful and manageable representation of aquifer flow properties. The following tasks will be performed in fiscal year 2005:

1. Numerous stratigraphic units have been identified in the SRPA beneath the INEEL, far too many to represent each unit individually in the SWGM. Stratigraphic units will be characterized and combined and/or segregated into a manageable number of hydrostratigraphic units in order to best represent the hydrogeologic conditions beneath the INEEL site.

2. Important aquifer properties, such as hydraulic conductivity, have been shown in numerous reports to vary by as many as six orders of magnitude. The effect of this variability on contaminant fate and transport will be assessed so that it can be adequately represented in the SWGM.

3. Water level data are the easiest and most widely available data to collect regarding the SRPA at the INEEL site. These data provide good information about the flow system; however, many uncertainties are inherent in these data. The historic water level data will be reviewed to ensure that future data-collection efforts are coordinated and consistent from year to year.

4. Hydrographs will be evaluated for geographical consistency as part of determining the appropriateness of selecting water table elevations from a single time point for calibrating steady-state flow models.

8.1.3.4 Modeling. The following subtasks will be performed in fiscal year 2005 for inclusion in the two-dimensional summary report:

1. Through the interpretation of existing data, primarily water levels, an assessment will be made of the smallest scale where the assumption of a porous media is still representative of flow in the SRPA. This will identify the smallest grid size that can be represented in the SWGM.

2. In order to take advantage of the rich and diverse data sets available for the SRPA beneath the INEEL site, a methodology and approach to use multiple performance objectives will be developed for incorporating these diverse data sets in the modeling effort. Calibration objectives will also be defined for each data set. Data sets that will be evaluated include the water levels and transmissivity data being used in the USGS and the State of Idaho modeling efforts. This review will ensure that the most complete data set possible is used for model calibration.

3. A two-dimensional, steady-state, aquifer-flow model will be developed at the subregional scale and will have the ability to test different aquifer scenarios (e.g., thick versus thin aquifer). This model will demonstrate consistency in flow velocities and boundary conditions with intermediate-scale models, such as those for WAGs 3 and 7.

4. A response surface modeling method will be developed that uses a convolution integral approach to simulate transport in the aquifer. In this method, unit source inputs from each identified source are integrated to estimate actual concentrations at predetermined aquifer receptor locations while mimicking simulated flow and transport conditions in two- or three-dimensional aquifer flow and transport simulations. Appendix B provides a brief overview of the methodology. A proof-of-principle white paper will be completed to describe the approach and demonstrate the utility of the method.

5. Reactive transport modeling will be applied along a one-dimensional flow path southward from INTEC. Stochastically distributed physical properties along this flow field will be developed for the reactive transport simulations. Comparisons to observed contaminant concentrations, and against transport simulations using the traditional K_d approach, will guide whether it is appropriate to expand the reactive transport simulations to additional dimensions as part of incorporating the approach into the SWGM.

6. The two-dimensional, steady-state, aquifer-flow model will be extended to include transient conditions by incorporating transient recharge from the Big Lost River, tributary basin influx, and the primary upgradient and downgradient boundaries as determined to be appropriate.

8.2 Fiscal Year 2006 Planning

The following deliverables are currently identified for fiscal year 2006. A final report will be prepared documenting the two-dimensional aquifer flow and transport model. A summary report for the subregional, three-dimensional, aquifer-flow model will be prepared and will consist of a conceptual model of groundwater flow and a numerical model that is capable of simulating flow in three dimensions. That report will be transmitted to DOE by September 30, 2006, as a part of the annual report.

8.2.1 Subregional-scale Two-dimensional Transport Model

The two-dimensional aquifer flow model will be used to simulate transport, within the aquifer, of contaminants from all INEEL WAGs that have undergone RI/FS analyses. This cumulative transport will be evaluated with both a traditional numerical simulation and with the response surface approach. The contaminant source term loading to the aquifer will need to be extracted from existing modeling studies for each WAG. As part of determining these source terms, the appropriateness of the individual WAG vadose zone models and the underlying assumptions included in their development will be reviewed. This model will also include a sensitivity evaluation to the method used to assign surface infiltration. Rather than a low uniform infiltration rate, a spatially variable infiltration rate based on exposed geologic media at the land surface will be assigned. The resulting impact on simulated concentrations at selected locations will be used to assess the impact. Lastly, in another sensitivity study, the two-dimensional transport

model will be used to evaluate the impact of including transient flow conditions. Comparisons of simulated concentrations at hypothetical receptor locations against both the observed contaminant monitoring data and the transport simulations with steady-state flow will be used to judge the importance of the transient effects.

8.2.2 Comprehensive Three-dimensional Subregional Conceptual Model

Geology, geophysics, hydrogeology, and geochemistry will be developed into an internally consistent interpretation of the SRPA at the subregional scale. The major components will include the following:

- Geologic model
- Thermal model
- Geochemical model
- Conceptual model of hydrogeologic properties.

The land use scenarios and potential receptor locations for determining groundwater pathway risk will be determined in a consensus process with the regulatory agencies. The assumptions in the use scenarios will be consistent with those most current with the RI/FS evaluations for WAGs 3 and 7.

8.2.3 Subregional-scale, Three-dimensional, Aquifer-flow Numerical Model

A three-dimensional, steady-state, aquifer-flow model will be developed at the subregional scale and will have the ability to test different aquifer interpretations. This model will demonstrate consistency in flow velocities and boundary conditions with intermediate-scale models, such as those for WAGs 3 and 7. As with the two-dimensional flow model, transient simulations will be performed with the three-dimensional aquifer-flow model to evaluate the impact from Big Lost River influx and boundary conditions.

8.3 Fiscal Year 2007 Planning

A fully three-dimensional, subregional-scale, flow and transport model will be developed and documented in a summary report due September 30, 2007. That report will contain the first flow and transport iteration based on the RI/FS data from WAGs 3 and 7 (see Figure 8-1). Like the two-dimensional aquifer transport model, the three-dimensional aquifer transport model will also be run with transient flow conditions to evaluate the impact on transport.

8.4 Fiscal Year 2008 Planning

The SWGM will continue to evolve and be updated with new information until it is used in the OU 10-08 RI/FS. At least one major update or iteration is planned (see Figure 8-1). Under the current schedule, the second iteration is planned to occur in the first half of fiscal year 2008. During fiscal year 2008, risk calculations will be added to the model. The final product of the SWGM effort will be a report that documents the modeling activity, and that report will be delivered to DOE by September 30, 2008. The report will serve as the basis for the OU 10-08 RI/FS, which will begin when the final major ROD is signed (OU 7-13/14 in June 2008).

9. REFERENCES

Ackerman, D. J., 1991, *Transmissivity of the Snake River Plain Aquifer at the Idaho National Engineering Laboratory, Idaho*, U.S. Geological Survey Water-Resources Investigations Report 91-4058.

Ackerman, D. J., 1995, *Analysis of Steady-State Flow and Advective Transport in the Eastern Snake River Plain Aquifer System*, *Idaho*, U.S. Geological Survey Water-Resources Investigations Report 94-4257.

Anderson, M. P., and W. W. Woessner, 1992, *Applied Groundwater Modeling, Simulation of Flow and Advective Transport*, San Diego: Academic Press.

Anderson, S. R., 1991, *Stratigraphy of the Unsaturated Zone and Uppermost Part of the Snake River Plain Aquifer at the Idaho Chemical Processing Plant and Test Reactor Area, Idaho National Engineering Laboratory*, *Idaho*, U.S. Geological Survey Water-Resources Investigations Report 91-4010.

Anderson, S. R., and B. Bowers, 1995, *Stratigraphy of the Unsaturated Zone and Uppermost Part of the Snake River Plain Aquifer at Test Area North, Idaho National Engineering Laboratory, Idaho*, U.S. Geological Survey Water-Resources Investigations Report 95-4130.

Anderson, S. R., M. A. Kuntz, and L. C. Davis, 1999, *Geologic Controls of Hydraulic Conductivity in the Snake River Plain Aquifer at and near the Idaho National Engineering and Environmental Laboratory, Idaho*, U.S. Geological Survey Water-Resources Investigations Report 99-4033.

Anderson, S. R., and M. J. Liszewski, 1997, *Stratigraphy of the Unsaturated Zone and the Snake River Plain Aquifer at and near the Idaho National Engineering Laboratory, Idaho*, U.S. Geological Survey Water-Resources Investigations Report 97-4183.

Arnett, R. C., 2002, *TAN OU 1-07B ISB Groundwater Model Development and Initial Performance Simulation*, INEEL/EXT-02-00560, Idaho National Engineering and Environmental Laboratory, June 2002.

Arnett, R. C., 2003, *Test Area North, Operable Unit 1-07B In Situ Bioremediation Groundwater Model Calibration Using the 2002 Pressure Response and Tracer Data*, INEEL/EXT-03-00528, Rev. 0, Idaho National Engineering and Environmental Laboratory, July 2003.

Arnett, R. C., J. M. McCarthy, G. T. Norrell, A. L Schafer-Perini, T. R. Wood, 1993, *Basis for Initial Code Selection for WAG 10 Groundwater and Contaminant Transport Modeling at the Idaho National Engineering Laboratory*, EGG-ERD-10532, Idaho National Engineering Laboratory, February 1993.

Arnett, R. C., and R. P. Smith, 2001, *WAG 10 Groundwater Modeling Strategy and Conceptual Model*, INEEL/EXT-01-00768, Rev. B, Idaho National Engineering and Environmental Laboratory, September 2001.

Arnett, R. C., and R. K. Springer, 1993, *Calibration of the Groundwater Flow Model for a Portion of the Snake River Plain Aquifer at the INEL*, ER&EM-EDF-0024-93, Idaho National Engineering Laboratory.

Barraclough, J. T., B. D. Lewis, and R. C. Jensen, 1981, *Hydrologic Conditions at the Idaho National Engineering Laboratory, Idaho – Emphasis 1974-1978*, U.S. Geological Survey Open-File Report 81-526.

Barraclough, J. T., J. B. Teasdale, and R. G. Jensen, 1966, *Hydrology of the National Reactor Testing Station, Idaho: Annual Progress Report, 1966*, U.S. Geological Survey Open-File Report IDO-22049.

Beasley, T. M., P. R. Dixon, and L. J. Mann, 1998, "^{99}Tc, ^{236}U, and ^{237}Np in the Snake River Aquifer at the Idaho National Engineering and Environmental Laboratory, Idaho Falls, Idaho," *Environmental Science and Technology*, Vol. 32, No. 24, pp. 3875-3881.

Bennett, C. M., 1990, *Streamflow Losses and Groundwater Level Changes along the Big Lost River at the Idaho National Engineering Laboratory, Idaho*, U.S. Geological Survey Water-Resources Investigations Report 90-4067.

Bestland, E. A., P. K. Link, D. Champion, and M. Lanphere, 2002, *Paleoenvironments of Sedimentary Interbeds in the Pliocene-Pleistocene Big Lost Trough (Eastern Snake River Plain, Idaho)*, P. K. Link and L. L. Mink (eds.), Geological Society of America Special Paper 353.

Blackwell, D. D., 1983, *Heat Flow in the Northern Basin and Range Province, the Role of Heat in the Development of Energy and Mineral Resources in the Northern Basin and Range Province*, Special Report 13, edited by Geothermal Resources Council, pp. 81 - 93.

Blackwell, D. D., 1989, "Regional Implications of Heat Flow of the Snake River Plain, Northwestern United States," *Tectnophysics*, Vol. 164, pp. 323-343.

Blackwell, D. D., 1990, *Temperatures and Heat Flow in INEL-GT1 and WO-2 Boreholes, Snake River Plain, Idaho*, EGG-NPR-10690, Idaho National Engineering Laboratory.

Blackwell, D. D., S. Kelley, and J. L. Steele, 1992, *Heat Flow Modeling of the Snake River Plain*, EGG-NPR-10790, Idaho National Engineering Laboratory.

Blackwell, D. D., and J. L. Steele, 1992, "Geothermal Map of North America: DNAG Continent-Scale Map-006," *Geological Society of America*, Decade of North American Geology series.

Blackwell, D. D., J. L. Steele, and L. S. Carter, 1991, "Heat Flow Patterns of the North American Continent: A Discussion of the DNAG Geothermal Map of North America," D. B. Slemmons, E. R. Engdahl, and D. D. Blackwell (eds.), *Neotectonics of North America, Geological Society of America*, DNAG Decade Map, Vol. 1, p. 498.

Blair, J. J., 2002, "Sedimentology and Stratigraphy of Sediments of the Big Lost Trough Subsurface from Selected Coreholes at the Idaho National Engineering and Environmental Laboratory, Idaho," Master's Thesis, Idaho State University, Pocatello, Idaho.

Blair, J. J., and P. K. Link, 2000, "Pliocene and Quaternary Sedimentation and Stratigraphy of the Big Lost Trough from Coreholes at the Idaho National Engineering and Environmental Laboratory, Idaho: Evidence for a Regional Pliocene Lake during the Olduvai Normal Polarity Subchron," L. Robinson (ed.), *Proceedings of the 35th Symposium on Engineering Geology and Geotechnical Engineering, Pocatello, Idaho State University*.

Brott, C. A., D. D. Blackwell, and J. P. Ziagos, 1981, "Thermal and Tectonic Implications of Heat Flow in the Eastern Snake River Plain, Idaho," *Journal of Geophysical Research*, Vol. 86, pp. 11,709-11,734.

BYU, 2002, "Groundwater Modeling System Software," Provo, Utah: Environmental Modeling Research Laboratory, Brigham Young University.

Cecil, L. D., J. R. Pittman, T. M. Beasley, R. L. Michel, R. L. Kubik, P. Sharma, U. Fehn, and H. E. Gove, 1992, "Water Infiltration Rates in the Unsaturated Zone at the Idaho National Engineering Laboratory Estimated from Chlorine-36 and Tritium Profiles, and Neutron Logging," Kharaka Yousifk and Ann S. Maest (eds.), *Proceedings of the 7th International Symposium on Water-Rock Interaction, July 13-18, 1992*, pp. 709-714.

Cecil, L. D., J. A. Welhan, J. R. Green, S. K. Frape, and E. R. Sudicky, 2000, "Use of Chlorine-36 to Determine Regional-Scale Aquifer Dispersivity, Eastern Snake River Plain Aquifer, Idaho/USA," *Nuclear Instruments and Methods in Physics Research*, B 172 (2000), pp. 679-687.

Champion, D. E., M. A. Lanphere, S. R. Anderson, and M. A. Kuntz, 2002, *Accumulation and Subsidence of Late Pleistocene Basaltic Lava Flows of the Eastern Snake River Plain, Idaho*, P. K. Link and L. L. Mink (eds.), Geological Society of America Special Paper 353, pp. 175-192.

Dahan, O., D. McGraw, E. Adar, G. Pohll, B. Bohm, and J. Thomas, 2004, "Multi-variable Mixing Cell Model as a Calibration and Validation Tool for Hydrogeologic Groundwater Modeling," *Journal of Hydrology*, Vol. 293.

Davis, J. A., S. B. Yabusaki, C. I. Steffel, J. M. Zachara, G. P. Curtis, G. D. Redden, L. J. Chriscenti, and B. D. Honeyman, 2004, "Assessing Conceptual Models for Subsurface Reactive Transport of Inorganic Contaminants", *Eos*, Vol. 85, No. 44, pp. 449, 455.

DOE M 435.1-1, 2001, *Radioactive Waste Management Manual*, Change 1, U.S. Department of Energy, June 2001.

DOE-ID, 1991, *Federal Facility Agreement and Consent Order for the Idaho National Engineering Laboratory,* Administrative Docket No. 1088-06-29-120, U.S. Department of Energy Idaho Operations Office; U.S. Environmental Protection Agency, Region 10; Idaho Department of Health and Welfare, December 4, 1991.

DOE-ID, 1997, *Comprehensive RI/FS for the Idaho Chemical Processing Plant OU 3-13 at the INEEL—Part A, RI/BRA Report (FINAL)*, DOE/ID-10534, U.S. Department of Energy Idaho Operations Office, November 1997.

DOE-ID, 2000, *Monitoring System and Installation Plan for Operable Unit 3-13, Snake River Plain Aquifer*, DOE/ID-10783, Rev. 1, U.S. Department of Energy Idaho Operations Office, November 2000.

DOE-ID, 2002a, *Waste Area Group 10, Operable Unit 10-08, Remedial Investigation/Feasibility Study Work Plan (FINAL)*, DOE/ID-10902, Rev. 0, U.S. Department of Energy Idaho Operations Office, August 2002.

DOE-ID, 2002b, *Central Facilities Area Landfills I, II, and III Five-Year Review Supporting Documentation*, DOE/ID-10981, Rev. 0, U.S. Department of Energy Idaho Operations Office, November 2002.

DOE-ID, 2003a, *New Pump and Treat Facility Remedial Action Work Plan for Test Area North Final Groundwater Remediation, Operable Unit 1-07B*, DOE/ID-10679, Rev. 1, U.S. Department of Energy Idaho Operations Office, September 2003.

DOE-ID, 2003b, *Monitored Natural Attenuation Remedial Action Work Plan for Test Area North Final Groundwater Remediation, Operable Unit 1-07B*, DOE/ID-11055, Rev. 0, U.S. Department of Energy Idaho Operations Office, June 2003.

DOE-ID, 2003c, *Monitored Natural Attenuation Operations, Monitoring, and Maintenance Plan for Test Area North, Operable Unit 1-07B*, DOE/ID-11066, Rev. 0, U.S. Department of Energy Idaho Operations Office, June 2003.

DOE-ID, 2003d, *First Five-Year Review Report for the Test Reactor Area, Operable Unit 2-13, at the Idaho National Engineering and Environmental Laboratory*, DOE/ID-11091, Rev. 0, U.S. Department of Energy Idaho Operations Office, September 2003.

DOE-ID, 2003e, *Annual INTEC Groundwater Monitoring Report for Group 5-Snake River Plain Aquifer (2003)*, DOE/ID-11118, Rev. 0, U.S. Department of Energy Idaho Operations Office, December 2003.

DOE-ID, 2004a, *Monitored Natural Attenuation 2003 Performance and Compliance Monitoring Annual Report for Test Area North Operable Unit 1-07B*, DOE/NE-ID-11148, Rev. 0, U.S. Department of Energy Idaho Operations Office, June 2004.

DOE-ID, 2004b, *In Situ Bioremediation Remedial Action Work Plan for Test Area North Final Groundwater Remediation, Operable Unit 1-07B*, DOE/ID-11015, Rev. 2, U.S. Department of Energy Idaho Operations Office, July 2004.

DOE-ID, 2004c, *Monitoring Report/Decision Summary for Operable Unit 3-13, Group 5, Snake River Plain Aquifer*, DOE/ID-11098, Rev. 0, U.S. Department of Energy Idaho Operations Office, January 2004.

Doherty, D. J., L. A. McBroome, and M. A., Kuntz, 1979, *Preliminary Geological Interpretation and Lithologic Log of the Exploratory Geothermal Test Well (INEL-1), Idaho National Engineering Laboratory, Eastern Snake River Plain, Idaho*, U.S. Geological Survey Open-File Report 79-1248.

Domenico, P. A., and F. W. Schwartz, 1990, *Physical and Chemical Hydrogeology*, New York: John Wiley and Sons, Inc.

Fetter, C. W., 1988, *Applied Hydrogeology*, New York: MacMillan Publishing, Inc.

Frederick, D. B., and G. S. Johnson, 1996, *Estimation of Hydraulic Properties and Development of a Layered Conceptual Model for the Snake River Plain Aquifer at the Idaho National Engineering Laboratory, Idaho*, State of Idaho INEL Oversight Program and Idaho Water Resources Research Institute Research and Technical Completion Report.

Freeze, R. A., and J. A. Cherry, 1979, *Groundwater*, Englewood Cliffs, New Jersey: Prentice-Hall.

Garabedian, S. P., 1992, *Hydrology and Digital Simulation of the Regional Aquifer System, Eastern Snake River Plain, Idaho*, U.S. Geological Survey Professional Paper 1408-F.

Gass, T. E., 1982, "Geothermal Heat Pumps," *Geothermal Resources Council Bulletin 11(11)*, pp. 3-8.

Goode, D. J., and L. F. Konikow, 1990, "Reevaluation of Large-Scale Dispersivities for a Waste Chloride Plume: Effects of Transient Flow," *International Conference on Calibration and Reliability in Groundwater Modeling, International Association of Hydrological Sciences, The Hague, The Netherlands, September 1990*.

Greeley, R., 1982, "The Style of Basaltic Volcanism in the Eastern Snake River Plain, Idaho," Bill Bonnichsen and R. M. Breckenridge (eds.), *Cenozoic Geology of Idaho*, Idaho Bureau of Mines and Geology Bulletin 25, pp. 407-421.

Hackett, W. R., R. C. Bartholomay, D. G. Disney, C. F. Hersley, L. G. Snider, and N. C. Zentner, 1987, *Volcanic Hazards Assessment for the Proposed Superconducting Supercollider*, Department of Geology, Idaho State University, Pocatello, Idaho, 33 pp.

Hackett, W. R., and R. P. Smith, 1992, "Quaternary Volcanism, Tectonics, and Sedimentation in the Idaho National Engineering Laboratory Area," J. R. Wilson (ed.), *Field Guide to Geologic Excursions in Utah and Adjacent Areas of Nevada, Idaho, and Wyoming*, Geological Society of America Rocky Mountain Section Guidebook, Utah Geological Survey Miscellaneous Publication 92-3, pp.1-18.

Harbaugh, A. W., E. R. Banta, M. C. Hill, and M. G. McDonald, 2000, *MODFLOW-2000, The U.S. Geological Survey Modular Ground-Water Model – User Guide to Modularization Concepts and the Ground-Water Flow Process*, U.S. Geological Survey Open-File Report 00-92.

Helm-Clark, C. M., D. W. Rodgers, and R. P. Smith, 2004, "Borehole Geophysical Techniques to Define Stratigraphy, Alteration and Aquifers in Basalt," *Journal of Applied Geophysics*, Vol. 55, pp. 1-38.

Holdren, K. J., B. H. Becker, N. L. Hampton, L. D. Koeppen, S. O. Magnuson, T. J. Meyer, G. L. Olson, and A. J. Sondrup, 2002, *Ancillary Basis for Risk Analysis of the Subsurface Disposal Area*, INEEL/EXT-02-01125, Rev. 0, Idaho National Engineering and Environmental Laboratory, September 2002.

Holdren, K. J., and B. J. Broomfield, 2004, *Second Addendum to the Work Plan for the OU 7-3/14 Waste Area group 7 Comprehensive Remedial Investigation/Feasibility Study*, DOE/ID-11039, Rev. 0, U.S. Department of Energy Idaho Operations Office, August 2004.

Hughes, S. S., J. L. Casper, and D. J. Geist, 1997, "Potential Influence of Volcanic Constructs on Hydrogeology beneath Test Area North, Idaho National Engineering and Environmental Laboratory, Idaho," *Proceedings, 32nd Symposium, Engineering, Geology, and Geotechnical Engineering*.

Hughes, S. S., M. McCurry, and D. J. Geist, 2002, "Geochemical Correlations and Implications for the Magmatic Evolution of Basalt Flow Groups at the Idaho National Engineering and Environmental Laboratory," P. K. Link and L. L. Mink (eds.), *Geology, Hydrogeology and Environmental Remediation, Idaho National Engineering and Environmental Laboratory, Eastern Snake River Plain*, Geological Society of America Special Paper 353, pp. 151-173.

Humphreys, E. D., K. G. Dueker, D. L. Schutt, and R. B. Smith, 2000, "Beneath Yellowstone: Evaluating Plume and Nonplume Models using Telesiesmic Images of the Upper Mantle," *GSA Today*, Vol. 10, No. 12, pp.1-7.

ICP, 2004a, *Evaluation of Tc-99 in Groundwater at INTEC: Summary of Phase I Results*, ICP/EXT-04-00244, Rev. 0, Idaho Completion Project, September 2004.

ICP, 2004b, *Central Facilities Landfills I, II, and III Annual Monitoring Report (2003)*, ICP/EXT-04-00149, Rev. 0, Idaho Completion Project, October 2004.

INEEL, 2003, *Central Facilities Landfills I, II, and III Annual Monitoring Report*, INEEL/EXT-03-00024, Rev. 0, Idaho National Engineering and Environmental Laboratory, September 2003.

Johnson, A. I., 1965, *Determination of Hydrologic and Physical Properties of Volcanic Rocks by Laboratory Methods*, D. N. Wadia (ed.), Commemorative Volume, Mining and Metallurgical Institute of India, pp. 50-63 and 78.

Johnson, G. S., and D. B. Frederick, 1997, *Depth and Temporal Variations in Water Quality of the Snake River Plain Aquifer in Well USGS-59 near the Idaho Chemical Processing Plant at the Idaho National Engineering and Environmental Laboratory, Idaho*, Idaho Water Resources Research Institute, 55 p.

Johnson, T. M., R. C. Roback, T. L. McLing, T. D. Bullen, D. J. DePaolo, C. Doughty, R. J. Hunt, R. W. Smith, L. D. Cecil, and M. T. Murrell, 2000, "Groundwater 'Fast Paths' in the Snake River Plain Aquifer—Radiogenic Isotope Ratios as Natural Groundwater Tracers," *Geology*, Vol. 28, No. 10, October 2000, pp. 871-874.

Kehew, A. H., 2000, *Applied Chemical Hydrogeology*, Upper Saddle River, New Jersey: Prentice-Hall.

Kipp, K. L., Jr., 1987, *HST3D: A Computer Code for Simulation of Heat and Solute Transport in Three-Dimensional Ground-Water Flow Systems*, U.S. Geological Survey Water-Resources Investigations Report 86-4095.

Knobel, L. L., R. C. Bartholomay, B. J. Tucker, L. M. Williams, and L. D. Cecil, 1999, *Chemical Constituents in Ground Water from 39 Selected Sites with an Evaluation of Associated Quality Assurance Data, Idaho National Engineering and Environmental Laboratory and Vicinity, Idaho,* U.S. Geological Survey Open-File Report 99-246.

Knutson, C. F., K. A. McCormick, J. C. Crocker, M. A. Glenn, and M. L. Fishel, 1992, *3D RWMC Vadose Zone Modeling (Including FY-89 to FY-90 Basalt Characterization Results)*, EGG-ERD-10246, Idaho National Engineering Laboratory.

Knutson, C. F., K. A. McCormick, R. P. Smith, W. R. Hackett, J. P. O'Brien, and J. C. Crocker, 1990, *FY-89 Report: RWMC Vadose Zone Basalt Characterization*, EGG-WM-8949, Idaho National Engineering Laboratory, July 1990.

Kuntz, M. A., S. R. Anderson, D. E. Champion, M. A. Lanphere, and D. J. Grunwald, 2002, "Tension Cracks, Eruptive Features, Dikes, and Faults Related to L Pleistocene-Holocene Basaltic Volcanism and Implementation for the Distribution of Hydraulic Conductivity in the Eastern Snake River Plain, Idaho," P. K. Link and L. L. Muele (eds.), *Geology, Hydrogeology, and Environmental Remediation, Idaho National Engineering and Environmental Laboratory, Eastern Snake River Plain, Idaho*, Geological Society of America Special Paper 353.

Kuntz, M. A., H. R. Covington, and L. J. Schorr, 1992, "An Overview of Basaltic Volcanism of the Eastern Snake River Plain, Idaho," P. K. Link, M. A. Kuntz, and L. B. Platt (eds.), *Regional Geology of Eastern Idaho and Western Wyoming: Geological Society of America,* Memoir 179, pp. 227-267.

Kuntz, M. A., P. K. Link, D. L. Boyack, J. K. Geslin, L. E. Mark, M. K. V. Hodges, M. E. Kauffman, D. E. Champion, M. R. Lanphere, D. W. Rodgers, and M. H. Anders, 2003, "Geologic Map of the Northern and Central Parts of the Idaho National Engineering and Environmental Laboratory, Eastern Idaho," Idaho Geological Survey Geologic Map 35.

Kuntz, M. A., B. Skipp, M. A. Lanphere, W. E. Scott, K. L. Pierce, G. B. Dalrymple, D. E. Champion, G. F. Embree, W. R. Page, L. A. Morgan, R. P. Smith, W. R. Hackett, and D. W. Rodgers, 1994, "Geologic Map of the Idaho National Engineering Laboratory and Adjoining Areas, Eastern Idaho," U.S. Geological Survey Miscellaneous Investigations Map I-2330, scale 1:100,000.

Leeman, W. P., and W. I. Manton, 1971, "Strontium Isotopic Composition of Basaltic Lavas from the Snake River Plain, Southern Idaho," *Earth and Planetary Science*, Letter 11, 420-434.

Lewis, B. D., and F. J. Goldstein, 1982, *Evaluation of a Predictive Ground-Water Solute-Transport Model at the Idaho National Engineering Laboratory, Idaho*, U.S. Geological Survey Water-Resources Investigations Report 82-25.

Lindholm, G. F., 1996, *Summary of the Snake River Plain Regional Aquifer-System Analysis in Idaho and Eastern Oregon*, U.S. Geological Survey Professional Paper 1408A.

Luo, S., T. Ku, R. Roback, M. Murrell, and T. L. McLing, 2000, "In-situ Radionuclide Transport and Preferential Groundwater Flows at the INEEL (Idaho)," Decay-series Disequilibrium Studies, *Geochimica et Cosmochimica Acta*, Vol. 64, No. 5, pp. 867-881.

Mann, L. J., 1986, *Hydraulic Properties of Rock Units and Chemical Quality of Water for INEL-1—A 10,365-Foot-Deep Test Hole Drilled at the Idaho National Engineering Laboratory, Idaho*, U.S. Geological Survey Water-Resources Investigations Report 86-4020.

Mann, L. J., and T. M. Beasley, 1994, *Iodine-129 in the Snake River Plain Aquifer at and near the Idaho National Engineering Laboratory, Idaho, 1990-91*, U.S. Geological Survey Water-Resources Investigations Report 94-4053.

McCarthy, J. M., R. C. Arnett, R. M. Neupauer, M. J. Rohe, and C. Smith, 1995, *Development of a Regional Groundwater Flow Model for the Area of the Idaho National Engineering Laboratory, Eastern Snake River Plain Aquifer*, INEL-95/0169, Rev. 1, Idaho National Engineering Laboratory, March 1995.

McLing, T. L., R. W. Smith, and T. M. Johnson, 2001, *Chemical Characteristics of Thermal Water Beneath the Eastern Snake River Plain*, Geological Society of America Special Paper 353.

McWhorter, D. B., and D. K. Sunada, 1977*, Ground-Water Hydrology and Hydraulics*, Fort Collins, Colorado: Water Resources Publications.

Meyer, W., and W. R. Souza, 1995, "Factors that Control the Amount of Water that can be Diverted to Wells in a High-level Aquifer, in Water Resources and Environmental Hazards—Emphasis on Hydrologic and Cultural Insight in the Pacific Rim," *American Water Resources Association*, June 1995.

Morse, L. H., and M. McCurry, 1997, "Possible Correlations between Basalt Alteration and the Effective Base of the Snake River Plain Aquifer at the INEEL," S. Sharma and J. H. Hardcastle (eds.), *Proceedings of the 32nd Symposium on Engineering Geology and Geotechnical Engineering, College of Engineering, Idaho State University, Pocatello*, pp. 1-13.

Morse, L. H., and M. McCurry, 2002, "Genesis of Alteration of Quaternary Basalts within a Portion of the Eastern Snake River Plain Aquifer," P. K. Link and L. L. Mink (eds.), *Geology, Hydrogeology, and Environmental Remediation, Idaho National Engineering and Environmental Laboratory, Eastern Snake River Plain, Idaho*, Geological Society of America Special Paper, Vol. 353, pp. 213-224.

Nace, R. L., M. Deutsch, and P. T. Voegeli, 1956, *Geography, Geology, and Water Resources of the National Reactor Testing Station, Idaho, Part 2: Geography and Geology*, U.S. Atomic Energy Commission Publication (IDO-22033), 225 pp.

Nace, R. L., J. W. Stewart, W. C. Walton, and others, 1959, "Geography, Geology, and Water Resources of the National Reactor Testing Station, Idaho, Part 3," *Hydrology and Water Resources*, U.S. Geological Survey, IDO 22034.

Olmsted, F. H., 1962, *Chemical and Physical Character of Groundwater in the National Reactor Testing Station, Idaho*, IDO-22043-USGS, U.S. Geological Survey.

Olmsted, F. H., 1965, *Radioactive Waste Disposal Data for the National Reactor Testing Station, Idaho*, U.S. Atomic Energy Commission, Idaho Falls, Idaho, 52 pp.

Osmond, J. K., and Cowart, J. B., 1992, *Ground Water in Uranium-series Disequilibrium; Applications to Earth, Marine, and Environmental Sciences*, M. Ivanovich and R. S. Harmon (eds.), Oxford, United Kingdom: Clarendon Press.

Parsons, T., and G. A. Thompson, 1991, "The Role of Magma Overpressure in Suppressing Earthquakes and Topography: Worldwide Examples," *Science*, Vol. 253, pp.1399-1402.

Parsons, T., G. A. Thompson, and R. P. Smith, 1998, "More Than One Way to Stretch: a Tectonic Model for Extension along the Track of the Yellowstone Hotspot and Adjacent Basin and Range Province," *Tectonics*, Vol. 17, No. 2, pp. 221-234.

Pierce, K. L., and L. A. Morgan, 1992, "The track of the Yellowstone Hot Spot: Volcanism, Faulting, and Uplift," P. K. Link, M. A. Kuntz, and L. B. Platt (eds.), *Regional Geology of Eastern Idaho and Western Wyoming*, Geological Society of America Memoir 179, pp. 1-53.

Roback, R. C., T. M. Johnson, T. L. McLing, M. T. Murrell, S. Luo, and T. Ku, 2001, *Uranium Isotopic Evidence for Groundwater Chemical Evolution and Flow Patterns in the Eastern Snake River Plain Aquifer, Idaho*, Geological Society of America Bulletin, September 2001.

Robertson, J. B., 1974, *Digital Modeling of Radioactive and Chemical Waste Transport in the Snake River Plain Aquifer at the National Reactor Testing Station, Idaho – 1952-1970*, U.S. Geological Survey Open-File Report IDO-22054.

Robertson, J. B., R. Schoen, and J. T. Barraclough, 1974, *The Influence of Liquid Waste Disposal on the Geochemistry of Water at the National Reactor Testing Station, Idaho, 1952-1970*, U.S. Geological Survey Open-File Report ID-22053, 231 p.

Rodgers, D. W., W. R. Hackett, and H. T. Ore, 1990, "Extension of the Yellowstone Plateau, Eastern Snake River Plain, Idaho," *Geological Society of America Abstracts with Programs*, 18, pp. 1138-1131

Rodgers, D. W., H. T. Ore, R. T. Bobo, N. McQuarrie, and N. Zentner, 2002, "Extension and Subsidence of the Snake River Plain, Idaho," Bill Bonnichsen, C. M. White, and Michael McCurry (eds.), *Tectonic and Magmatic Evolution of the Snake River Plain Volcanic Province*, Idaho Geological Survey Bulletin 30, pp. 121-155.

Rohe, M. J., 2002, "Tributary Streamflow Influence on a High Desert, Deep Aquifer System," *Proceedings for American Water Resources Association 2002 Summer Specialty Conference on Ground Water/Surface Water Interactions, Keystone, Colorado, July 2002*.

Shaw, R. Mark, DOE Idaho Operations Office, to Nicholas Ceto, EPA Region 10, and Daryl F. Koch, Idaho DEQ, July 28, 2004, "Documentation of Agency Consensus on Waste Area Group 10, 10-08 Groundwater Modeling Objectives and Transmittal of Meeting Presentation Materials," EM-ER-04-167.

Smith, R. B., and L. W. Braile, 1994, "The Yellowstone Hotspot," *Journal of Volcanology and Geothermal Research*, Vol. 61, pp. 121-187.

Smith, R. P., 2002, *Variability of the Aquifer Thickness Beneath the Idaho National Engineering and Environmental Laboratory (INEEL)*, INEEL/EXT-02-01022, Rev. 0, Idaho National Engineering and Environmental Laboratory, August 2002.

Smith, R. P., D. D. Blackwell, and T. L. McLing, 2001, "Temperature Distribution in the Snake River Plain Aquifer beneath the Idaho National Engineering and Environmental Laboratory (INEEL) — Implications for Aquifer Flow and Geothermal Input," *Geological Society of America Abstracts with Programs*, Vol. 33, No. 6, p. A-107.

Southern Methodist University, 2004, "Geothermal Map of the United States," http://www.smu.edu/geothermal/heatflow/geothermal_all_us_clipped_150dpi_pagesize_legend.gif, Web page visited April 5, 2004.

Spinazola, J. M., 1994, *Geohydrology and Simulation of Flow and Water Levels in the Aquifer System in the Mud Lake Area of the Eastern Snake River Plain, Eastern Idaho*, U.S. Geological Survey Water-Resources Investigations Report 93-4227.

Welhan, J. A., and M. Reed, 1997, *Geostatistical Analysis of Regional Hydraulic Conductivity Variations in the Snake River Plain Aquifer, Eastern Idaho*, Bulletin of the Geological Society of America, Vol. 109, pp. 855-868.

Whitehead, R. L., 1992, *Geohydrologic Framework of the Snake River Plain Regional Aquifer System, Idaho and Eastern Oregon*, U.S. Geological Survey Professional Paper 1408-B.

Wood, S. H., and W. Bennecke, 1994, "Vertical Variation in Groundwater Chemistry Inferred from Fluid Specific-Conductance Well Logging of the Snake River Plain Aquifer, Idaho National Engineering Laboratory, Southeastern Idaho," *Proceedings of the 30th Symposium on Engineering Geology and Geotechnical Engineering*, pp. 267-283.

Wood, W. W., and W. H. Low, 1986, *Aqueous Geochemistry and Diagenesis in the Eastern Snake River Plain Aquifer System, Idaho*, Bulletin of the Geological Society of America, Vol. 97, pp. 1456-1466.

Wylie, A. H., 2003, *Delineating the Bottom of the Aquifer, Eastern Snake Plain Aquifer Model Enhancement*, Model Design and Calibration Document Number DDM-012, Idaho Water Resources Research Institute, University of Idaho, March 2003.

Wymore, R. A., J. M. Bukowski, and K. S. Sorenson, Jr., 2000, *Site Conceptual Model – 1998 and 1999 Activities, Data Analysis, and Interpretation for Test Area North, Operable Unit 1-07B*, INEEL/EXT-2000-00188, Rev. 0, Idaho National Engineering and Environmental Laboratory, December 2000.

Ziagos, J. P., and D. D. Blackwell, 1986, "A Model for the Transient Temperature Effects of Horizontal Fluid Flow in Geothermal Systems," *Journal of Volcanology and Geothermal Research*, Vol. 27, pp. 371-397.